MASTER IN BIOCHEMISTRY AND MOLECULAR AND CELL BIOLOGY RESEARCH FOCUS

Study of the role of succinate in naïve murine embryonic stem cells two-cell-like reprogramming

Feller, Louise

Award date:
2022

Awarding institution:
University of Namur

UNIVERSITE DE NAMUR

Faculté des Sciences

STUDY OF THE ROLE OF SUCCINATE IN NAÏVE MURINE EMBRYONIC STEM CELLS TWO-CELL-LIKE REPROGRAMMING

Mémoire présenté pour l'obtention

du grade académique de master 120 en biochimie et biologie moléculaire et cellulaire

Louise FELLER

Janvier 2022

Université de Namur
FACULTE DES SCIENCES
Secrétariat du Département de Biologie
Rue de Bruxelles 61 – 5000 NAMUR
Téléphone : +32(0)81.72.44.18 – Téléfax : +32(0)81.72.44.20
E-mail : joelle.jonet@unamur.be – http://www.unamur.be

ETUDE DU RÔLE DU SUCCINATE DANS LA REPROGRAMMATION 2-CELL-LIKE DES CELLULES SOUCHES EMBRYONNAIRES MURINES NAÏVES

Louise FELLER

Résumé

Au sein de la population des cellules embryonnaires souches naïves de souris (mESC), originellement dérivée de la masse cellulaire interne (ICM) du blastocyste, une sous-population de cellules oscille spontanément entre un état naïf et un état *totipotent-like*. Ces cellules réminiscentes de l'embryo au stade 2-cellule (2C), se nomment *2C-like cells* (2CLC). De précédents résultats produits au laboratoire ont montré qu'une inhibition en amont de la biosynthèse de l'hème augmente l'expression de marqueurs *2C-like* dans les mESC. Ce phénotype n'est pas restauré par une supplémentation en hémine mais par le diethyl-butylmalonate (BM), qui inhibe le transport du succinate hors de la mitochondrie. Puisqu'il a été reporté que des métabolites pouvaient induire la reprogrammation *2C-like* des mESC, nous avons émis l'hypothèse que le succinate pourrait être impliqué dans ce phénomène. Nous avons démontré ici que l'atpenin A5 (AA5), un inhibiteur de la succinate déshydrogénase (SDH), peut provoquer une élévation des niveaux en succinyllysine dans les cellules and sur-réguler les marqueurs spécifiques des 2C à l'échelle des transcrits et des protéines, ce qui est reflété également par l'augmentation de la population des 2CLC ($ZSCAN^+$ et $MERVL^+$). Dans la recherche des mécanismes moléculaires sous-jacents à la reprogrammation *2C-like* associés à l'accumulation de succinate, nous avons tout d'abord investiguer son rôle dans la succinylation des résidus lysine. Par l'utilisation de SIRT7i, un inhibiteur d'une dessucinylase nucléaire, la sirtuine 7, nous avons observé qu'alors cet inhibiteur intensifie les niveaux nucléaires de pan-succinyllysine (Pan-SuccK), cela n'augmente pas la reprogrammation *2C-like*. Un autre rôle du succinate étant l'inhibition des dioxygénases dépendantes du 2-oxoglutarate (2OGX) ceci nous a incité à utiliser l'octyl-α-ketoglutarate (OAKG) qui prévient des effets de l'AA5. Trois 2OGX pertinentes ont été investiguées ici : la prolyl hydroxylase (PHD) liée à l'hypoxie, les histone déméthylases (HDM) contenant un domaine JMJC, et les 5-methylcytosine (5mC) déméthylase de la famille ten eleven (TET). Aucune implication d'HIF-1α dans la reprogrammation *2C-like* n'a été montrée. Les rôles putatifs des HDM et des TET ont été explorées grâce à deux inhibiteurs spécifiques, JIB et C35, respectivement. Des analyses d'immunofluorescence ont montré que H3K4me3 et H3K27me3 sont enrichies lors du traitement à l'AA5 et aussi apparemment avec un traitement combinatoire usant de

JIB et C35. Ces résultats sont soutenus par l'augmentation du pourcentage des cellules ZSCAN$^+$ au sein de la population totale naïve chez les cellules traitées avec AA5, JIB, C35, ou JIB+C35, cependant cette augmentation ne s'avère pas significative. Malheureusement, même si une tendance est observée vers une réduction nucléaire du signal 5hmC dans les cellules traitées à l'AA5, aucune conclusion définitive ne peut être établie à propose des niveaux de méthylation de l'ADN. Tout cela nous permet donc de conclure que la reprogrammation *2C-like* des mESC naïves provoquée par l'accumulation du succinate est caractérisée par une activité déméthylase réduite agissant sur les histones et l'ADN, ce qui soutient une régulation métabolique du paysage épigénétique de l'état pluripotent des mESC.

Mémoire de master en biochimie et biologie moléculaire et cellulaire

Janvier 2022

Promotrice : Prof. Patricia RENARD, co-promoteur : Prof. Thierry ARNOULD,

Encadrant : Dr. Damien DETRAUX.

University of Namur
FACULTY OF SCIENCES
Secretariat of the Department of Biology
Rue de Bruxelles 61 – 5000 NAMUR
Phone : +32(0)81.72.44.18 – Fax : +32(0)81.72.44.20
E-mail : joelle.jonet@unamur.be – http://www.unamur.be

ETUDE DU RÔLE DU SUCCINATE DANS LA REPROGRAMMATION 2-CELL-LIKE DES CELLULES SOUCHES EMBRYONNAIRES MURINES NAÏVES

Louise FELLER

Summary

In the population of naïve murine embryonic stem cells (mESCs), primarily derived from the inner cell mass (ICM) of the mouse blastocyst, a subpopulation of cells spontaneously oscillates in and out a totipotent-like state. These cells, reminiscing of the 2-cell stage embryo, are called 2-cell-like cells (2CLCs). Previous results in the laboratory showed that upstream inhibition of the heme biosynthesis increased the expression of 2-cell-like markers in mESCs. This phenotype was not recovered by hemin supplementation but by diethyl-butylmalonate (BM), inhibiting succinate transport out of the mitochondria. Since metabolites have been previously reported to induce 2CL reprogramming in mESCs, we hypothesized that succinate could be involved in this phenomenon. We demonstrated here that atpenin A5 (AA5), an inhibitor of the succinate dehydrogenase (SDH), is able to provoke a rise in succinyllysine levels in the cells and to upregulate 2C-specific markers at transcript and protein levels, also reflected in the 2CLCs ($ZSCAN4^+$ and $MERVL^+$) population increase. Searching for the molecular mechanisms underlying the 2C-like reprogramming associated with succinate build-up, we first investigated its role in lysine residue succinylation. Using SIRT7i, an inhibitor of the nuclear dessucynilase sirtuin 7, we observed that while this inhibitor intensifies pan-succinyllysine (Pan-SuccK) nuclear levels in naïve cells, it does not increase the 2C-like reprogramming. Another role of succinate being the inhibition of 2-oxoglutarate-dependent dioxygenases (2OXs), this prompted us to use octyl-α-ketoglutarate (OAKG) that prevented AA5 effects. Three relevant 2OGXs were investigated here: the hypoxia-related prolyl hydroxylase (PHD), the JMJC-containing domain histone demethylase (HDM), and 5-methylcytosine (5mC) demethylase of the ten eleven (TET) family. No implication of HIF-1α in 2C-like reprogramming was shown. The putative roles of HDMs and TETs were explored by the means of two specific inhibitors, JIB and C35, respectively. Immunofluorescence analyses showed that H3K4me3 and H3K27me3 were enriched upon AA5 treatment and also seemingly when treated with a combination of JIB and C35. These results were supported by the increase of the percentage of $ZSCAN4^+$ cells in the naïve total population in AA5, JIB, C35, or JIB+C35-treated cells, although not significant. Unfortunately, even if a trend is observed for a reduced nuclear 5hmC signal in AA5-treated cells, no definite conclusion

can be drawn on the levels of methylated DNA. Together, this enables us to conclude that the 2C-like reprogramming of naïve mESCs following succinate accumulation is characterised by a reduced demethylase activity on histones and DNA, supporting a metabolic regulation of the epigenetic landscape of the pluripotent state of mESCs.

Master's thesis in biochemistry, molecular and cellular biologie

January 2022

Promoter: Prof. Patricia RENARD, co-promoter: Prof. Thierry ARNOULD,

Tutor: Dr. Damien DETRAUX.

REMERCIEMENTS

Je voudrais tout d'abord remercier l'ensemble de l'URBC de m'avoir accueillie en tant que mémorante, de m'avoir permis à produire ce travail d'un peu moins d'un an ainsi que de goûter une première fois au monde de la recherche scientifique académique.

Je tiens à remercier très fortement la Professeure Patricia Renard pour ses avis et relectures bienveillants, vis-à-vis de ce mémoire. De plus, elle a pu suivre mon évolution et ce, depuis ma toute première année en Biologie à l'Université de Namur. Elle a fait partie de ces professeurs qui je pense m'auront permis à valider mon choix à me diriger vers la Biologie. Et pour cela, je l'en remercie sincèrement.

Ensuite, je remercie l'ensemble des chercheurs et techniciens de l'URBC, et plus particulièrement Sébastien Meurant, qui en plus d'avoir produit les transects de la Figure 20, aura joyeusement égayé certains moments passés sur le bench de part des discussions pour le moins intéressantes.

Je tiens également à remercier Alexis Khelfi de l'URPHYM pour m'avoir fait prêt et formée à la technique du dot blot.

Et puis forcément, je souhaite souligner l'incroyable ribambelle de mémorants avec qui j'ai vécu ce mémoire haut en couleur. Chers Amandine, Coline, Inès, Laura, Lisa, Manon, Thomas, Youri, notre cohésion, notre bonne entente et nos différences nous auront soudés plus que jamais malgré nos très différentes personnalités. Ce mémoire vous est en partie dédié et j'espère que nos fous rires résonneront encore quelques temps dans les couloirs du 5^{e} étage. Je ne peux que vous souhaiter le meilleur quelques soient vos ambitions.

Plus personnellement, merci à mes parents, Nathalie et Didier, à mon frère, Florent, à ma grand-mère et mes cokotteurs, dont Charlotte, qui ont fait du peu de ce qui me restait de temps libre un réel support lors de ce mémoire.

Enfin et non des moindres… Merci à toi Damien, ou plutôt merci au Dr. Damien Detraux pour son encadrement jusqu'aux dernières minutes. Ta dévotion à me former à une myriade de techniques, à une réflexion poussée, à l'interprétation de résultats (pas toujours concluants) ainsi que ton énergie auront fait la qualité de ce mémoire. Je ne te remercierais jamais assez pour tout ce temps partagé au laboratoire, comme en dehors. De plus, j'espère que tu es fier de cet accomplissement. Ceci n'est pas un adieu mais un au revoir car je pense qu'on n'en a pas tout à fait terminé.

Ad astra per aspera.

TABLE OF CONTENTS

1. INTRODUCTION

Stem cells are very promising models as they enable applications in transplant and regenerative medicine, but also in fundamental research, such as disease modelling, drug discovery screening and developmental biology. To cite some examples, in 2014, two Japanese patients affected by age-related macular degeneration underwent autologous implantation of retinal pigment epithelial cells derived from induced pluripotent stem cells (iPSCs) priorly originating from skin fibroblasts, enabling patients to recover their sight (Mandai *et al.*, 2017). In regard to treat patients with vascular disorders and thanks to biocompatible 3-dimensional printing techniques, iPSCs have been derived into primary vascular smooth muscle cells in order to generate tissue-engineered blood vessel grafts. For now they have only been successfully implanted in rats (Gui *et al.*, 2016; Melchiorri *et al.*, 2016). Stem cells are also used as models to study human diseases thanks to cell reprogramming and differentiation *e.g.*, congenital heart defect (Zakariyah *et al.*, 2019), Parkinson's disease (Amano *et al.*, 2009), or organoids [reviewed in (Fatehullah, Tan and Barker, 2016; Lancaster and Huch, 2019)]. Moreover, stem cells organoids in combination with high-throughput analyses are suitable tools for drug screening applicable for uncountable disorders. Through the modulation of signalling pathways in dish-controlled differentiating iPSCs or organoids, the development of several tissues is also studied. This enables the generation of organoids offering a notable architectural fidelity with their *in vivo* tissue counterparts [reviewed in (Lancaster and Huch, 2019)]. Finally, an ultimate goal would be to fill up the lack of available organs destined for transplantation in human patients who cannot benefit from a donation in time.

1.1. Stem cells *per se*

By definition, stem cells are characterized by three features: self-renewal (these cells highly proliferate), clonality (colonies arise from a single cell) and the potency to differentiate in several cell types (Wobus and Boheler, 2005; Kolios and Moodley, 2012; Romito and Cobellis, 2016). These cells are generally classified either according to their origin or their differentiation potency.

1.1.1. Stem cells classified based on their origin

Following their origin, three main groups can be distinguished. Adult stem cells (ASCs) also named resident, somatic or tissue-specific stem cells, are originating from diverse tissues *e.g.*, bone marrow, intestine, adipose tissue, placenta, brain, muscle, etc. Within these tissues they are located in a microenvironment called niche, where conditions are adequate for their growth and maintenance. Most of the time these cells are quiescent but they can generate new mature tissue-specific cells to counteract cellular loss or injuries. Many studies have been focusing on this type of stem cells for regenerative medicine *e.g.*, treatment of cardiac and neuronal injuries, auto-immune diseases (*i.e.*, diabetes mellitus), etc. However, some challenges remain to be overcome such as failure of ASC-made grafts to survive

post-transplantation, their restricted availability in tissues, and their *in vitro* culture which might alter their repair abilities to enable cell proliferation. Unfortunately, no drastic functional improvement has been observed so far following transplantation on patients reducing their appeal for regenerative medicine use [reviewed in (Gurusamy *et al.*, 2018)].

To circumvent these flaws, the famous iPSCs have been stabilized as pluripotent progenitors by Takahashi and Yamanaka in 2006 thanks to the reprogramming of fibroblasts, owing to the expression of four factors, OCT3/4, KLF4, SOX and c-MYC, thereby named the OKSM factor cocktail (Takahashi and Yamanaka, 2006). Despite the fact that iPSCs may offer tremendous advances in the field of regenerative medicine, the unlimited proliferative capacities of these cells can be a double-edged sword because tumours could emerge from the transplanted iPSCs or even their iPSCs progeny [reviewed in (Yamanaka, 2020)]. Despite this, iPSCs offer the advantage of a high differential potential, reminiscent of the embryonic stem cells (ESCs).

Due to their natural potential, ESCs have received a lot of attention from the scientific community for their potential role in regenerative medicine. Their isolation from the mouse early embryo the first time in 1981 by Evans and Kaufman, and Martin teams raised a lot of hope in the scientific community (Evans and Kaufman, 1981; Martin, 1981). It is only seventeen years later that human embryonic stem cells (hESCs) were successfully stabilized (Thomson *et al.*, 1998). However, the use of hESCs raised lots of ethical issues concerning the use of human embryos while maintaining the risk for immune rejection (Yamanaka, 2020).

1.1.2. Stem cells classified upon cell fate potency

The main interest behind the use of stem cells is the generation of a wide spectrum of more or less committed cell lineages depending on their differentiation potential. Starting from the lowest differentiation potential, unipotent stem cells can only give rise to one unique differentiated cell type. Multipotent cells have the potency to differentiate into several cell types within one germ layer (Sobhani *et al.*, 2017). Then, cells owning the ability to generate progeny from all three germ layers (endo-, meso- and ectoderm lineages) are defined as pluripotent *e.g.*, iPSCs and ESCs. Stem cells with the highest potential are characterized as totipotent as a single cell, according to the stringent definition, can give rise to an entire organism, which means that it can generate the three embryonic layers and the extra-embryonic tissues (Baker and Pera, 2018; Genet and Torres-Padilla, 2020). Interestingly and so far, despite the remarkable perspectives that an *in vitro* totipotent model offers, no cell culture model of totipotency has been developed (Genet and Torres-Padilla, 2020).

A

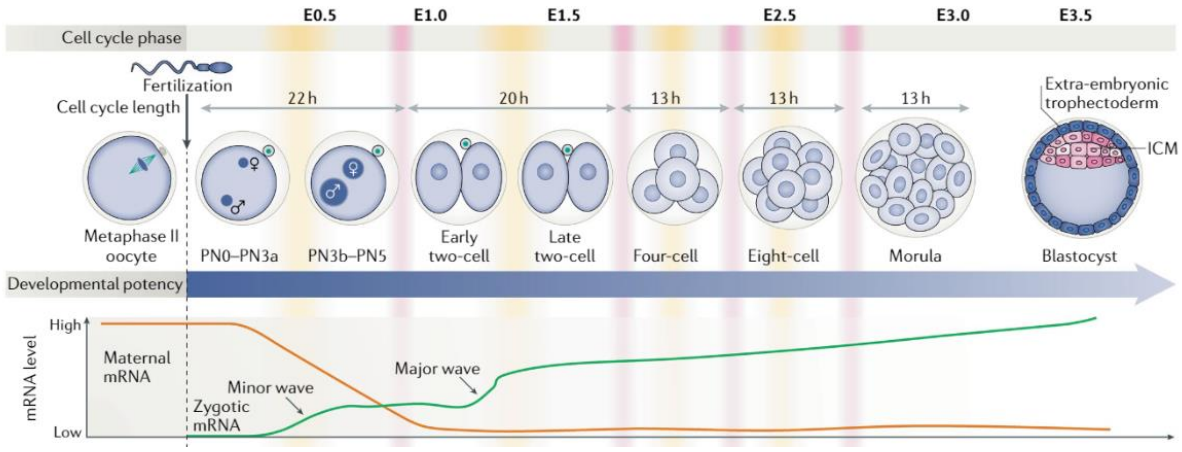

B

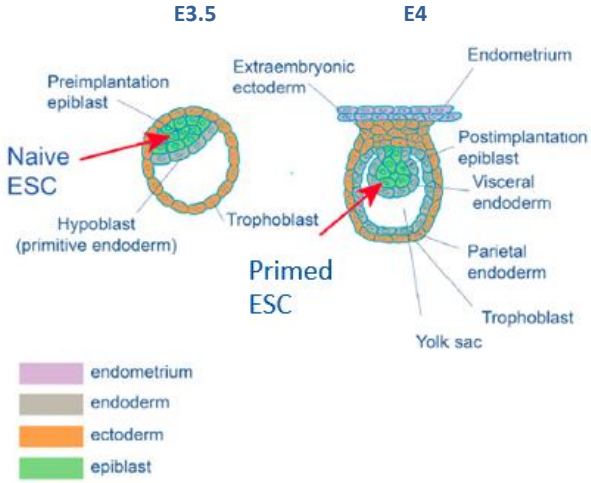

Figure 1. Schematic illustration of the early murine embryonic development.

(A) From fertilization to embryonic day 3.5. After the gametes fusion and the first division, the zygote undergoes around the 2-cell (2C) stage the zygotic genome activation (ZGA). Briefly, this corresponds to the timepoint when the developmental duty is passed on from the mother to the zygote. The ZGA occurs in two waves, the minor wave occurring in the male pronucleus (PN), and the major wave when 2C-specific genes such as *Dux*, *Zscan4*, and other retrovirus-like elements such as *MERVL*, are expressed due to chromatin decompaction events. In order to engender an entire organism, successive cell fate restrictions occur in the zygote. At first, the trophoblast and inner cell mass (ICM) lineages are discriminated from one another. The green line represents the ZGA, the orange line the maternal transcripts [adapted from (Eckersley-Maslin *et al.*, 2016)].

(B) Pre- and post-implantation stages. Before the implantation step, the ICM splits into the epiblast (or primitive ectoderm) and the hypoblast (or primitive endoderm). Naïve mESCs are primarily derived from the pre-implantation ICM whereas primed mESCs mirror the post-implantation blastocyst [adapted from (Baker and Pera, 2018)].

1.2. Development and totipotency

1.2.1. From the fertilized oocyte to the 2-cell stage embryo

Developmentally speaking, in the mouse embryo, only the zygote and the 2-cell (2C) stage blastomeres are strictly totipotent meaning that even a single cell can generate an entire embryo. It is not the case for 4- and 8-cell-stage blastomeres, unless they are in presence of supportive cells such as in tetraploid complementation assays (Wobus and Boheler, 2005; Nichols and Smith, 2009; Zhang *et al.*, 2016; Genet and Torres-Padilla, 2020). In this totipotent 2C embryo, the zygotic genome activation (ZGA) is a major event that occurs right after fertilization when the developmental duty is passed on from the mother to the zygote, coinciding with the depletion of the transcripts and proteins originating from the oocyte (Ko, 2016; Jukam, Shariati and Skotheim, 2017; Eckersley-Maslin, Alda-Catalinas and Reik, 2018). The ZGA is occurring in two waves that are distinguished by different expression profiles, the minor ZGA taking place before the second round of DNA duplication and the major ZGA happening after (Abe *et al.*, 2018). Expressed during the minor ZGA and regulating gene expression during the major wave of ZGA (Sugie *et al.*, 2020), the transcription factor (TF) DUX encoded by a double homeodomain gene (*Dux*) is considered as one of the pioneer TF and is associated with events of drastic chromatin relaxation observed during the ZGA **(Figure 1A)** (De Iaco *et al.*, 2017).

1.2.2. Epigenetic remodelling mediates the early embryonic development

As depicted in **Figure 2**, epigenetics play a substantial role during the development of the embryo enabling adequate gene network program activation towards the following developmental paths. After fertilization, most of the repressive marks of the pre-implantation embryo *i.e.*, methylated DNA, H3K27me3 and H3K9me3 are either absent or in an 'immature' state [nicely reviewed in (Xia and Xie, 2020)]. Some of these immature repressive marks at early embryo stages actually sometimes herald future epigenetic marks of the late embryo. For example, whereas it is generally considered as a repressive histone modification, *de novo* SUV39H1-deposited H3K9me3 is inconsistent with inactive expression in the 1-cell embryo and rather indicate future chromatin compaction later during the embryo development (Burton *et al.*, 2020).

This *primitive* chromatin state is underscored by relaxed and extensively open chromatin, active marks and compromised heterochromatin. Nonetheless, this permissive chromatin state is mirroring the events occurring during the ZGA. The activation of the zygote's genome around the 2C stage correlates with the transcription of retrotransposons *i.e.*, endogenous retroviruses (ERVs). Indeed, the repression of murine endogenous retrovirus with leucine tRNA primer (MERVL) retrovirus-like elements expression is transiently lifted during the pre-implantation 2C-stage because of chromatin decompaction (Peaston *et al.*, 2004). Another transposable element (TE) referred to as long-interspaced element 1 (LINE-1) is also activated in the pre-implantation embryo and it has been demonstrated that both its silencing or its forced activation negatively impacts further development (Jachowicz *et al.*, 2017). One

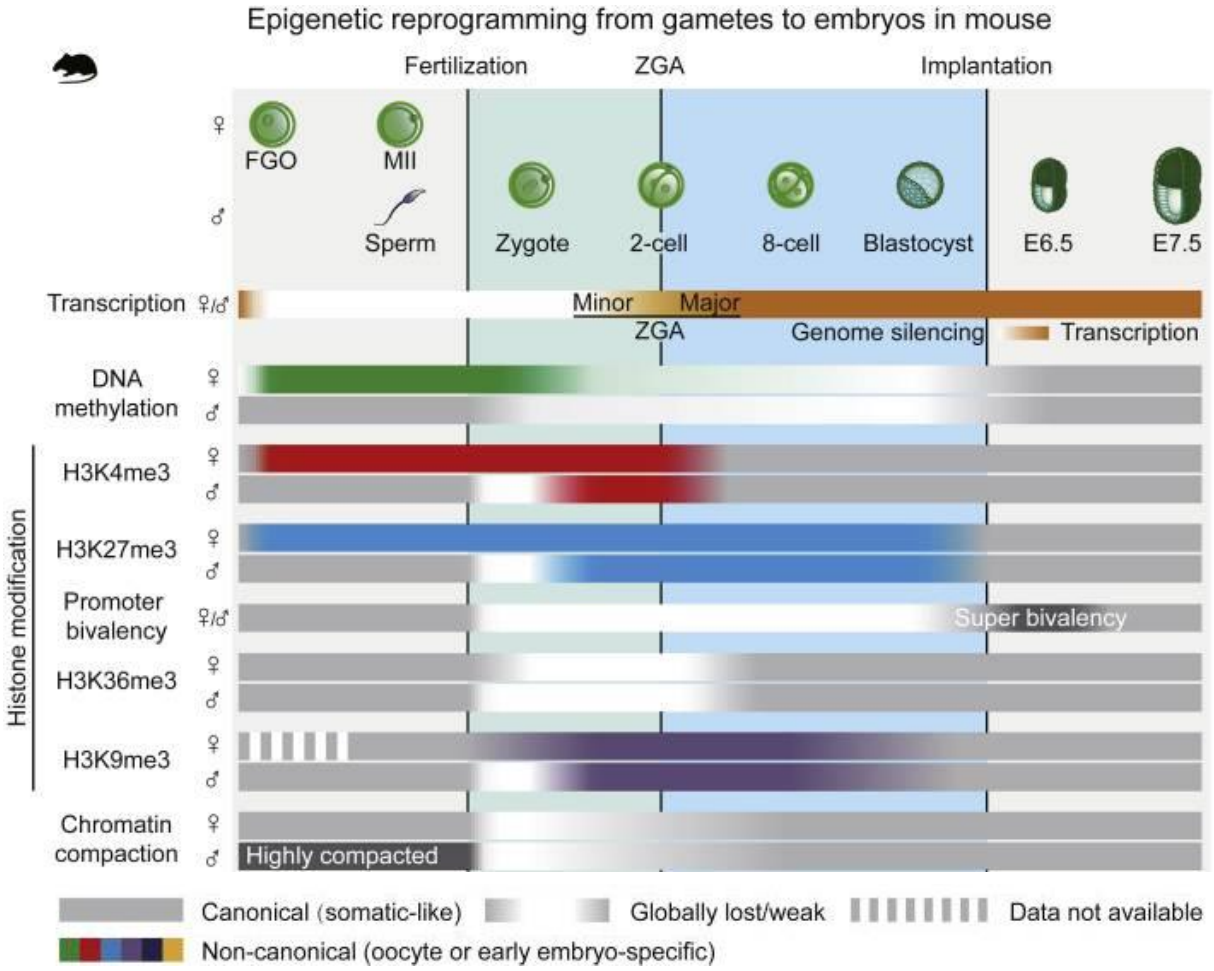

Figure 2. Epigenetic marks through the early murine development.

During the mouse early development, the genome is globally silenced starting from late mature gametes to the ZGA (zygotic genome activation). **DNA methylation**: in the gametes, DNA methylation is deposited in a transcription-dependent fashion in the oocytes and at both transcribed or not regions in the sperm. Following fertilization, DNA undergoes global methylation erasure ultimately restored around implantation. **H3K4me3**: after fertilization, the previous H3K4me3 in sperm is replaced by new broad H3K4me3 domains on the paternal allele. In the oocyte, H3K4me3 domains are broad and can be found also in a non-canonical form (ncH3K4me3), these imprints can be inherited partly by the embryo, except H3K4me3 at promoters. During ZGA, H3K4me3 on the maternal allele is remodelled into a canonical pattern. **H3K27me3**: H3K27me3 repressive marks are conserved upon the blastocyst and promoter H3K27me3 marks are only lately canonically re-established upon implantation. Similar to the H3K4me3, sperm H3K27me3 is substituted by broad *de novo* H3K27me3 regions after fertilization. **Bivalent promoters (H3K4me3/H3K27me3)**: at key developmental genes, the bivalency undergoes a fall at the pre-implantation stage, to reappear strongly at E6.5 to decrease at E7.7. **H3K36me3**: this histone mark is particular to transcribed genes and is first deposited in gametes to be erased post-fertilization and to be inscribed again after the ZGA. **H3K9me3**: typical of LTRs in gametes, the epigenetic mark undergoes a transient state towards the blastocyst stage. H3K9me3 is also specific to the embryonic lineages after implantation. In gray are canonical (somatic-like) patterns whereas colours represent non-canonical (specific to the oocyte or the early embryo). FGO, full-grown embryo; ZGA, zygotic genome activation [adapted from (Xia and Xie, 2020)].

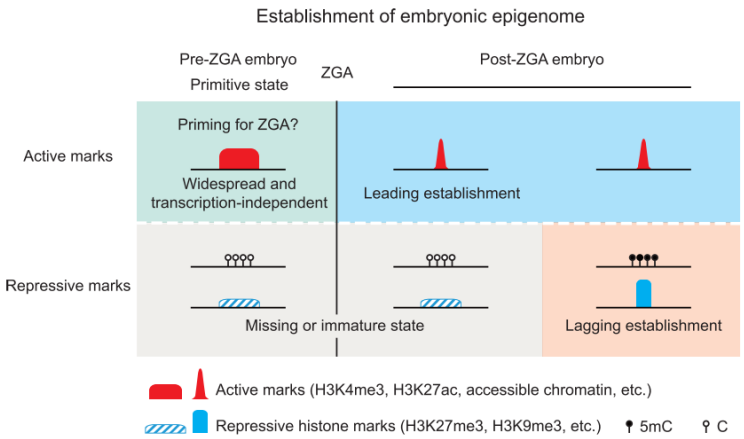

Figure 3. Establishment of the epigenome in mammalian early embryo. Before the ZGA, it is hypothesised that the embryo epigenome is in a primitive and transient state characterised by widespread and transcription-independent active histone marks, resulting into permissive chromatin, and by missing or immature repressive marks. Following the ZGA, the epigenome becomes more "mature", through rapid establishment of active marks ("leading establishment") and a slower instauration of repressive marks ("lagging establishment") occurring more progressively (Xia and Xie, 2020).

report hypothesized that LINE-1 inhibition impedes the ZGA because transcribed LINE-1 can recruit nucleolin/KAP1 for 2C-genes (*e.g.*, *Zscan4*, *MERVL*) repression through downregulation of *Dux* (Percharde *et al.*, 2018). So far, the role of TE activation during this developmental timing remains obscure. Nonetheless, it is hypothesized that from TE expression (*i.e.*, HERVK, human endogenous retrovirus K) results the synthesis of related viral-like particles that activate pathways that can counteract viral infections of human early embryos (Grow *et al.*, 2015).

Aside from TE expression, other transcripts are specifically expressed by the 2C embryo. The zinc finger and SCAN domain containing 4 (*Zscan4*) gene cluster encoding 6 paralog genes (*Zscan4a-f*) is thought to be involved in telomere elongation, thus in genomic stability in the embryo (Le *et al.*, 2021) and mESCs, as well as their self-renewal. In comparison with DUX that drives the ZGA, ZSCAN4 more likely reinforces the gene activation (Eckersley-Maslin *et al.*, 2019) [reviewed in]. The Krüppel-like factor ZFP352 from a family of zinc-finger containing transcription factors (TFs) is also specific of the 2C embryo but its function is yet to be understood (Pei and Grishin, 2013).

Throughout the ZGA, active epigenetic marks are also established. Among others, while broad non-canonical (nc) H3K4me3 are disappearing during the pre-ZGA phase when the chromatin is in its primitive state, canonical H3K4me3 marks are inscribed on CpG-rich regions of putative promoters during the ZGA. Canonical H2K4me2 and H3K27ac are deposited at specific enhancers and active promoters, respectively, during the ZGA **(Figure 2)** [reviewed in (Xia and Xie, 2020)].

Besides histones modifications, the DNA methylation landscape is also recognised before or during the ZGA. On the one hand, DNA methylation is written transcription-dependently during follicular growth in mouse oocytes, resulting on the methylation only of transcribed genic bodies (Sendžikaitė and Kelsey, 2019). On the other hand, methylation of the genome in sperm is unspecific to expressed genes (Hammoud *et al.*, 2014). After fertilization of the oocyte, a global DNA demethylation event occurs **(Figure 2)** (Smith and Meissner, 2013; Amouroux *et al.*, 2016).

Dynamically-speaking, after these drastic epigenetic modifications, all active marks patterns are readily established right after the ZGA. This fast instauration of activating epigenetic marks is referred to as *leading establishment*, that establishes active epigenetic marks that will drive the early embryo development transcriptional programs. On the flip side of the coin of the ongoing epigenetic regulations, repressive marks undergo a deposition known as *lagging establishment* that will occur later during the embryo development **(Figure 3)** [reviewed in (Xia and Xie, 2020)].

1.2.3. From the 2-cell stage embryo to lineage-specific commitment

Following this totipotent 2C stage and the ZGA, the embryo goes through successive divisions leading to the formation of a blastocyst, that later implants itself in the uterine wall and that concomitantly develops, ultimately leading to a whole organism. To pursue its developement, the blastocyst cells will undergo a number of cell fate decisions restricting its pluripotency. The first cell

fate decision occurs between the cells in the periphery and in the core of the morula **(Figure 1A)**. They respectively restrict their fate potency to the trophectoderm and the inner cell mass (ICM) lineages, the former giving rise to extra-embryonic envelopes such as the placenta. The latter, after the blastocyst implantation, develops into the embryonic ectoderm or epiblast, later becoming the embryo, and the primitive endoderm or hypoblast that will engender some layers of the yolk sac **(Figure 1B)** (Lu, Brennan and Robertson, 2001; Avilion *et al.*, 2003; Chazaud *et al.*, 2006; Mihajlović and Bruce, 2017).

1.3. *In vitro* culture of murine embryonic stem cells

To develop a pluripotent cell culture model, mESCs originally deriving from the murine early blastocyst ICM were first isolated in 1981 (Evans and Kaufman, 1981; Martin, 1981). This *in vitro* pre-implantation cell model is named *naïve*, as opposed to the post-implantation epiblast cells later isolated and termed *primed* **(Figure 1B)** (Nichols and Smith, 2009; Romito and Cobellis, 2016). The common feature of these two states is that they are grown in a suitable medium sustaining their self-renewal and their potency to differentiate.

1.3.1. LIF serum mESC cultures

Historically, naïve mESCs were first cultured in a medium constituted of foetal bovine serum and leukaemia inhibitory factor (LIF). Serum acts as an activator of proteins inhibiting differentiation . LIF binds to gp130 signal transducer receptors, known as LIF receptor, resulting into the activation of the JAK/STAT3 pathway, holding up the self-renewal capabilities of mESCs, thus impeding differentiation and promoting survival (Niwa *et al.*, 1998; Smith, 2001; Ying *et al.*, 2003). Serum LIF medium can sustain the stability of mESC cell lines yet not for all mice embryo strains (Nichols *et al.*, 2009). Subsequently, cells grown in serum LIF do not reiterate pre-implantation epiblast features *i.e.,* 5-methylcytosine (5mC) profile that is rather similar to post-implantation embryo and somatic cells (Kinoshita and Smith, 2018), unless an inhibitor of the mitogen-activated protein kinase (MAPK)/extracellular-signal-regulated kinase (ERK) kinase (MEK) pathway is added (Q. L. Ying *et al.* 2008).

1.3.2. 2iL medium mESCs and ground state

For maintaining mESCs more alike to the ICM but also due to encountered batch-to-batch variability of serum, two additional inhibitors referred as *2i* are added to LIF, resulting into *2iL*. These inhibitors act on the MEK and the glycogen synthase kinase 3 (GSK3β) pathways. MEK inhibitors, such as PD0325901, prevent mESCs differentiation whereas GSK3β inhibitors, like CHIRON (CHIR99021), activate the canonical WNT signalling favouring self-renewal (Batlle-Morera, Smith and Nichols, 2008; Wray, Kalkan and Smith, 2010).

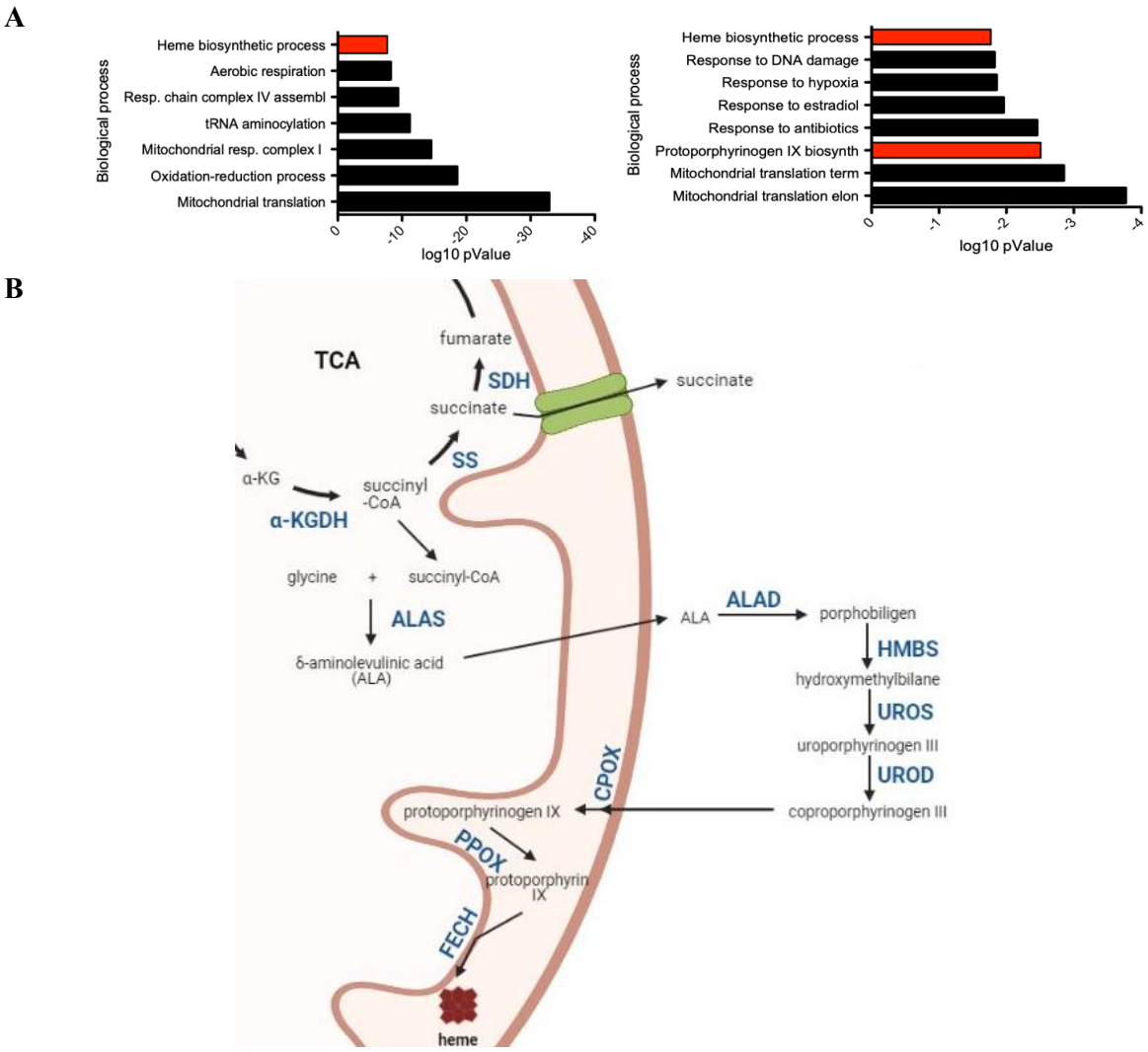

Figure 4. The 2-cell-like reprogramming of naïve mESCs is heme-independent but might involve the succinyl-CoA/succinate couple.

(A) Heme-related biological processes are critical for the naïve-to-primed transition of mESCs. Biological processes gene ontologies (GO) enrichment of two CRIPR-Cas9 screening studies conducted in hESCs (Mathieu *et al.*, 2019) on the left, and in mESCs (Li *et al.*, 2018) on the right, with the aim to highlight essential genes for the naïve-to-primed transition (Detraux *et al.*, submitted manuscript).

(B) The heme biosynthesis pathway drains succinyl-CoA from the TCA cycle. Schematic representation of the heme biosynthesis pathway and the TCA (tricarboxylic acid) cycle at its upstream. Glycine and succinyl-CoA are first condensed into δ-aminolevulinic acid (ALA) by the aminolevulinate synthase (ALAS) in the mitochondrial matrix. The following steps of the synthesis occur in the cytosol where ALA converted into porphobiligen by the δ-aminolevulinic acid dehydrogenase (ALAD), then into hydroxymethylbilane thanks to the hydroxymethylbilane synthase (HMBS), into uroporphyrinogen III by the uroporphyrinogen III synthase (UROS), into corproporphyrinogen III by the uroporphyrinogen III decarboxylase (UROD). The coproporphyrinogen oxidase (CPOX) located in the intermembrane space of the mitochondria is taking in charge the following reaction resulting into the formation of protoporphyrinogen IX, then another enzyme located in the inner mitochondrial membrane, the protoporphyrinogen oxidase (PPOX), converts the metabolite into protoporphyrin IX into which ferrous iron is finally inserted by the ferrochelatase (FECH) to form the heme. SDH, succinate dehydrogenase; SS, succinyl-CoA synthetase; α-KGDH, α-ketoglutarate (α-KG, or 2-oxoglutarate) dehydrogenase.

A

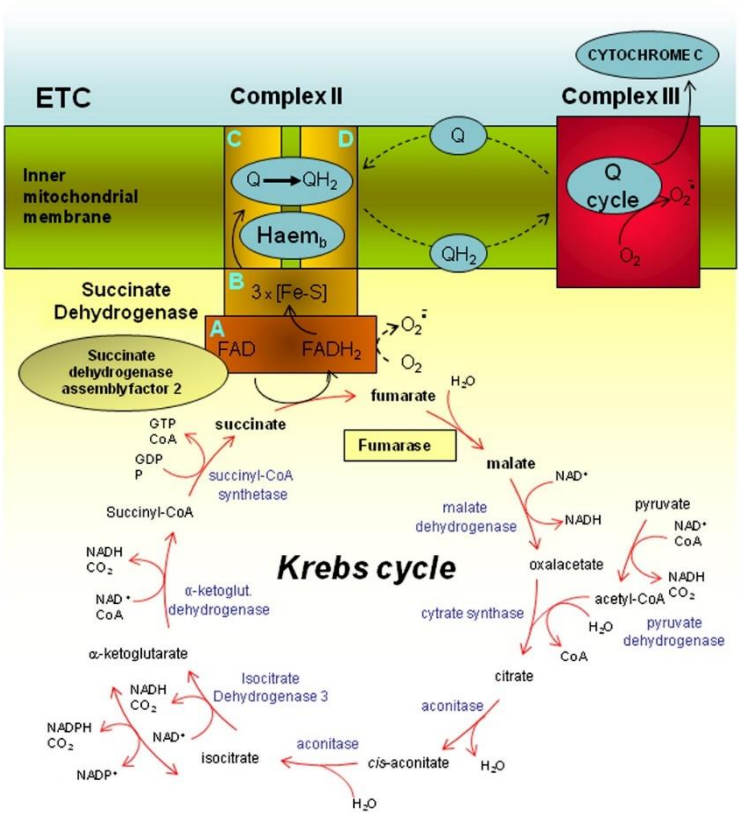

Figure 5. Succinate acts as a metabolite in cells, but not only.

(A) SDH known as complex II, couples the respiratory chain and the TCA cycle. The succinate dehydrogenase (SDH), also called complex II of the electron transport chain is embedded in the inner mitochondrial membrane (IMM) thanks to its two subunits SDHC and SDHD. Between these two subunits is found a heme b group. SDHA and SDHB are in charge of the catalytic activity of the complex. Coupled with the flavin adenine nucleotide (FAD) reduction, succinate is oxidized into fumarate that are both metabolites of the Krebs cycle. The electrons reduced by the succinate are thus transferred via $FADH_2$ to three iron-sulfur clusters (subsequently, [2Fe-2S], [4Fe-4Fe] and [3Fe-3S]), to be finally donated to the ubiquinone (Q) that is mobile in the IMM. Electrons can be then conveyed to the third complex of the respiratory chain (Bardella, Pollard and Tomlinson, 2011).

Remarkably, mESCs grown in a serum-containing medium exhibit more permissiveness in their cell fate compared to 2iL medium mESCs (Macfarlan *et al.*, 2013; Hackett and Azim Surani, 2014; Baker and Pera, 2018). Nevertheless, compared to cells grown in LIF serum that bear heterogeneity, 2iL mESCs are more controlled and are therefore designated as a *ground state* showing no restriction to further differentiate into all three embryonic lineages. The ground state is characterized by its epigenetic and molecular features like the double activation of the X chromosomes in female cells and a ERK pathway independence (Bao *et al.*, 2009; Nichols and Smith, 2009).

1.3.3. Heterogeneity within mESC population and 2-cell-like cells

Intriguingly, as mentioned especially for the LIF serum-cultured ESCs, heterogeneity has been observed in mESCs, as variable epigenetics and gene expression profiles were noticed amidst subpopulations of cells from the same colony (Šustáčková *et al.*, 2012; Macfarlan *et al.*, 2013). Interestingly, the emergence of subpopulations resembling the 2C-stage blastomeres has been reported among the naïve mESC populations, reaching from 0.5% up to 5% of the total naïve population (Romito and Cobellis, 2016). Enhanced histone mobility (Massagué, Seoane and Wotton, 2005), transcriptional and chromatin accessibility (Ye *et al.*, 2013; Itoh, Watabe and Miyazono, 2014), and scattered chromocenters (Romero-Lanman *et al.*, 2012) are molecular traits shared with the 2C embryo, closely related to its totipotent and pluripotent abilities thus called 2-cell-stage-like cells (2CLCs). This population is ZSCAN4-positive ($ZSCAN4^+$) and/or MERVL-positive ($MERVL^+$) and approximates between 0.5 to 5% of the global naïve population (Zalzman *et al.*, 2010; Macfarlan *et al.*, 2013).

1.4. Heme biosynthesis involvement in the naïve-to-primed transition

Initially based on the comparison of two CRISPR-Cas9 genome-wide knock out screening studies carried out on human ESCs (hESCs) (Mathieu *et al.*, 2019) and on mESCs (Li *et al.*, 2018), the genes required for the naïve-to-primed ESC transition were compared **(Figure 4A)**. This list of genes was analysed by the means of functional annotation tools. The top gene ontologies (GO) emphasized several biological processes, including the heme biosynthesis. At a first glance, such a result was intriguing in non-hematopoietic cells and suggested an important role for heme during the naïve-to-primed ESC transition (Detraux *et al.*, submitted manuscript).

1.4.1. mESCs naïve-to-primed transition is heme-dependent

Previous studies in the laboratory investigated the implication of the heme biosynthesis pathway in ESCs by the inhibition of the δ-aminolevulinic acid (ALA) dehydrogenase (ALAD) enzyme by succinylacetone (SA) **(Figure 4B)**. SA has been reported as a suicide substrate of the enzyme with a greater affinity compared to the initial ALAD substrate, the ALA. As SA and ALA structures are close

B

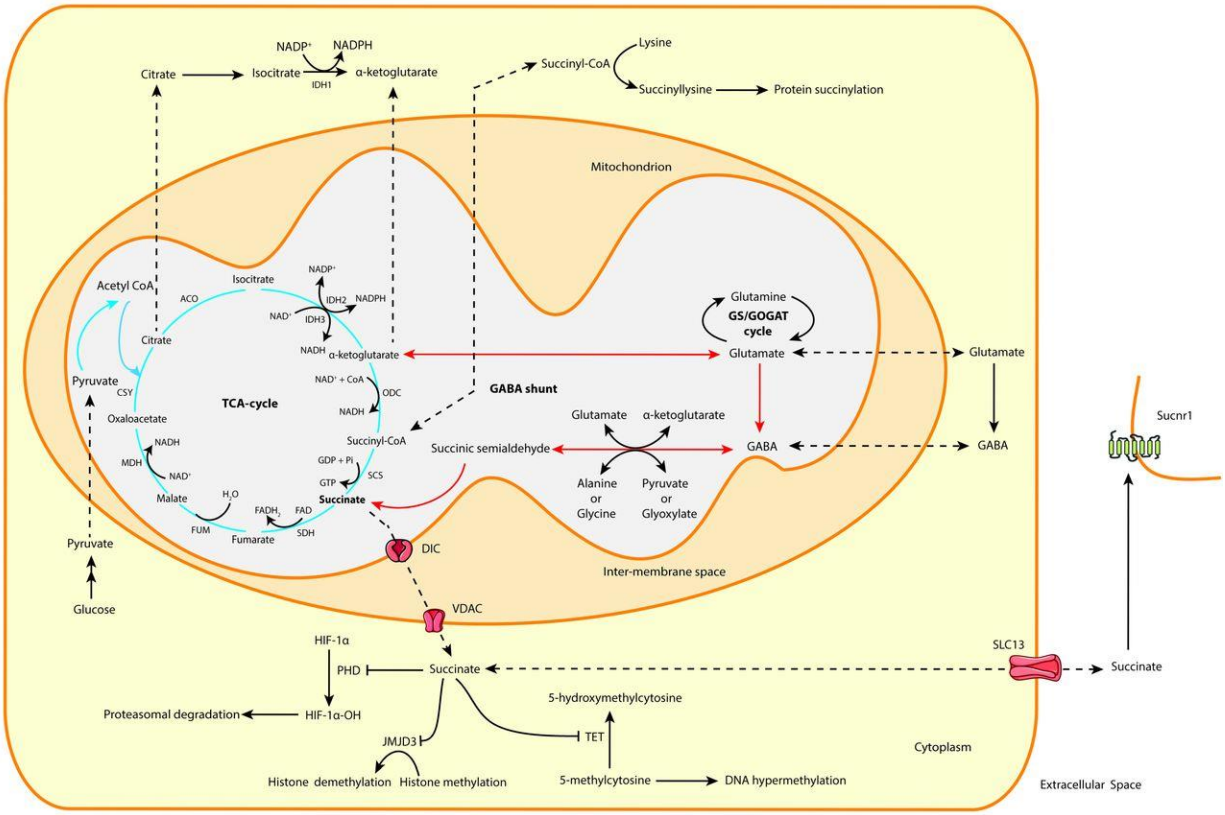

Figure 5. Succinate acts as a metabolite in cells, but not only.

(B) Succinate is located at a metabolic crossroad. Succinate is the product of the reversible of SCS (succinyl-CoA synthetase) reaction of substrate-level phosphorylation. Being part of the TCA cycle, succinate can be drained by other metabolic pathways such as the GABA (γ-aminobutyric acid) shunt but also heme biosynthesis, branched-chain amino acids and ketone bodies syntheses (not represented). In addition, succinyl-CoA can escape out the mitochondria to the cytosol through the DIC (dicarboxylate carrier, or SLC25A10) antiport located at the IMM and the VDAC (voltage-dependent anion-selective channel) at the outer mitochondrial membrane. DIC is sensitive to BM (butylmalonate) inhibition. Succinate can spontaneously succinylate proteins in different cellular compartments such as the cytosol and the nucleus provoking drastic mass and charge changes on the succinylated lysine residues. Also, as 2OG (2-oxoglutarate) is a cosubstrate for 2OGX reactions, succinate can impede such enzymes through product inhibition. As represented, the PHD (prolylhydroxylase) responsible for HIF-1α destabilisation and thus proteasomal degradation is sensitive to succinate inhibition. JMJD3-containing histone demethylases and TET 5-mC (5-methylcytosine) DNA demethylases are also prone to succinate inhibition which could result in important epigenetic modifications as these enzymes can remodel the cell epigenetic landscape (Tretter, Patocs and Chinopoulos, 2016).

to each other, it was suggested that the inhibitor binds the catalytic pocket of the enzyme instead of ALA (Sassa and Kappas, 1983). It was formerly demonstrated that the treatment of naïve mESCs with SA for 48h blocks their transition to the primed state. The global gene expression profile of naïve mESCs treated with SA for 48h largely differed from the control, and unexpectedly displayed an increase in the expression of 2C markers, suggesting an increase in the 2CLC population. Even more unforeseen, a supply of hemin does not prevent the observed phenotype on naïve cells, suggesting that the process might be hemin-independent (Detraux *et al.*, submitted manuscript). As supplementation with the end product does not rescue the phenotype, the upstream of the heme biosynthesis pathway must be investigated.

The synthesis of heme starts with the condensation of tricarboxylic acid (TCA) cycle-originating succinyl-coenzyme A (succinyl-CoA) and glycine by the aminolevulinate synthase (ALAS) resulting in the formation of ALA **(Figure 4B)**. This biochemical reaction finally yields 1 mole of tetrapyrrole ring out of 8 moles of succinyl-CoA and 8 moles of glycine. This 1:8:8 ratio is actually largely underestimated since a portion of porphyric by-products is excreted. This means that heme biosynthesis drains glycine from the mitochondrial pool, but also succinyl-CoA out of the TCA cycle (Atamna, 2004).

1.4.2. Succinate and the heme biosynthesis pathway

Detraux *et al.* have speculated that this inhibition of the heme pathway might results in a build-up in the succinyl-CoA/succinate couple, as it stands at a metabolic crossroad [reviewed in (Tretter, Patocs and Chinopoulos, 2016)]. In case of succinate accumulation within the mitochondrion, succinate way out of the organelle would be the dicarboxylate carrier (DIC), or SLC25A10, located in the inner mitochondrial membrane (IMM) **(Figure 5A)**. DIC has been shown to mediate inorganic phosphate (P_i)/dicarboxylate anion and dicarboxylate/dicarboxylate anions exchange, the dicarboxylic compounds being succinate, malate and malonate (Palmieri *et al.*, 1971). Furthermore, DIC is sensitive to 2-butylmalonate (BM) inhibition (Robinson and Williams, 1970). Strikingly, RT-qPCR conducted on mESCs treated with both SA and BM exhibit a prevention of the upregulation of 2C-like-specific markers, advocating that the 2C-like reprogramming of naïve mESCs is heme-independent but instead involve succinate (Detraux *et al.*, submitted manuscript).

As recently demonstrated by the team of Dr Torres-Padilla metabolites in mESCs can impact the emergence of 2CLCs. Dimethylsuccinate (DMS), a more cell-permeable form of succinate has been shown to enhance the 2C-like reprogramming in a concentration-dependent manner (Rodriguez-Terrones *et al.*, 2020). Subsequently, we hypothesized that succinate and succinyl-CoA molecules are potential actors of the emergence of 2CLCs subpopulation owing to their close relation with the heme biosynthetic pathway and several reasons discussed further below.

Besides being a metabolite of the TCA cycle, succinate is also at the metabolic crossroads of several pathways such as the branched-chain amino-acids, heme synthesis as explained before, ketone

bodies, or the γ-aminobutyric acid (GABA) shunt **(Figure 5B)** [reviewed in (Tretter, Patocs and Chinopoulos, 2016)].

In the TCA cycle, succinate, CoASH and ATP are produced out of succinyl-CoA, inorganic phosphate and ADP, during the reversible substrate-level phosphorylation reaction catalysed by the succinyl-CoA synthetase (Nishimura, 1986; Johnson *et al.*, 1998). Along the TCA cycle, the newly formed succinate is then oxidized by the next enzyme, succinate dehydrogenase (SDH).

The SDH or complex II of the ETC is a tetrameric complex embedded in the inner mitochondrial membrane (IMM) **(Figure 5A)** (Sun *et al.*, 2005). It is constituted of two hydrophilic subunits, SDHA and SHDB, which are respectively a protein containing a covalently-linked flavin adenine nucleotide (FAD) and an iron-sulfur (Fe-S) clusters-containing protein. Electrons are conveyed from the succinate via FAD, [2Fe-2S], [4Fe-4S] and [3Fe-4S] clusters to the ubiquinone (Hägerhäll, 1997; Sun *et al.*, 2005). These two first subunits are related to the oxidoreductive activity of the enzyme performing the reversible conversion of succinate into fumarate on the matrix side of the IMM (Tretter, Patocs and Chinopoulos, 2016). SDHC and SDHD are IMM-integrated subunits and achieve the anchoring of the complex in the membrane. A heme b group is inserted between the C and D subunits (Sun *et al.*, 2005), and appears to rather serve as an assembly factor than an electron carrier (Hägerhäll, 1997; Lemarie and Grimm, 2009).

1.5. Multiple roles of succinate

1.5.1. Post-translational succinylation

Besides its metabolic role, succinyl-CoA can be implicated in protein succinylation as a post-translational modification (PTM) on lysine residues **(Figure 5B)** [reviewed in (Chinopoulos and Valenti, 2021)]. The addition of a succinyl moiety represents a drastic change in the global charge of the lysine residues in comparison with acetylation or methylation that are commonly studied PTMs. At physiological pH, the lysine net charge shifts from +1 to -1 due to the two carboxylate groups of succinate. Moreover, this PTM induces a modification in the global mass, adding 100 Daltons (Zhang *et al.*, 2011; Weinert *et al.*, 2013).

Nowadays, the mechanism of lysine succinylation is still contentious as it is not clear whether it is enzymatically or non-enzymatically driven (Sreedhar, Wiese and Hitosugi, 2020). Succinyl-CoA could spontaneously succinylate lysine residues as it is a CoA-activated form of succinate. The enzymatic mechanism is thought to be performed by the means of a lysine succinyl transferase (KSTase). So far, three enzymes have been described with such activity: lysine acetyltransferase 2A (KAT2A), the carnitine palmitoyltransferase 1A (CPT1A) and the histone acetyltransferase 1 (HAT1). The latter, being the more recently discovered as KSTase, was previously identified in the context of

A

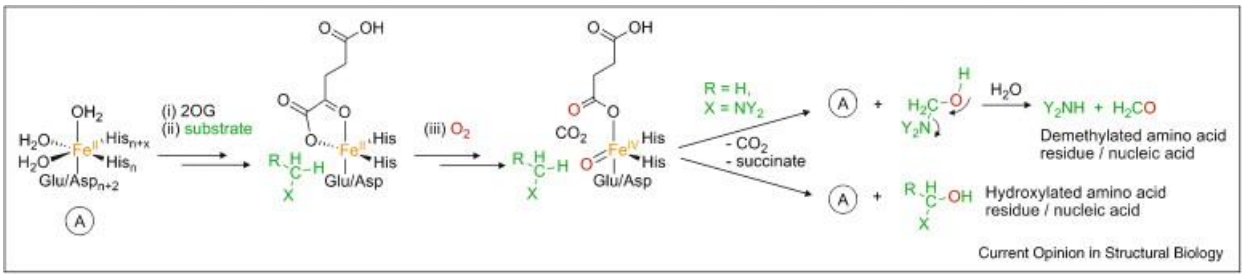

B1 **B2**

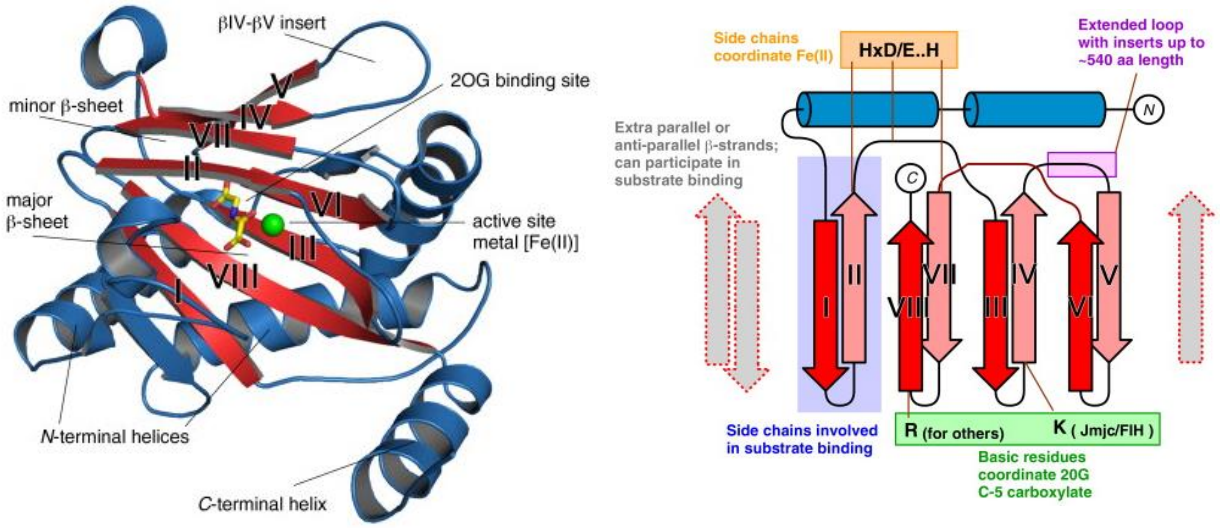

Figure 6. 2-oxoglutarate-dependent dioxygenases general features.

(A) Global hydroxylation reaction of 2OGXs. 2-OGXs (2-oxoglutarate-dependent dioxygenases) are able to catalyse the hydroxylation C-H bonds and *N*-demethylation through hydroxylation. The catalytic site contains a ferrous iron [Fe(II)] binding a *facial triad* motif (HXD/E…H), in addition of two coordination sites for 2-OG and water. The binding of the substrate of the enzyme releases water enabling the binding of oxygen, provoking the formation of a reactive Fe(IV)=O ferryl species. 2-OGXs being dioxygenases, one of the oxygen atoms of O_2 is incorporated into the substrate (R-H) through a step of oxidative decarboxylation of 2-OG. CO_2 is produced out of the C1 of 2-OG, as the second oxygen atom is incorporated, thereby forming succinate. α-Helixes at the C- and N- termini are most of the time in charge of substrate recognition and stabilization of the protein, respectively (McDonough *et al.*, 2010).

(B) 2-OGXs contorted fold forms a squashed *β*-barrel owning conserved Fe(II) and 2-OG binding sites. 1) Ribbon representation of a typical 2-OGX crystal structure (blue and red), metal (green sphere) and a non-reactive co-substrate analogue of 2-OG (yellow sticks; NOG, *N*-oxalyglycine). Double stranded *β*-helixes (DSBH) strands are numbered from I to VIII. Accessory elements commonly observed in these enzymes are labelled. **2)** Two-dimensional topology diagram using same colour code as (B).1 (McDonough *et al.*, 2010).

tumorigenesis as a histone acetyltransferase (Nagarajan *et al.*, 2013). HAT1 is able to succinylate histone and non-histone proteins, such as H3K122 and K19 of phosphoglycerate mutase 1 (PGAM1), resulting in upregulated gene expression and an enhanced enzymatic activity stimulating glycolysis, respectively, ultimately favouring the progression of tumours in HepG2 cancer cells (Yang *et al.*, 2021).

1.5.2. Desuccinylation by sirtuins

On the flip side of the coin, desuccinylation of the lysine residues is crucial for balancing protein succinylations. Sirtuins 5 and 7 (SIRT5 and SIRT7) were firstly detected as nicotinamide dinucleotide (NAD^+)-dependent deacetylases, and were soon attributed a desuccinylase activity (Du *et al.*, 2011; Li *et al.*, 2016). SIRT5 is mainly present in the mitochondria and/or the cytosol depending on the isoform (Matsushita *et al.*, 2011) whereas SIRT7 is found in the nucleus and active on histones. Its action is linked to genome stability and chromatin compaction (Li *et al.*, 2016). SIRT5 has been reported to desuccinylate the urea cycle carbamoyl phosphate transferase 1 (CPS1) as a SIRT5 knock-out augments the succinylation of CPS1, especially on the 1291 lysine residue (K1291) (Du *et al.*, 2011). Park *et al.* pointed out the presence of succinylated lysine residue (SuccK) sites on enzymes such as complex II's SDHA subunit, the pyruvate dehydrogenase complex (PDH) and the isocitrate dehydrogenase (IDH). Interestingly, SuccK sites were overlapping substrate and cofactor binding sites, suggesting a regulatory function over metabolism. Furthermore, SuccK sites have been correlated with other PTM sites mainly of lysine acetylation but also ubiquitination and malonylation (Park *et al.*, 2013). Acting as a histone desuccinylase, SIRT7 seems to be recruited dependently of poly(ADP-ribose) polymerase 1 (PARP1) at double strand break (DSB) sites and to desuccinylate H3K122, leading to chromatin compaction and DSB repair. Chromatin condensation and DNA repair is indeed altered in the case of SIRT7 knock-down (Li *et al.*, 2016).

1.5.3. Inhibition of 2-oxoglutarate-dependent dioxygenases

Besides the succinate role in PTMs, the metabolite is also involved in the inhibition of 2-oxoglutarate (2OG)-dependent dioxygenases (2OGXs) **(Figure 5B & 7)**. The first 2OGX that has been described is a procollagen prolyl hydroxylase (PHD) involved in collagen biosynthesis by hydroxylating lysine and proline residues (Myllyharju and Kivirikko, 2004). 2OGX enzymes are known to hydroxylate C-H bonds and also to demethylate *N*-methyl bonds (McDonough *et al.*, 2010). A feature of dioxygenases is the incorporation of two oxygen atoms into the substrates, in the case of 2OGX, one atom ends up in succinate and the second one in the hydroxylated resulting product (Welford *et al.*, 2005). Such catalytic activity requires a ferrous iron [Fe(II)] as cofactor and two cosubstrates, O_2 and 2OG further converted into CO_2 and succinate **(Figure 6)** (Hausinger, 2015).

Functionally speaking, 2OGX are implicated in metabolism *i.e.*, collagen and collagen-related proteins biosynthesis, lipid metabolism, nucleic acid repair, but also in oxygen level sensing, epigenetic regulation of transcription and protein biosynthesis (Islam *et al.*, 2018).

1.6. Prolyl hydroxylase and hypoxia-inducible factor 1α

Among the 2OGX enzyme family stands a group of PHDs, inhibited in hypoxia and regulating the HIF-1α subunit. HIF-1, the hypoxia-inducible factor 1 is composed of the constitutive β/aryl hydrocarbon receptor nuclear translocator (β/ARNT) and of the highly regulated α subunits (Wang and Semenza, 1995), the latter being determinant for the global protein activity. In the case of normoxia, HIF-1α undergoes hydroxylation of its 402 and 564 proline residues (Ivan *et al.*, 2001) by favouring HIF-1α von Hippel-Lindau (vHL) E3 ubiquitin ligase-dependent ubiquitination and its degradation by the proteasome **(Figure 5A)** (Maxwell, Pugh and Ratcliffe, 2001).

Apart from a regulation of its degradation, other 2OGX have been shown to regulate HIF-1α activity. As an example, the factor inhibiting HIF (FIH-1) protein, containing a Jumonji C (JMJC) domain (such enzymes being discussed later on) catalyses an asparaginyl hydroxylation on the 803 asparagine residue located in the C-terminal region of HIF-1α. Consequently, HIF-1α coactivators such as p300/CBP (CREB (cAMP-response element)-binding protein) histone acetyltransferase cannot interact with the protein, partially repressing target gene expression (Mahon, Hirota and Semenza, 2001; Kenneth and Rocha, 2008). However, contrarily to the PHDs, FIH-1 is less sensitive to succinate inhibition (Koivunen *et al.*, 2007).

The relation between succinate and hypoxia is actually reciprocal. Under hypoxic conditions, on the one hand, the ETC undergoes a build-up in reducing equivalents as a result of the lack of O_2, occasioning the accumulation of succinate due to a reverse electron transport. High levels of succinate and concomitant low 2-oxoglutarate (2OG) levels provoke a reduction in 2OG-dependent dioxygenases activity of PHDs (Selak *et al.*, 2005; Kluckova and Tennant, 2018). On the other hand, the deficit in O_2 as PHDs' substrate also alters their activity (Zhou *et al.*, 2012). Consequently, succinate accumulation and O_2 deprivation are thus stabilising the HIF-1α/β complex that can act as a transcriptional factor mediating the expression of genes related to hypoxia response (Selak *et al.*, 2005; Kluckova and Tennant, 2018).

In mESCs, it has been shown that hypoxia, thus HIF-1α stabilization, suppresses *Oct4* expression by the binding of HIF-1α to reverse hypoxia-responsive elements (rHREs) located at the promoting sequence of this pluripotency gene, thereby promoting mESC early differentiation (Lee *et al.*, 2012). Also, when mESC are left to spontaneously differentiate following LIF withdrawal, hypoxic conditions (1% and 5% O_2) did not prevent the downregulation of pluripotency markers (*i.e.,* OCT4, NANOG) (Binó *et al.*, 2016), suggesting once more that HIF-1α stabilisation favours the shift towards a differentiated state in ESCs. HIF-1α/β is indeed involved in the drastic metabolic changes happening during the naïve-to-primed transition. In hESCs, Sperber *et al.* demonstrated that HIF-1α gets stabilized upon the primed state due to increased repressive H3K27me3 marks on the promoter region of the

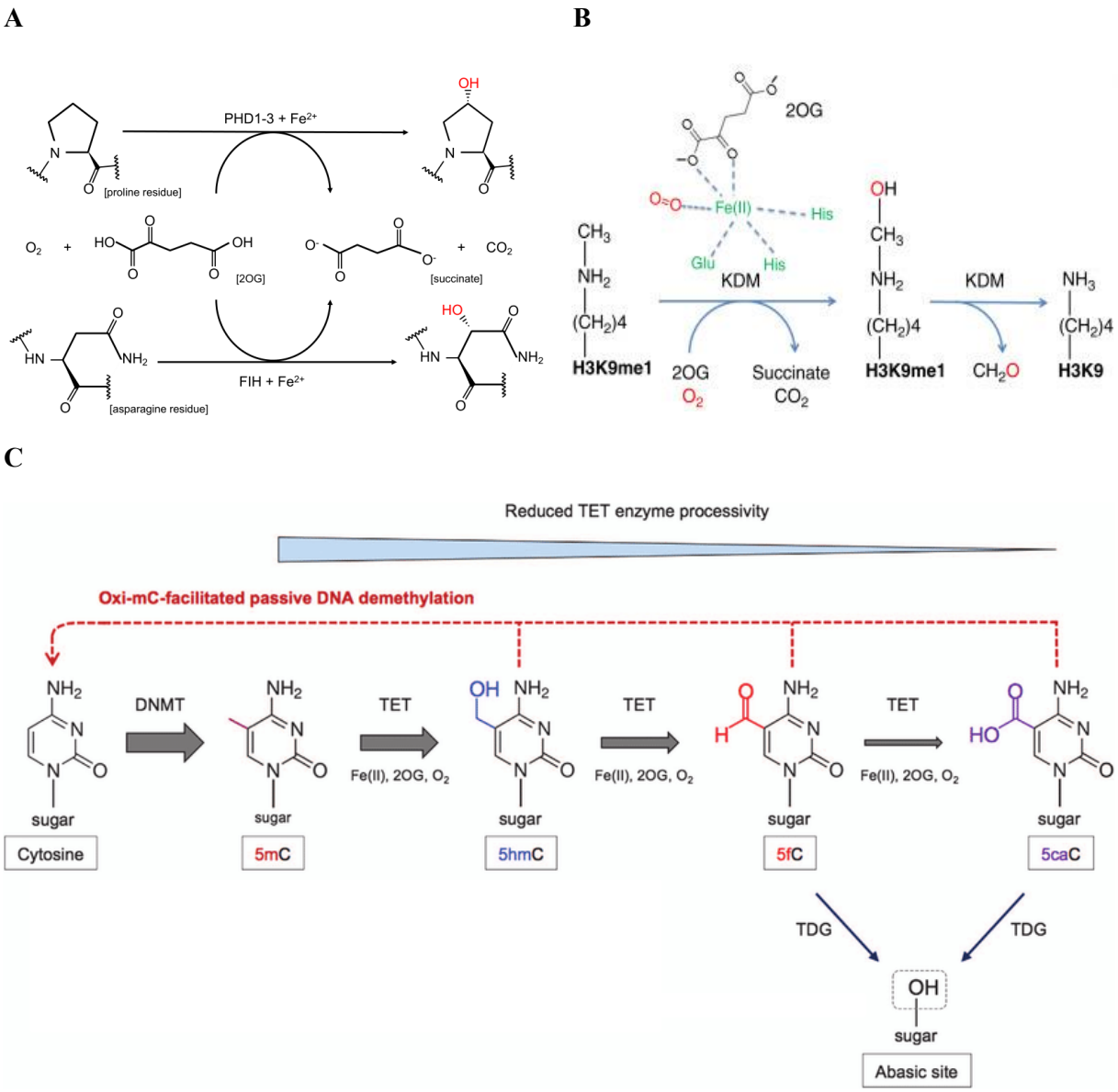

Figure 7. Global catalytic reactions of three types of 2OGXs.

(A) PHDs (prolylhydroxylases) hydroxylate HIF-1α (hypoxia-inducible factor 1α) on two of its proline residues (Pro402, Pro564), further causing HIF-1α proteasome degradation. FIH (factor inhibiting HIF) is a JMJC (Jumonji C) domain-containing dioxygenase and catalyses HIF-1α hydroxylation on an asparagine residue (Asn803), impairing interactions with HIF-1α co-activators (Strowitzki, Cummins and Taylor, 2019).

(B) HDMs (histone demethylases) demethylate lysine residues of histones by a two-step reaction; first, the hydroxylation of N^{ε}-methyllysine into a N^{ε}-hydroxymethyllysine intermediate, second, the intermediate is split into formaldehyde and a demethylated lysine residue (Bovee *et al.*, 2017).

(C) TET (Ten eleven translocation) 5mC (5-methylcytosine) demethylases can sequentially convert 5mC into 5hmC (5-hydroxymethylcytosine), 5fC (5-formylcytosine) and 5caC (5-carboxycytosine). TDG, thymine DNA (An, Rao and Ko, 2017).

hydroxylase domain-containing protein 2 (PHD2, encoded by *EGLN1*) inducing a downregulation of the protein and thus stabilizing HIF-1α. Thanks to a CRIPSR-Cas9 HIF-1α KO cell line, the author showed that HIF-1α is required for the primed transition (Sperber *et al.*, 2015). Another study conducted with mESCs proved that HIF-1α is an important regulator during the transition towards the primed state and also able to cause the observed metabolic switch (Zhou *et al.*, 2012). This role of hypoxia is in relation to the post-implantation *in vivo* embryo niche, embedded within the endometrium hypoxic environment (Lee *et al.*, 2001).

1.7. Jumonji C domain-containing histone demethylases

Other 2OG-dependent dioxygenases are the JMJC domain-containing histone demethylases (HDMs) that catalyse the demethylation of N^{ε}-methylated lysines of histone tails. Such demethylation occurs in two steps, *(i)* the N^{ε}-methyllysine is first hydroxylated into unstable intermediate being accompanied by the oxidation of 2OG and its decarboxylation then, *(ii)* the N^{ε}-hydroxymethyllysine is split into a demethylated lysine and formaldehyde (Ng *et al.*, 2007; Hopkinson *et al.*, 2010). Another characteristic of these histone demethylases is that they are able to demethylate mono-, di- and tri-methylated lysine residues by serial reactions **(Figure 7B)** (Klose, Kallin and Zhang, 2006).

1.7.1. Histone (de-)methylation

The methylation of lysine residues of histones is part of the now well-known post-translational modifications of these proteins that organize the genome. As a brief reminder, the DNA is a strictly organised entity within the cell nucleus (Schardin *et al.*, 1985; Hadlaczky, Went and Ringertz, 1986), entwined around the nucleosome complex made of histone 1 (H1), as known as the linker histone, and of a double set of histones (H2A, H2B, H3 and H4) (Oudet, Gross-Bellard and Chambon, 1975). 145 to 147 bp of DNA are twisted around one nucleosome, these protein complexes being scattered approximately every 200 bp along the genome (Kornberg, 1974). Due to their physical interaction with DNA, nucleosomes and their constituting histones are able to influence the access to transcriptional factors (Luger *et al.*, 1997) in order to regulate gene expression. In the context of development, PTMs such as acetylation, methylation, phosphorylation, ubiquitinylation, sumoylation, ADP-ribosylation, deamination (Kouzarides, 2007), propionylation and butyrylation (Kebede, Schneider and Daujat, 2015) of various histone residues can initiate and maintain transcriptional programs towards specific lineages (Shpargel *et al.*, 2014). However, histone methylation of lysine residues can be related either to activated or repressed gene expression (Santos-Rosa *et al.*, 2002; Klose, Kallin and Zhang, 2006).

Histone modifications are part of epigenetics regulation depicted at three levels **(Figure 8)**. First, the chromatin structure can be modified by *remodelers*, influencing chromatin accessibility of *trans*-factors to *cis*-elements [reviewed in (Quan *et al.*, 2020)]. Secondly, as cited previously, tail and core of

histones can be post-translationally modified, regulating transcription and other processes [reviewed in (Lawrence, Daujat and Schneider, 2016)]. Finally, DNA itself can be tagged by (hydroxy)methyl moieties on the fifth carbon of cytosine pyrimidine ring recruiting diverse complexes [reviewed in (Moore, Le and Fan, 2013)]. Both histone modifications and DNA (hydoxy)methylation can be either deposited by *writers* or removed by *erasers*, but also recognized and bound by *readers*.

Throughout early embryo development, drastic histone modifications occur **(Figure 2)**. Three histone marks draw literature's attention: H3K27me3, H3K4me3 and H3K9me3. To begin with, trimethylated H3K27, this mark usually reflects inactive gene expression, whereas monomethylation is associated with active gene promoters (Barski *et al.*, 2007). On the maternal allele, H3K27me3 at promoters of developmental genes is erased right after fertilization to be restored later during the blastocyst stage. In addition, distal H3K27me3 domains are maintained until implantation (Zheng *et al.*, 2016). On the paternal allele, following fertilization, sperm canonical H3K27me3 imprint is converted into broad non-canonical modified histone pattern (Xia and Xie, 2020).

H3K9me3, which is a repressive histone modification, rather tags promoters for future compaction in this case. A *de novo* deposition on both alleles of the embryo occurs post-fertilization, owing to SUV39H2 on the paternal allele (C. Wang *et al.*, 2018; Burton *et al.*, 2020). This H3K9me3 state is transient as it disappears around the 4C stage for the benefit of blastocyst-specific patterns and later on of lineage-specific patterns at gene promoters at E6.5 to 7.5 following implantation (C. Wang *et al.*, 2018). This histone modification is also linked to LTRs. Notably, MERVL after its activation during the ZGA is repressed around the 4C stage in parallel with an increase in methylation of H3K9, suggesting an action of the DNA replication-coupled histone deposition chaperone (CHAF1A) (C. Wang *et al.*, 2018).

Even if there is no transcription happening before the ZGA, *de novo* non-canonical broad and weak domains of H3K4me3 are inscribed on the paternal allele in gene-rich regions whereas the maternal imprint results from oocyte inheritance (Zhang *et al.*, 2016). Mechanistically speaking, this deposition could be enabled by the unusual permissive chromatin state and the temporary absence of epigenetic marks. It is speculated that such activating histone marks might favour an open chromatin and thus upcoming gene expression (Xia and Xie, 2020). Further on, while pre-ZGA typical broad H3K4me3 and relaxed chromatin is loss, canonical H3K4me3 is deposited at active promoters (Dahl *et al.*, 2016; Zhang *et al.*, 2016; Xia *et al.*, 2019). This removal of broad H3K4me3 is mediated by KDM5A (aka. JARID1A or RBP2) and KDM5B (aka. JARID1B or PLU-1) enabling canonical inscribing. KDM5A/B knockdown impairs ZGA and development to the blastocyst stage (Dahl *et al.*, 2016).

Interestingly, repressive H3K27me3 and active H3K4me3 marks were found nearby chromatin domains which are said to be *bivalent* that coincide with genomic regions of key developmental genes. Bivalent chromatin domains have been observed in the early embryo, ESCs, lineage progenitors and the

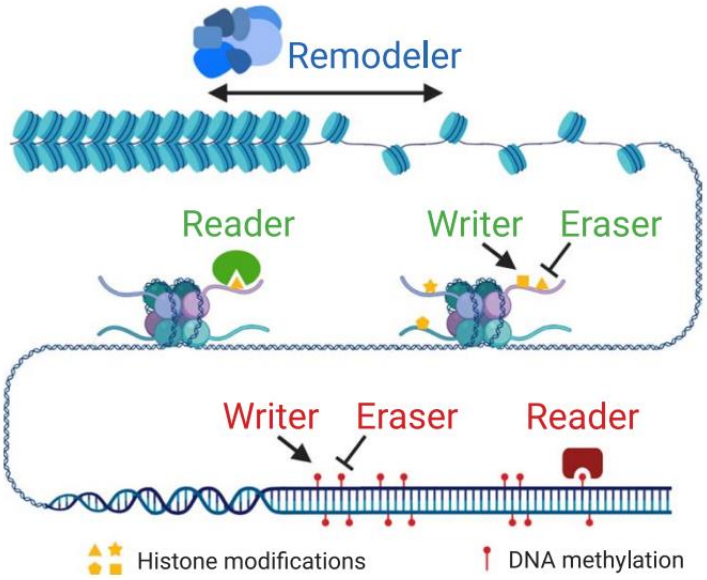

Figure 8. Basic epigenetic mechanisms modulating gene expression.

The epigenetic landscape of a genome is depicted at three levels. The 3-dimensional state of the chromatin can be changed by entities named remodelers. DNA methylation and histone post-translational modifications can be deposited by *writers* but also removed by *erasers*. *Readers* are able to recognize such marks and influence transcription (Cao and Yan, 2020).

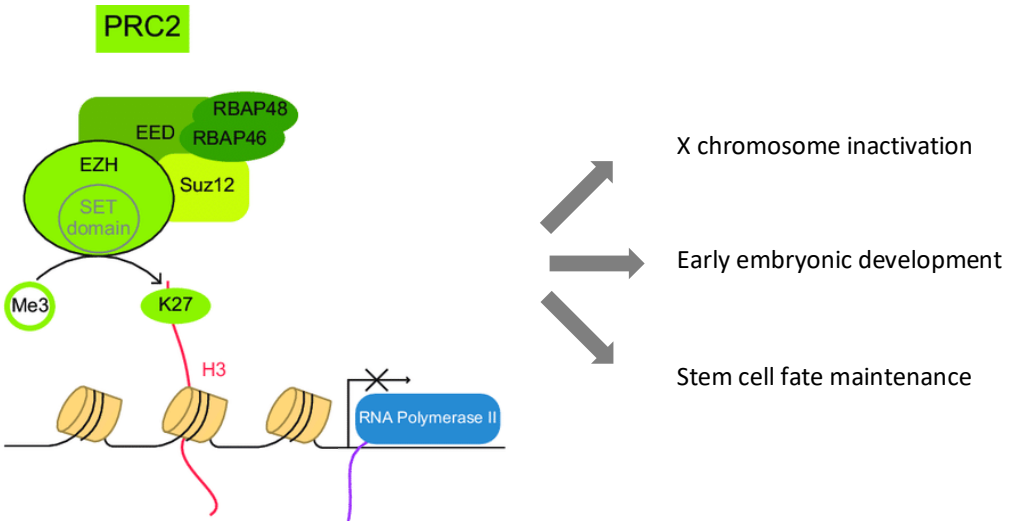

Figure 9. Schematic representation of the human EED-EZH2 complex.

The EED-EZH2 (Embryonic ectoderm development-Enhancer of zeste homolog 2) complex part of the PRC2 (Polycomb repressive complex 2) is a lysine 27 histone 3 methylator provoking DNA silencing. Several core proteins constitute this complex. EZH1 and especially EZH2 are in charge of the catalytic histone methyltransferase activity thanks to their conserved SET domain. This activity occurs in the proximity of two other subunits, EED and SUZ12. PRC2 is involved in X chromosome inactivation, early embryonic development and maintenance of pluripotency [adapted from (Vissers, Van Lohuizen and Citterio, 2012)].

germline, suggesting that the related genes are poised with the objective to reactively induce transcription accordingly to developmental necessities (Bernstein *et al.*, 2006; Mikkelsen *et al.*, 2007). However, this bivalency is absent during pre-implantation stages and rises at E6.5 in the epiblast (Xiang *et al.*, 2019).

1.7.2. H3K27me3

When it comes to epigenetic marks on histones, modifications on lysine 27 of H3 are deposited by protein complexes such as the Polycomb repressive complex 2 (PRC2) that inscribes trimethylation. The PRC2 (in *Drosophila*, ESC-E[Z], Extra sex comb-Enhancer of zeste; in human and mouse, EED-EZH2, embryonic ectoderm development-enhancer of zeste homolog 2) is an important chromatin modifier throughout the deposition of mono-, di- or trimethyl groups on histones (Laugesen, Højfeldt and Helin, 2019) and acts as silencer. The complex is constituted of core subunits being EZH1/2, EED, SUZ12 and RBBP4/7 **(Figure 8)** (Müller *et al.*, 2002). EZH2 possesses a conserved and 130-residue SET (SU[VAR3-9], Enhancer of zeste, trithorax) domain (Jones and Gelbart, 1993; Tschiersch *et al.*, 1994) suggesting a histone methyltransferase (HMTase) activity. EZH2 is a more efficient HMTase compared to its paralog EZH1. However, EZH2 requires to be in the vicinity of EED and SUZ12 subunits for its catalytic activity (Wu *et al.*, 2013). PRC2 is implicated in X chromosome inactivation, early embryonic development and maintenance of stem cell fate (Cao and Zhang, 2004; Morey and Helin, 2010). PRC2 has been demonstrated to be essential for embryonic development as mice embryos with mutated PRC2 stop developing at the gastrulation step (Cao and Zhang, 2004). In human and murine ESCs, PRC2-deficient cells can still proliferate but the complex is required for differentiation to late embryonic lineages (Chamberlain, Yee and Magnuson, 2008; Pasini *et al.*, 2010; Adam Collinson *et al.*, 2016).

Although, while writers like PRC2 deposit epigenetic repressive imprints on histones, other protagonists act as erasers of histone modifications. Methyl groups of H3K27me3 are actually erased through differentiation towards one of the three embryonic layers [reviewed in (Burchfield *et al.*, 2015)]. The active demethylation of H3K27me3 requires for example one of the three histone demethylases of the lysine-specific demethylase 6 (KDM6) family characterized by a catalytic JMJC domain: JMJD3 (KDM6B, autosomally encoded), UTX (KDM6A, X-linked) and UTY (encoded in the Y-chromosome). Nevertheless, the latter shows a decreased demethylase activity due to mutations located in the JMJC catalytic domain as compared to the corresponding UTX sequence, even though murine UTY shares 82% of homology with UTX (Shpargel *et al.*, 2012). Mutagenesis on mouse have demonstrated that *Jmjd3*$^{-/-}$ mutants show post-natal lethality owing to respiratory issues (Burgold *et al.*, 2012). Hemizygous *Utx*$^{-/y}$ males go through adulthood with a usual mouse lifespan. Homozygous *Utx*$^{-/-}$ females and hemizygous *Utx*$^{-}$*; Uty*$^{-}$ males have a lethal phenotype around the half of gestation and show developmental delays and a deficient cardiac development (Shpargel *et al.*, 2012), advocating a crucial implication of JMJD3 in mice development. *In vitro*, it was demonstrated that JMJD3 and UTX are

favouring naïve pluripotency (Carey *et al.*, 2015) and the maintenance of the stemness and the self-renewal capacity does not appear to be impaired in *Jmjd3*-deficient ESCs (Mansour *et al.*, 2012; Ohtani *et al.*, 2013). Moreover, KDM5 (or JARID1) is implicated into neural differentiation (Schmitz *et al.*, 2011).

1.7.3. H3K4me3

The team of J. Arne Dahl, thanks to a micro-scale chromatin immunoprecipitation and sequencing (μChIP-Seq) method they developed, achieved a genome-wide profiling of H3K4me3 and H3K27ac on immature and mature (metaphase II) oocytes, 2C and 8C-stage embryos. From this study, they concluded that around 22% of the oocyte genome is correlated with H3K4 trimethylation and the absence of DNA methylation, suggesting that H3K4me3 deposition might interfere with DNA methylation of the oocyte genome. In addition, H3K4me3 levels markedly fell in the 2C-stage embryos where this imprint is restricted to transcriptional-start-site (TSS) regions whereas in oocytes, H3K4me3 are mainly (~75%) further away from TSSs. In opposition, H3K27ac increases in the 2C embryo compared to the oocyte (Dahl *et al.*, 2016). Recently, H3K27ac has been proposed as a markers of enhancer regions, although it has not been shown to alter chromatin accessibility, transcription and self-renewal in mESCs (Zhang *et al.*, 2020).

In the oocyte, H3K4me3 is mainly deposited by the methyltransferase KMT2B, regulating chromatin modification on promoter-specific regions. KMT2B deficiency provokes oocyte apoptosis and failure to develop. Furthermore, this writer enzyme is necessary for functional ZGA (Andreu-Vieyra *et al.*, 2010). On the erasers' side, two H3K4 demethylases are shown to be highly expressed in 2C embryos; KDM5A and KDM5B. Depletion of these two demethylases in embryos results in high and conserved levels of H3K4me3 (Dahl *et al.*, 2016). During the mouse ZGA, occurs a switch from ncH3K4me3 to canonical H3K4me3, as mentioned previously. This results from the erasure of ncH3K4me3 by KDM5A/5B demethylases at untranscribed loci. This is advocated by KDM5A/5B KO causing high levels in H3K4me3 and downregulation of ZGA-related genes (Dahl *et al.*, 2016). KMT2B-dependent genes are upregulated in 2C- and 8C-embryos as broad non-canonical H3K4 trimethylation is erased. Likewise, a significant number of ZGA-specific genes get downregulated and almost all of the depleted embryos cannot develop towards the blastocyst stage (Dahl *et al.*, 2016). The loss of ncH3K4me3 is an outcome of zygotic transcription and overexpression of KDM5B, causing a downregulation H3K4me3 marks that engender shortcomings of genomic silencing. Accessorily, an overlap of ncH3K4me3 and partially methylated DNA regions has been noticed in the oocyte (Zhang *et al.*, 2016). Taken together, this illustrates an implication of KDM5A and KDM5B-mediated H3K4me3 removal during the ZGA.

Another histone demethylase, KDM1A, has been proven to silence MERVL expression in mESCs. However, the exact mechanism remains obscure because this HDM can target both H3K4me1

and H3K9me2 (Macfarlan *et al.*, 2011). Quite controversially, monomethylated H3K4 is related to active expression whereas H3K4me2 is associated with compacted chromatin and repressive H3K9me3. Nevertheless, H3K9me2 mark is the most suitable suspect as it is inscribed on MERVL locus and H3K4me1 is not (Sun *et al.*, 2021).

1.8. Ten eleven translocation cytosine dioxygenases

In the 2010s, 5-methylcytosine (5mC) demethylase family from the AlkB family known as Ten eleven translocation (TET) enzymes was identified as 2OGXs and is composed of three isoforms, TET1-3 (Tahiliani *et al.*, 2009; Ito *et al.*, 2010). TET enzymes acts as demethylases of 5mC through serial oxidations of the methyl moiety on CpG dinucleotides where the methylated cytosine is gradually transformed into 5-hydroxymethylcytosine (5hmC), 5-formylcytosine (5fC) and 5-carboxylcytosine (5caC) (Ito *et al.*, 2011). TET enzymes are constituted a catalytic double-stranded β-helix (DSBH) fold at their C-terminus containing an essential cysteine-rich domain (McDonough *et al.*, 2010). Moreover, TET1 and TET3 have CXXC zinc fingers that tightly bind unmethylated DNA **(Figure 9)** (Xu *et al.*, 2012). For the cytosine to entirely reach its initial unmethylated state, thymine DNA glycosylase (TDG) involved in DNA base-excision repair (BER) is able to excise either the carboxyl or the formyl group of the cytosine **(Figure 7C)** (He *et al.*, 2011; Maiti and Drohat, 2011).

TET1 and *TET2* expression is high in ESCs. TET1 appears to be related to 5hmC levels at promoter and TSS sites while TET2 is more likely responsible of 5mC enrichment in gene bodies and exon boundaries of active genes (Ito *et al.*, 2011; Huang *et al.*, 2014). Single and triple TET knockouts studies concluded that TETs are not essential for ESC maintenance while they are critical for ESC ability to differentiate and for normal embryonic development. More precisely, TET1 facilitate the reprogramming into a naïve state and triple TET KO impairs differentiation. Nevertheless, double KO of TET1/2 and triple KO provoke serious abnormalities through lineage differentiation (Dawlaty *et al.*, 2011, 2013, 2014; Lu *et al.*, 2014).

Beyond their catalytic activity, TETs can recruit chromatin modifiers as the *O*-linked β-d-*N*-acetylglucosamine (*O*-*N*-GlcNAc) transferase (OGT) (Vella *et al.*, 2013) that is involved in the viability maintenance of male mESCs and in the development of extra-embryonic tissues that requires paternal X chromosome inactivation (Shafi *et al.*, 2000). Furthermore, TETs also associate with SIN3 co-repressor complex (Williams *et al.*, 2011) that provokes transcriptional repression through histone deacetylation (Grzenda *et al.*, 2009). SIN3A has been emphasized to repress LINE-1 in a TET1-dependent manner (de la Rica *et al.*, 2016).

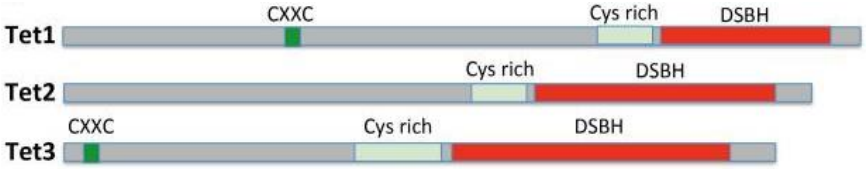

Figure 9. Schematic representation of constitutive domains of TET isoforms.

All three TET (Ten eleven translocation dioxygenases) isoforms share a catalytic DSBH (double-stranded β-helix) fold and a Cys-rich (cysteine-enriched) domain. TET1 and TET3 also have a CXXC zinc fingers that binds strongly to unmethylated DNA (Meng *et al.*, 2015).

A

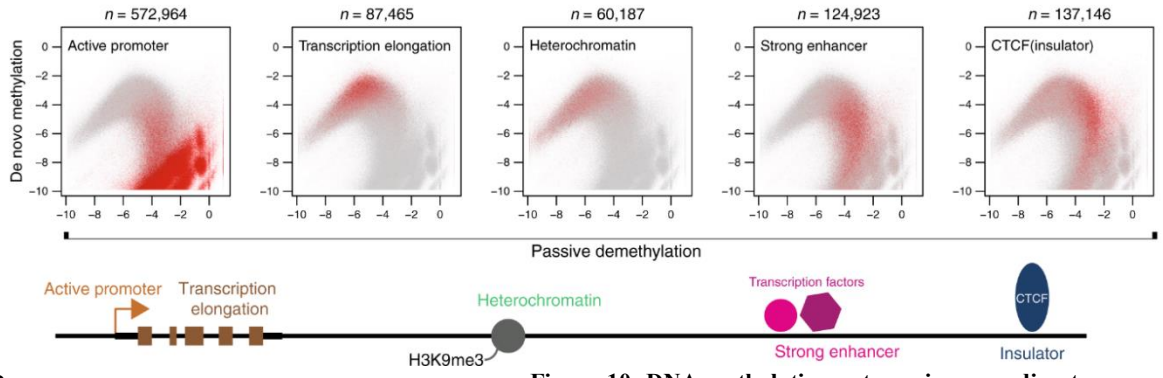

B

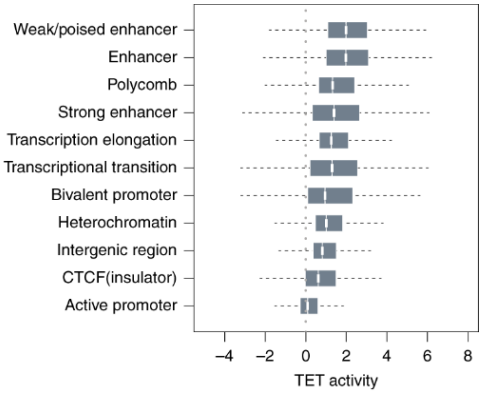

Figure 10. DNA methylation rate varies according to genomic context.

(A) Scatterplots of *de novo* methylation and passive demethylation for all cytosines in mESCs. Red dots represent CpGs that overlap with the indicated genomic annotation (*e.g.*, active promoter), *n* is the number of identified CpGs (Ginno *et al.*, 2020).

(B) TET activity levels are specific to the chromatin context. Genomic regions in mESCs are organised by decreasing mean change of TET activity. Boxes represent 50% of the data, the white line shows the median, whiskers represent the most extreme values comprised within the 1.5 times the interquartile range (Ginno *et al.*, 2020).

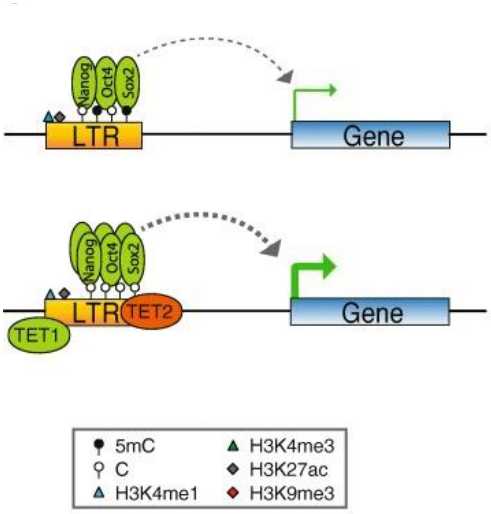

Figure 11. TET1/2-mediated enhanced expression of genes targeted by pluripotency transcriptional factors.

In mESCs, pluripotency-specific TFs (transcriptional factors) such as Nanog, Oct4 and Sox2 bind to TE (transposable elements)-derived enhancer LTR regions. The related genes of these enhancers undergo higher expression when TET 1 and 2 co-bind to the enhancer promoting activating 5mC demethylation (de la Rica *et al.*, 2016).

A **B**

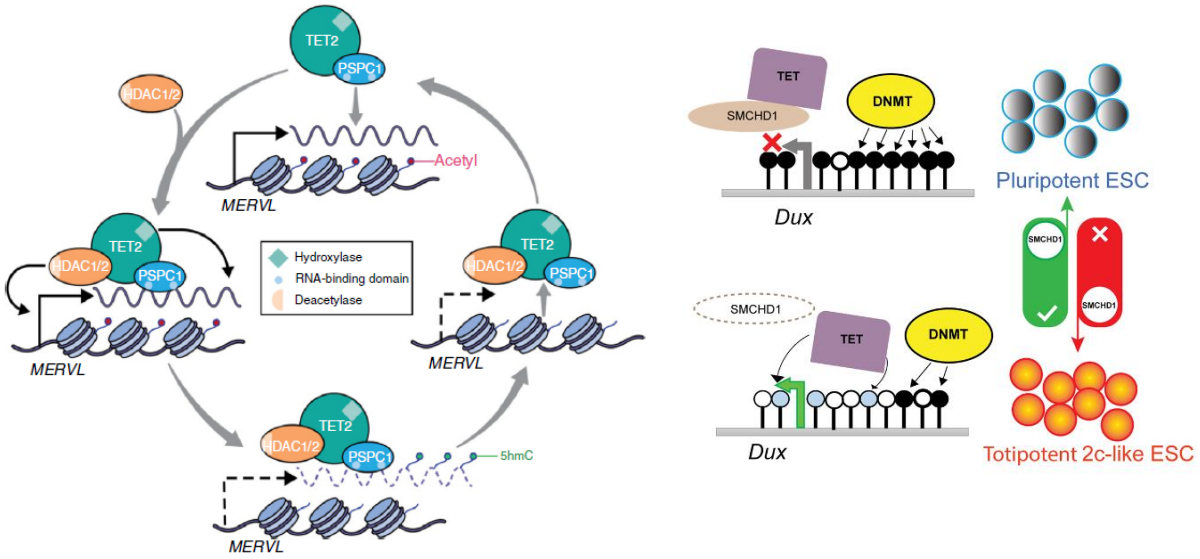

Figure 12. Models of TET-mediated regulation of expression in 2CLCs.

(A) *MERVL* expression TET2-dependent repression model. PSPC1 (Paraspeckle component 1), an RNA-binding protein, recruits TET2 (ten eleven translocation DNA demethylase 2) to the transcript of *MERVL*, with subsequent recruitment of HDAC1/2 (histone deacetylases 1 and 2) to the chromatin. This results in *i)* the hydroxylation of 5mC into 5hmC mediated by TET2, and *ii)* the HDAC1/2 deacetylation of acetyl histone marks. The two events provoke respectively the destabilisation of the transcript and the repression of expression at *MERVL* locus, leading to the release of the PSPC1/TET2/HDAC1/2 complex (Guallar *et al.*, 2018).

(B) SMCHD1 repression of TET-mediated *Dux* expression model. TET-mediated DNA demethylation activates Dux expression, thus promoting the emergence of 2CLC subpopulation in ESCs. However, the presence of SMCHD1 (chromosomes flexible hinge domain containing 1) at *Dux* promoter impedes the chromatin demethylation and concomitantly represses transcription. 5mC are represented in black circles, 5hmC in light blue circles and unmethylayed CpGs in white circles (Huang *et al.*, 2021).

1.8.1. 5-methylcytosine and 5-hydroxymethylcytosine

5mC is mostly found at CpG islands in somatic cells (Lister *et al.*, 2009) and is associated with gene silencing events and epigenetic imprinting such as X chromosome inactivation, silencing of repetitive elements, regulation of gene expression [reviewed in (Meng *et al.*, 2015)]. However, 5-cytosine methylation has been observed at other sites than CpG islands in iPSCs and in ESCs, where they were found at CpA and also less significantly at CpT sites (Ramsahoye *et al.*, 2000; Lister *et al.*, 2009). Strikingly, 70 to 80% of CpG-rich regions in mammals are methylated (Li and Zhang, 2014) and usually unmethylated CpG islands located near promoters are related to tissue-specific expressed genes in early embryos. Nevertheless, in female embryo these regions can be highly *de novo* methylated to ensure X chromosome silencing for dosage compensation (Wolf *et al.*, 1984).

Contrarily to 5mC, 5hmC [reviewed in (Shi *et al.*, 2017)] is associated with active gene expression due to its presence in active gene bodies, promoters and TF-binding sites. Additionally, TET1 has been noticed at transcription start sites (TSSs) possessing promoters with abundant CpG and being tagged by bivalent H3K27me3/H3K4me3 marks at poised genes in mESCs. This evokes the role of TET1 and 5hmC in expression regulation through the modulation of chromatin accessibility (Nestor *et al.*, 2012) and in association with bivalent histone marks epigenetic code. Indeed, TET1 forms a complex with PRC2 complex (an H3K27me3 writer) at bivalent regions (Neri *et al.*, 2013). Alongside with this, 5hmC was correlated with repressed expression in case of bivalent TET1/PRC2-cobound regions and with active expression at only TET1-bound promoters (Wu *et al.*, 2011), suggesting a potential action in pluripotent states switch (Shi *et al.*, 2017).

1.8.2. DNA (de-)methylation

Among DNA methylation events, a distinction is made between *de novo* methylation, accomplished by the DNA methyltransferases (DNMTs) 3A and 3B (Okano *et al.*, 1999), and methylation maintenance conducted by DNMT1 (Hermann, Goyal and Jeltsch, 2004). These effectors are required for functional mammalian development (Okano *et al.*, 1999). In accordance with their different N-terminal domains, DNMT3A and DNMT3B do not overlie their function as DNMT3A appears to imprint differentially methylated maternal regions whereas DNMT3B methylates pericentromeric repeated sequences and CpG islands on inactive X chromosome (Li and Zhang, 2014).

Contrariwise, demethylation can be due either to an incomplete post-replication maintenance (exercised by DNMT1), denoted as passive demethylation (Kagiwada *et al.*, 2013), or to active demethylation through the TET dioxygenases (Tahiliani *et al.*, 2009; Ito *et al.*, 2010). Passive demethylation is explained by the more unstable intermediates that are 5fC and 5caC compared to 5mC and 5hmC that are thus exercising epigenetic functions (Maiti and Drohat, 2011).

In a recent study, the authors managed to model de- and methylation kinetics of identified CpG sites in ESCs and they inferred that cytosines have a strikingly large variety in their methylation kinetics.

Additionally, the study revealed an overlap of context-specific genomic regions (*i.e.,* promoters, enhancers, insulators, transcribed genes) with specific methylation rate regimes **(Figure 10)** (Ginno *et al.*, 2020).

In mESCs, OCT4 and SOX2 have been shown to bind TF-binding sites of which 19.0% were embedded within an LTR-repeat TE (Bourque *et al.*, 2008). This suggests that evolutionary speaking, TEs have played a significant role in enlarging the collection of TF-binding sites in eukaryotes. Interestingly, pluripotency-specific TFs can co-bind with TET1 and TET2 to these TEs that act as enhancers. As a consequence, expression is boosted as a result of the TF binding to enhancing sequence and of the DNA demethylation mediated by the TETs **(Figure 11)** (de la Rica *et al.*, 2016).

TET is also known to control pluripotent states. Indeed, in mESC populations, triple TET KO have been reported to provoke expected rise in DNA methylation. Also, an upregulation of 36 out of 220 2C-specific genes in triple TET KO mESCs was observed as well as an increase in ZSCAN4^{+} cell subpopulation. Additionally, TETs are suspected to be involved in KAP1 binding to *MERVL*, repressing *MERVL* expression as well as 2C gene transcription in the vicinity. In parallel with *Zscan4* upregulation, triple KO mESCs cycle more frequently in and out the 2C-like state and show correlated features such as elongated telomeres. These observations support the idea of a TET-influenced 2C-like reprogramming of naïve mESCs (Lu *et al.*, 2014). In accordance, an interesting report suggested a model for TET2 regulation over *MERVL* expression. Paraspeckle component 1 (PSPC1) RNA-binding protein is suggested to bind the newly transcribed *MERVL* RNA ending up in the recruitment of TET2 and histone deacetylases 1 and 2 (HDAC1/2) to the chromatin. TET2 then destabilizes the *MERVL* transcript by the hydroxylation of 5mC into 5hmC. In parallel, HDAC1/2 remove the acetyl moieties on histones impeding *MERVL* transcription and ultimately provokes the release of the PSPC1/TET2/HDAC1/2 complex from the chromatin **(Figure 12A)** (Guallar *et al.*, 2018). This model favours the hypothesis that TET activity would antagonize the emergence of 2CLCs in naïve mESC populations.

In the opposite, an other model of DNA demethylation regulation presents a role of structural maintenance of chromosomes flexible hinge domain containing 1 (SMCHD1) in the expression of *Dux*. In this report, it has been demonstrated that SMCHD1-knockout in ESCs upregulates *Dux* expression owing to TET active demethylation of the gene promoter locus. As a consequence, SMCHD1 is thought to act as a shielding factor against the TET2 demethylase activity, engendering *Dux* repression. The negative effect of SMCHD1 observed on demethylation is suggested to be due either to a direct binding to DNA or its recruitment to heterochromatin, favouring *de novo* methylation instead of favouring methylation maintenance. This underlies a role of TET demethylation activity in the emergence of 2CLCs in global mESC population **(Figure 12B)** (Huang *et al.*, 2021), opposing the assumption made in this Master's thesis.

1.9. Succinate build-up impacting histone and DNA methylation

Because of the critical epigenetic landscape described here during early zygote and embryo development, succinate could have a significant impact on the epigenetic processes at that developmental timepoint, especially through its inhibition of 2OGXs. Indeed, in previous reports, histone demethylases (HDMs) and the ten-eleven translocation (TET) family of 5-methylcytosine (5mC) hydroxylases (TET1-3) have been shown to be inhibited by succinate and fumarate accumulation in neuroblastoma cells (Laukka *et al.*, 2016). In addition, in a context of tumorigenesis, a hypermethylated phenotype has been observed in two reports after the loss of SDH activity leading to succinate accumulation. This phenotype was the outcome of a competitive inhibition by succinate of the 2-oxoglutarate-dependent dioxygenases Jumonji domain-containing protein D3 (JMJD3) HDM and TET 5mC hydroxylases (Cervera *et al.*, 2009; Xiao *et al.*, 2012). The 2OG/succinate ratio is critical for HDMs and TET activity, and by consequence for a proper embryonic development. This role of the 2OG/succinate couple has also been highlighted in the differentiation of primed ESCs. 2OG seemed to maintain low DNA and histone demethylation levels, enhancing cell permissiveness through the differentiation of the primed cells (TeSlaa *et al.*, 2016). Even closer to the mESC model used in this Master's thesis, it has been shown that 2OG favours naïve mESCs self-renewal probably via DNA and histone demethylation (Carey *et al.*, 2015). Moreover, succinate (under its more permeable form, dimethylsuccinate) has been emphasized as capable to favour 2C-like reprogramming of naïve cells, an effect that is dependent on the metabolite concentration (Rodriguez-Terrones *et al.*, 2020).

1.10. Objectives

Provoking succinate endogenous accumulation through SDH inhibition

Detraux *et al.* results suggest that heme biosynthesis pathway inhibition leads to an increase in the 2CLC subpopulation within mESCs and that this might be an outcome of succinate build-up in the mitochondria, leaking to the cytosol (Detraux *et al.*, submitted manuscript). We thus decided to mimic this succinate accumulation although more directly, thanks to SDH inhibition.

To do so, we will use atpenin A5 (AA5), a specific inhibitor of SDH. This compound actually shows some structure similarities with the ubiquinone which receives electrons from the SDH complex. AA5 can substitute UQ at the UQ-binding site of the complex, resulting in its inhibition (Miyadera *et al.*, 2003). Preliminarily, AA5 will be tested to verify that this molecule does not alter naïve mESCs fitness by inhibiting the SDH as it is part of both the TCA cycle and mitochondrial ETC, both involved in cellular energy production. After that, we will confirm whether AA5-mediated inhibition of the respiratory complex II causes a noteworthy succinate accumulation within mESC mitochondria and a potential leakage of the metabolite to the cytosol.

Furthermore, if the effect is confirmed, the emergence either of 2CLCs or 2C-like features in the naïve cells treated with AA5 will be investigated.

Understanding the underlying mechanisms through which succinate build-up could engender a rise of 2CLC subpopulation in naïve mESCs

Once it will be demonstrated that succinate accumulation can enhance the 2C-like characteristics of naïve mESCs, we will focus on the potential mechanisms via which succinate could mediate such a reprogramming into 2CLCs.

Firstly, post-translation succinylation of proteins will be investigated. Indeed, it was previously shown that a knock-down (KD) of SDHB is intensifying lysine succinylation in the mitochondria and other cellular compartments, strongly suggesting a succinate accumulation and its leak out of the mitochondria to the cytosol and nucleus. These succinyllysines residues were also detected on chromatin proteins especially at active gene promoters, supporting the hypothesis that these succinylations turn on gene expression (Smestad *et al.*, 2018). We speculate that succinate cytosolic build-up will increase the succinylation of some targets that will mediate the 2C-like reprogramming in mESCs.

Alternatively, succinate inhibition of 2OGXs will be explored. Interesting connexions have been repeatedly reported in literature between pluripotency in mESCs and, PHD or HIF-1α (Zhou *et al.*, 2012; Laukka *et al.*, 2016), JMJC-domain-containing HDMs (Cervera *et al.*, 2009; Xiao *et al.*, 2012; Carey *et al.*, 2015; Sperber *et al.*, 2015; TeSlaa *et al.*, 2016) and TET DNA demethylases (Xiao *et al.*, 2012; Carey *et al.*, 2015; Laukka *et al.*, 2016; TeSlaa *et al.*, 2016). We will focus on whether an inhibition by succinate of these dioxygenases is sufficient to induce the 2C-like reprogramming.

2. MATERIALS AND METHODS

2.1. Tbg4 cell line

Tbg4 mESCs (kindly offered by Rodriguez-Terrones *et al.*, 2020) contain a turboGFP reporter construct (*2C*::3XturboGFP-NLS-PEST reporter) within the long terminal repeat (LTR) of Mervl and a neomycin resistance cassette conferring aminoglycoside antibiotics resistance such as geneticin (G418). 250 mg/µL G418 was used for *2C*::3XturboGFP-NLS-PEST reporter-containing cells selection.

2.2. Naïve mESCs culture

mESCs (ES-E14TG2a) were cultured on 0.2% porcine gelatin (Sigma, G1393)-coated plates in 2iL N2B27 medium composed of a 1:1 mixture of DMEM/F12 (Gibco, 31330-038) and Neurobasal Medium (Gibco, 21103-049), supplemented with 1x N-2 Supplement (Gibco, 17502-048), 1x B-27 Supplement (Gibco, 17504-044), 1:100 penicillin-streptomycin (Gibco, 15140-122), 1x MEM nonessential amino acids (NEAA) (Gibco,11140-035), 1x GlutaMAX (Gibco, 35050-038), 1x sodium-pyruvate (Gibco, 11360-039) and 0.1 mM β-mercaptoethanol (Gibco, 31350-010), and complemented with 1 µM MEK inhibitor (PD0325901) (SelleckChem, S1036), 3 µM GSK3 inhibitor (CHIR99021) (Peprotech, 2520691) and 10^3 U/mL of mLIF (ESGRO, ESG1107). Naïve mESCs were seeded at a 50,000 cells/cm²-density and were passaged every 2 to 3 days with accutase (Stemcell Technologies, #07920).

2.3. Naïve mESCs treatments

All inhibitors used in the Master's thesis are listed in **Appendix 1** where the abbreviation, name, reference and used concentration(s) are mentioned.

2.4. MTT

AA5 inhibition efficiency was semi-quantitatively determined by a MTT (3-[4,5-dimethylthiazol-2-yl]-2,5 diphenyl tetrazolium bromide) assay. Naïve mESCs were priorly plated and incubated for 2 days in 2iL medium treatment with SA, SABM 100 nM, 250 nM, 500 nM, 750 nM and 1 µM AA5, and AA5 and BM at the respective AA5 concentrations. 2.5 mg/mL MTT was added to the wells before a 2-hour incubation in a humidified incubated (37°C, 5% CO_2). Medium was discarded, pure sterile DMSO added and cells were incubated for 5 min at 37°C. After homogenisation, formazan crystals absorbance was read at 570 nm.

APPENDIXES

Appendix 1. List of inhibitors used for mESCs treatment.

Compound (abbreviation, name)		Target	Reference	Final concentration
SA	Succinylacetone	δ-aminolevulinic acid dehydrogenase	Sigma #D1415	0.5 mM
BM	Diethyl-butylmalonate	Dicarboxylate carrier	Sigma #112038	1 µM
AA5	Atpenin A5	Succinate dehydrogenase	Santa Cruz biotechnology #sc-202475	250 nM
SIRT7i	Sirtuin7 inhibitor 97491	Sirtuin 7	MedChemExpress #HY-135899	1 µM, 5 µM
JIB	JIB	Jumonji histone demethylases		250 nM, 500 nM
C35	TET-INH-C35	TET1-3		2.5 µM, 5 µM
$CoCl_2$	Cobalt chloride	Enables HIF-1α stabilization		100 µM

Appendix 2. List of antibodies used for immunofluorescence and western blotting.

Antibody	Reference	Species	Source	Dilution
Anti-IDH2	GeneTex #GTX628487	Mouse	IF	1:200
Anti-MERVL-GAG	Novus #NBP2-66963	Rabbit	IF	1:200
Anti-Oct3/4	Santa-Cruz #sc-5279	Mouse	IF	1:100
Anti-Pan-succinyllysine	PTM Bio #PTM-401	Rabbit	IF	1:300
Anti-Zscan4	Millipore Corp. #AB4340	Rabbit	IF WB	1:300 1:1,000
IRDye 680RD anti-mouse	LI-COR Biosciences #926-68070	Goat	WB	1:10,000
IRDye 800RD anti-rabbit IgG	LI-COR Biosciences #926-32211	Goat	WB	1:10,000
Anti-mouse Alexa Fluor 568	ThermoFisher #A11004	Goat	IF	1:1,000
Anti-rabbit Alexa Fluor 488	ThermoFisher #A11008	Goat	IF	1:1,000

Anti-dsDNA	Abcam #ab27156	Mouse	DB	1:1,000
Anti-5hmC	Active motive #AB_10013602	Rabbit	IF DB	1:250 1:2,000
Anti-H3K27me3	Active motive #AB_39157	Rabbit	IF WB	1:500 1:1,000
Anti-H3K4me3	Active motive #AB_39916	Rabbit	IF WB	1:500 1:2,000

Appendix 3. List of primers used for the qPCR.

Gene	**Sequence**	
DUB1	F: GCAGGCCAACCTCAAACAG	R: CGCAGGGCTCTCCTAAATCTT
DUX	F: AAAGGAAGAGCATGTGCCAGC	R: GCAGTAAGCTGTCCTGGGAAC
GAPDH	F: CATGGCCTTCCGTGTTCCT	R: CCTGCTTCACCACCTTCTTG
MUERVL	F: CCCATCATGAGCTGGGTACT	R: CGTGCAGATCCATCAGTAAA
OCT4	F: CACGAGTGGAAAGCAACTCA	R: AGATGGTGGTCTGGCTGAAC
TCSTV1	F: TGAACCCTGATGCCTGCTAAGACT	R: AGATGGCTGCAAAGACACAACTGC
ZFP352	F: AAGTCCCACATCTGAAGAAACAC	R: GGGTATGAGGATTCACCCACA
ZSCAN4C	F: CCGGAGAAAGCAGTGAGGTGGA	R: CGAAAATGCTAACAGTTGAT

2.5. Live/dead assay

LIVE/DEAD® Viability/Cytotoxicity Kit (L3224) from ThermoFisher was used. mESCs were seeded on Lab-Tek® at a density of 10,000 cells/cm² with 2iL medium. Lab-Tek® were coated before seeding with 3.5 µg/cm² Cell-Tak^{TM} (VWR, 734-1577) in 0.1 M $NaHCO_3$. After 2-day incubation (37°C, 5% CO_2), cells were treated with the kit according to the manufacturer advice before confocal microscopy observations (Leica TCS SP5 confocal microscope, Leica Microsystems). Micrographs for the counting were taken by an uninformed and neutral observer.

2.6. Immunofluorescence staining

2iL mESCs were plated on sterilized cover glass slips coated with 3.5 µg/cm² Cell-Tak^{TM} (VWR, 734-1577) in 0.1 M $NaHCO_3$ and were incubated for 2 days with SA, SABM, 500 nM AA5 and 500 nM AA5 BM. Cells were then washed with sterile PBS, fixated for 15 minutes with 4% paraformaldehyde (Sigma, 30525-89-4), blocked and permeabilized for 1 hour with 2% BSA containing 0.1% Triton. Fixed cells were incubated at 4°C o/n with a 30-µL drop containing the primary antibody diluted in BSA-Triton solution. After 5-minute BSA-Triton washes, cells were incubated in the dark for 1 hour with a 30-µL drop of the secondary antibody and DAPI (Sigma, 10 236 276 001). Before confocal microscopy observations, cover glasses were washed again with BSA and Triton solution to be assembled on microscope slides with pre-heated Mowiol. Confocal micrographs (Leica TCS SP5 confocal microscope, Leica Microsystems) were taken by an uninformed and neutral examiner. Used antibodies are listed in **Appendix 2**.

2.7. 5hmC immunostaining

This procedure is similar to the other immunostaining method mentioned previously in the PFA fixation step and the cover slip assembling. Following PFA fixation, cover slips were first permeabilized with 0.1% Triton X-100 for 10 minutes. Then, cells were treated with RNase for 2h and incubated at 37°C, before a 15-minute treatment with 4N HCl at RT. Cover slips were then rinsed with H_2O, before another 15-minute incubation but with 100 mM HCl at RT for dsDNA denaturation. This was followed by a PBS washing step and the blocking step (2% BSA-0.1% Twenn-PBS) lasting for 1H at RT. After that, the immunostaining was followed as already described. For the anti-5hmC antibody concentration, it is listed in **Appendix 2**.

2.8. Confocal micrographs analysis

2.8.1. ZSCAN4⁺/MERVL⁺ cells counting

ZSCAN4$^+$ and MERVL$^+$ cells were counted following the different treatments. The total number of cells were counted thanks to the FIJI Software (Schindelin *et al.*, 2012). The percentage of these sub-populations to the naïve mESCs global population was calculated.

2.8.2. Fluorescence intensity quantification

Pan-SuccK, HIF-1α, H3K4me3, H3K27me3 immunofluorescence signal intensities were quantified thanks to the FIJI Software (Schindelin *et al.*, 2012), by the use of the "Analyze particles" command on the DAPI channel micrograph, which data were saved into the region of interest (ROI) manager for a copy-paste on the other channel for measurements. The fluorescence intensities were corrected with background correction following this equation:

$$CTCF\ (corrected\ total\ cell\ fluorescence) = IntDen_{ROI} - (Area_{ROI} - Mean_{BG}),$$

where $IntDen_{ROI}$ is the integrated density of the ROI, $Area_{ROI}$, the area of the ROI and $Mean_{BG}$, the mean of the selected background.

2.8.3. 5hmC immunofluorescence intensity quantification

Transects were drawn on micrographs and quantified thanks to the FIJI Software (Schindelin *et al.*, 2012), by the use of the "plot profile" analysis that was added to the ROI manager and copy-pasted to the other channel of interest. The quantification has been assessed according to the following protocol, (Dunn, Kamocka and McDonald, 2011).

2.9. RNA extraction and RT-qPCR

RNAs were harvested and extracted using the ReliaPrep^{TM} RNA Tissue MiniPrep System (Promega) following the manufacturer's instructions. Samples RNA concentration and purity was quantified with Nanophotometer N60 (Implen). Retrotranscription was conducted by the means GoScript^{TM} Reverse Transcriptase kit Random Primers (Promega, A2801). qPCR was performed using 5 ng/µL of cDNA using SYBR Green GoTaq® qPCR Master Mix (Promega, A6002) and ViiA 7 Real-Time PCR system (ThermoFisher). Primer sequence of 2-cell-like markers are listed in **Appendix 3**. Murine *Gapdh* was chosen as endogenous control.

2.10. Western blot analysis

Cells were lysed with protein lysis buffer (20 mM Tris-HCl pH 7.5, 150 mM NaCl, 15% glycerol, 2% SDS, 25x protease inhibitor cocktail (PIC, Roche, 11697498001), 25x phosphatase inhibitor cocktail (PIB, constituted of 25 mM Na_3VO_3, 250 mM 4-nitrophenylphosphate, 250 mM β-glycerophosphate and 125 mM NaF), 1% Triton X-100, SuperNuclease (Sino Biologicals, 25 U/10 µL) by up-and-down pipetting motion. Protein content was assessed by Pierce 660 nm assay (ThermoFisher, 22660) and samples were prepared by mixing Laemmli buffer (SDS, β-mercaptoethanol and bromophenol blue) at 95°C for 5 minutes. 20 µg of proteins were loaded on 12% polyacrylamide gels. After electrophoresis at 200 V, 400 mA, proteins were transferred on PVDF membranes (IPFL00010) by Trans-Blot® Turbo™ Transfer System (Bio-Rad). Membranes were placed in LI-COR Intercept Blocking buffer PBS for 1h at RT. Membranes were then incubated with primary antibodies o/n at 4°C. After 3 consecutive 5-minute washes with PBS 0.1% Tween-20 (PBST), membranes were incubated for 1h with the secondary antibodies at RT. Membranes were scanned and protein abundance quantified with Amersham™ Typhoon scanner and software. Gapdh was used as endogenous loading control. Primary and secondary antibodies were incubated for 45 minutes for Gapdh detection. Used antibodies are listed in **Appendix 2**.

2.11. Flow cytometry

2iL or serum LIF Tbg4 line mESCs were suspended in PBS containing 2% FBS before flow cytometry analysis with BD FACSVerse™ Flow Cytometer (BD). The BD FACSuite Software was used for data acquisition. Data were analysed thanks to the same software and cells were gated following a 1.2×10^3 GFP signal.

2.12. Pull-down data analysis

A pull-down of succinylated peptides of 2il and SA-treated mESCs has been previously conducted in the laboratory and was followed by mass spectrometry analysis (Detraux *et al.*, submitted manuscript). Out of the identified peptides, proteins with a succinylation fold-change ≥1.5 were selected for GO cellular component analysis thanks to DAVID Annotation Tool (Huang, Sherman and Lempicki, 2009a, 2009b).

2.13. Dot blot

DNA was isolated and purified from mESCs plated in 6-well plates (50,000 cells/well) thanks to Promega Wizard™ Genomic DNA Purification kit (Promega, A1120) according to manufacturer advices. The following dot blot protocol was inspired from (Park and Kang, 2015). Genomic DNA concentration was then adjusted with distilled H_2O to 100 ng/condition for 75 µL. After that, 75 µL of 0.8 M NaOH and 20 mM EDTA buffer. DNA was then boiled at 100°C for 10 minutes. Samples were cooled down and DNA neutralized with 100 µL 2 M ammonium acetate (pH 7), vortexed, spined and kept on ice. PVDF membranes (IPFL00010) was activated in methanol for 1 minute and equilibrated in 6xSSC (pH7) buffer (0.5 M sodium chloride, 57 mM sodium citrate) as well as 3 Watman papers. Meanwhile, the Dot-Blot Apparatus (Bio-Rad, #1706545) was assembled. Once the whole manifold ready and the excess buffer from membrane and pre-soaked papers aspirated thanks vacuum, slots were rinsed with 1 M Tris-HCl buffer (pH 7.5) and EDTA (TE) solution. Then, DNA was placed in slots whereas empty slots were filled up with TE buffer, to finally be gently vacuumed. Slots were subsequently washed with 2xSSC (1.5 M sodium chloride,0.17 M sodium citrate). Once all the solutions were vacuumed, the manifold has been disassembled and the membrane baked at 50°C for 20 minutes. The membrane is then blocked in 5% non-fat dry milk TBS-0.1% Tween-20 for 1 hour. Following the blocking step, the membrane was incubated in the primary antibody at 4°C overnight. The day after, the membrane was washed three times for 5 minutes with TBS-T before to be incubated with secondary antibody at RT for 1 hour. The membrane underwent three 5-minute washes to be then let dry before scanning. After that, double strand DNA was also labelled on the membrane following the same procedure. **Appendix 2** contains a detailed list of used antibodies.

2.14. Statistical analyses

All statistical analyses were conducted on all results using GraphPad Prism version 6.0c for Mac OS X, GraphPad Software, San Diego, California USA, www.graphpad.com.

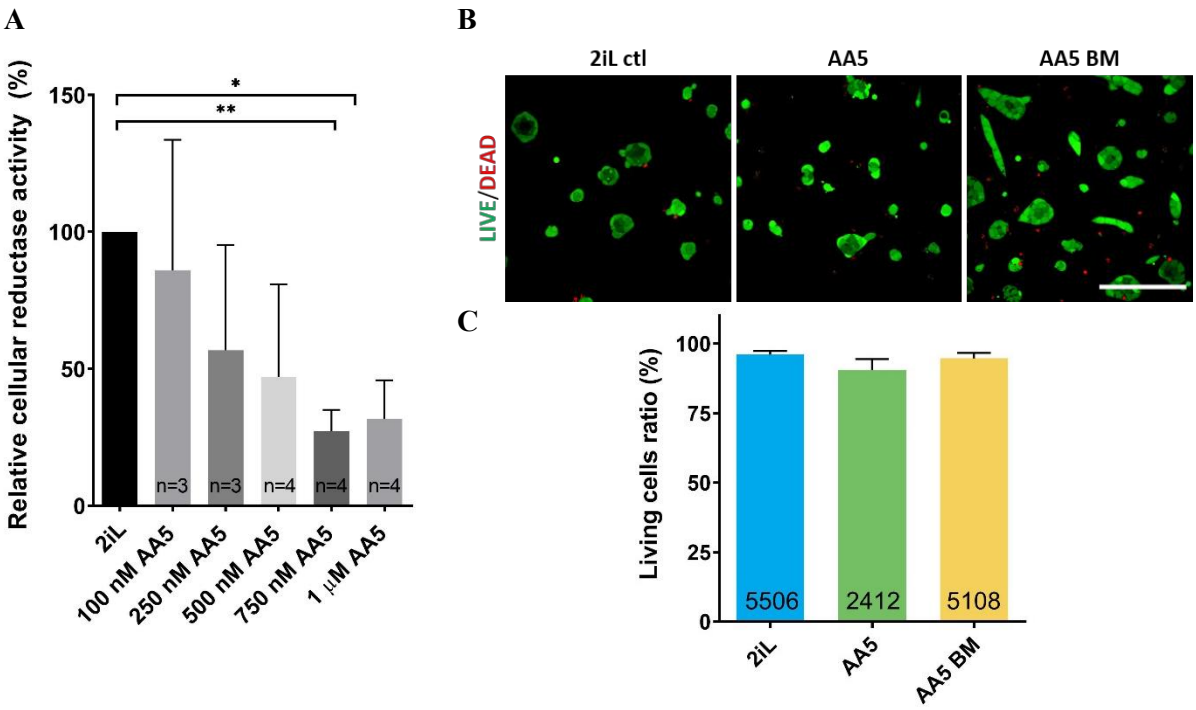

Figure 13. AA5 treatment does not alter naïve mESCs viability.

(A) Relative cellular reductive activity of 2iL mESCs exposed to various concentration of AA5 (100, 250, 500, 750 nM and 1 µM) assessed by a MTT assay carried out on n=3 or 4 independent biological replicates. Absorbance was read at 570 nm after DMSO-solubilisation and corrected to 2iL control condition. The MTT assay enables to measure cells global reductase activity thanks to their reduction of the water-soluble yellow tetrazole ([3-(4,5-dimethylthiazol-2-yl)-2,5-diphenyltetrazoliumbromide], or MTT) into DMSO-soluble purple formazan. All results are expressed as mean + S.D. One-way ANOVA was conducted, * $P < 0.05$, ** $P < 0.01$.

(B) Confocal micrographs representative of 3 independent replicates obtained with the live/dead assay with naïve 2iL mESCs treated with 500 nM AA5, AA5 and 1 µM BM. Living cells are labelled in green and dead cells in red. Scale bar=150 µm.

(C) Quantification of the proportion of living cells in 2iL control, 500 nM AA5, and 500 nM AA5 + 1 µM BM-treated naïve population. The total number of observed cells for each condition is indicated. n=3 independent biological replicates. All results are expressed as mean + S.D. One-way ANOVA was conducted, no results are significant.

3. RESULTS

3.1. AA5 can induce 2C-like reprogramming as SA

3.1.1. AA5 is not cytotoxic to naïve mESCs

As we hypothesized that AA5 is able provoke succinate accumulation due to SDH inhibition, we first assessed to which extent this molecule could alter naïve mESCs fitness and to select its working concentration. First, to investigate AA5 cytotoxicity in naïve mESCs, we conducted a MTT assay consisting in the reduction of a water-soluble yellow tetrazole ([3-(4,5-dimethylthiazol-2-yl)-2,5-diphenyltetrazoliumbromide], or MTT) compound by intracellular reductases, into DMSO-soluble purple formazan in living cells. Absorbance after DMSO-solubilisation is then read out at 570 nm (Mosmann, 1983; Kumar, Nagarajan and Uchil, 2018). A range of AA5 concentrations (100, 250, 500, 750 nM and 1 µM) was tested. Results show an expected decreasing cellular reductase activity as concentration increases **(Figure 13A)**. However, as phase-contrast microscopic observation of cells suggested intense cell stress after treatment with 750 nM and 1 µM of AA5, the concentrations selected for addressing cell viability did not exceeded 500 nM. It is not that surprising that a certain inhibition of the SDH is acceptable for naïve mESCs accounting their bivalent metabolism, flexible between glycolysis, pentose phosphate pathway and oxidative phosphorylation (Rodriguez-Terrones *et al.*, 2020).

To verify that 500 nM AA5 is not provoking any cell mortality in naïve mESCs, a live/dead assay was performed. Treated cells were exposed to a mixture of calcein-acetomethoxy (calcein-AM) that is labelling living cells as the AM group is cleaved by intracellular esterase activity, and ethidium homodimer-1 that can only stain dead cells that have lost plasma membrane integrity (**Figure 13B-C**). As the DIC transporter expelling succinate out of the mitochondria is sensitive to BM inhibition (Robinson and Williams, 1970), we also assessed the toxicity of the combined AA5+BM treatment. BM will be further used in order to prevent the phenotype induced by AA5. Results demonstrate very low cell death amongst the AA5-exposed mESCs, indicating that a 48h-treatment with 500 nM AA5 is not cytotoxic to the cells. However, due to some observable modifications of the cell morphology exposed to 500 nM AA5 especially with the double AA5-BM treatment **(data no shown)**, we opted for a working concentration of 250 nM that is thus by extension also not toxic to the cells.

3.2. AA5 provokes succinate accumulation in 2iL mESCs

To evaluate the extent of succinate accumulation in the different cell compartments after treatment with AA5, pan-succinyllysine residues have been labelled by immunostaining in naïve mESCs treated with AA5 in the presence or absence of BM, an inhibitor of DIC, the IMM transporter of succinate. SA is used as positive control since we previously showed that heme synthesis inhibition induces a succinate

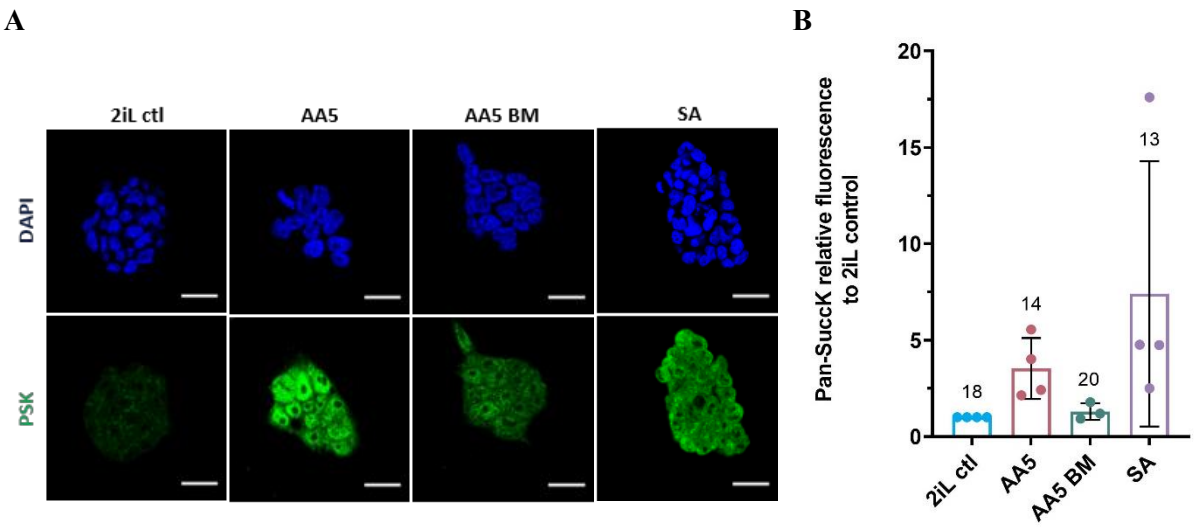

Figure 14. Accumulation of succinyllysine residues in mESCs compartments under AA5 treatment.

(A) Immunostaining of pan-succinyllysine residues (Pan-SuccK) (green) in 2iL mESCs treated with 0.5 mM SA, 1 µM BM, 250 nM AA5 assessed by confocal analysis. Nuclei are counterstained with DAPI. Confocal micrographs are representative of 3 independent replicates. Scale bar=20 µm.

(B) Quantification of pan-succinyllysine fluorescence (Pan-SuccK) relative to 2iL control total colony fluorescence (n=4). All results are expressed as mean + S.D. The number of colonies quantified are indicated on the graph for each condition. One-way ANOVA and post-hoc Turkey analysis were conducted, * $P < 0.05$, although no results were significant.

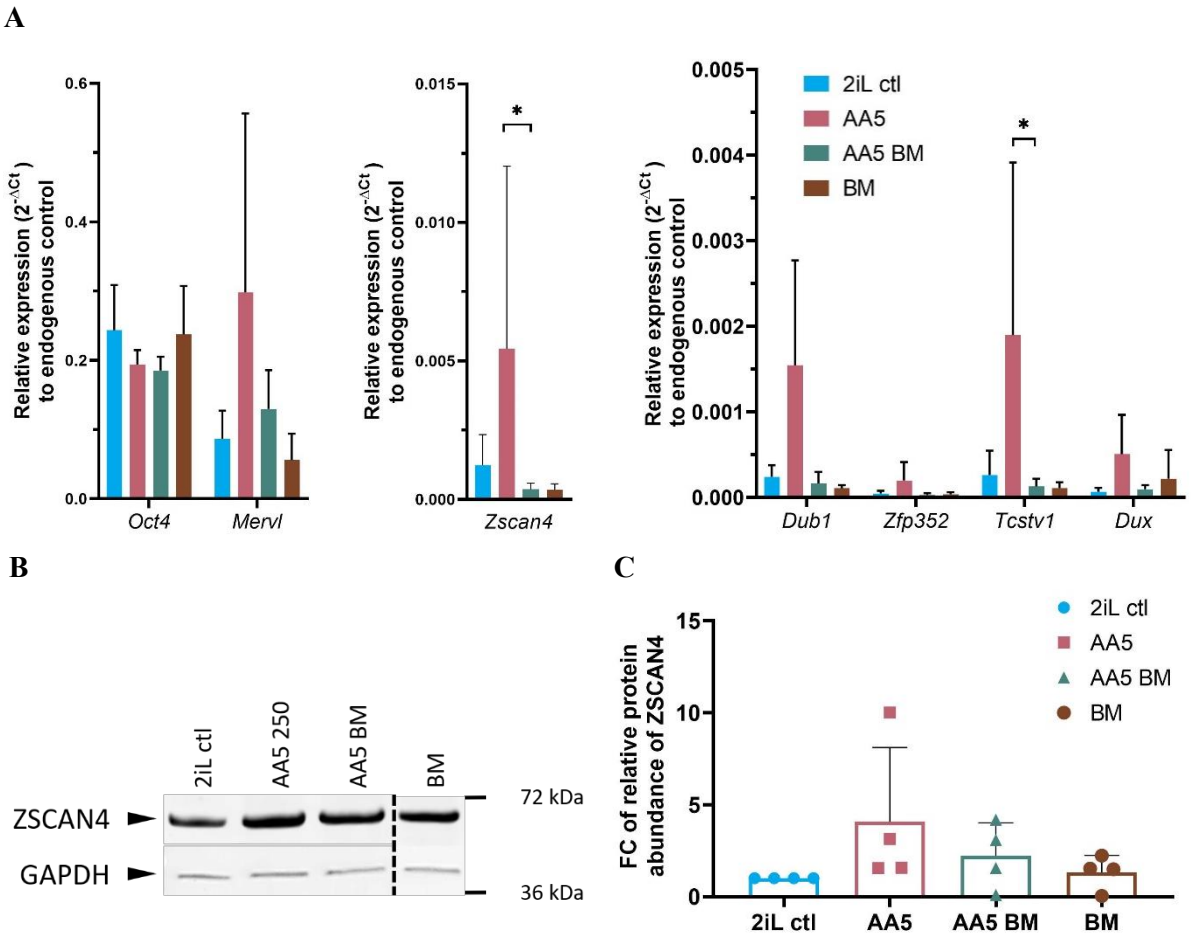

Figure 15. AA5 induces the expression of 2-cell-like markers in naïve mESCs.

(A) Relative expression of 2-cell-like-specific markers determined by RT-qPCR, relative to *Gapdh* (glyceraldehyde-3-phosphate dehydrogenase) as endogenous control of naïve mESCs exposed to 250 nM AA5 and/or 1 µM BM. *Oct4* (octamer-binding transcription factor) is considered as pluripotency control, while *Zscan4* (zinc finger and SCAN domain-containing protein 4), *Dub1* (ubiquitin specific peptidase 36), *Zfp352* (zinc finger protein 352), *Mervl* (murine endogenous retrovirus with leucine tRNA primer), *Tcstv1* (2-cell stage variable group member 1) and *Dux* (double homeobox) are 2C-like specific markers. n=4 independent biological replicates. All results are expressed as mean + S.D. One-way ANOVA and post-hoc Turkey analysis were conducted, * $P < 0.05$.

(B) Western blot analysis of the abundance of ZSCAN4 after 250 AA5, 0.5 mM SA treatments and/or 1 µM BM supplementation, relative to GAPDH as loading control. Representative blot of 4 independent replicates.

(C) Western blot quantification of the fold change of ZSCAN4 protein abundance relative to GAPDH endogenous loading control. Results are represented as mean (n=4) + S.D. One-way ANOVA with post-hoc Turkey test was conducted for western blot quantification results. Non-significant results are not labelled. * $P < 0.05$.

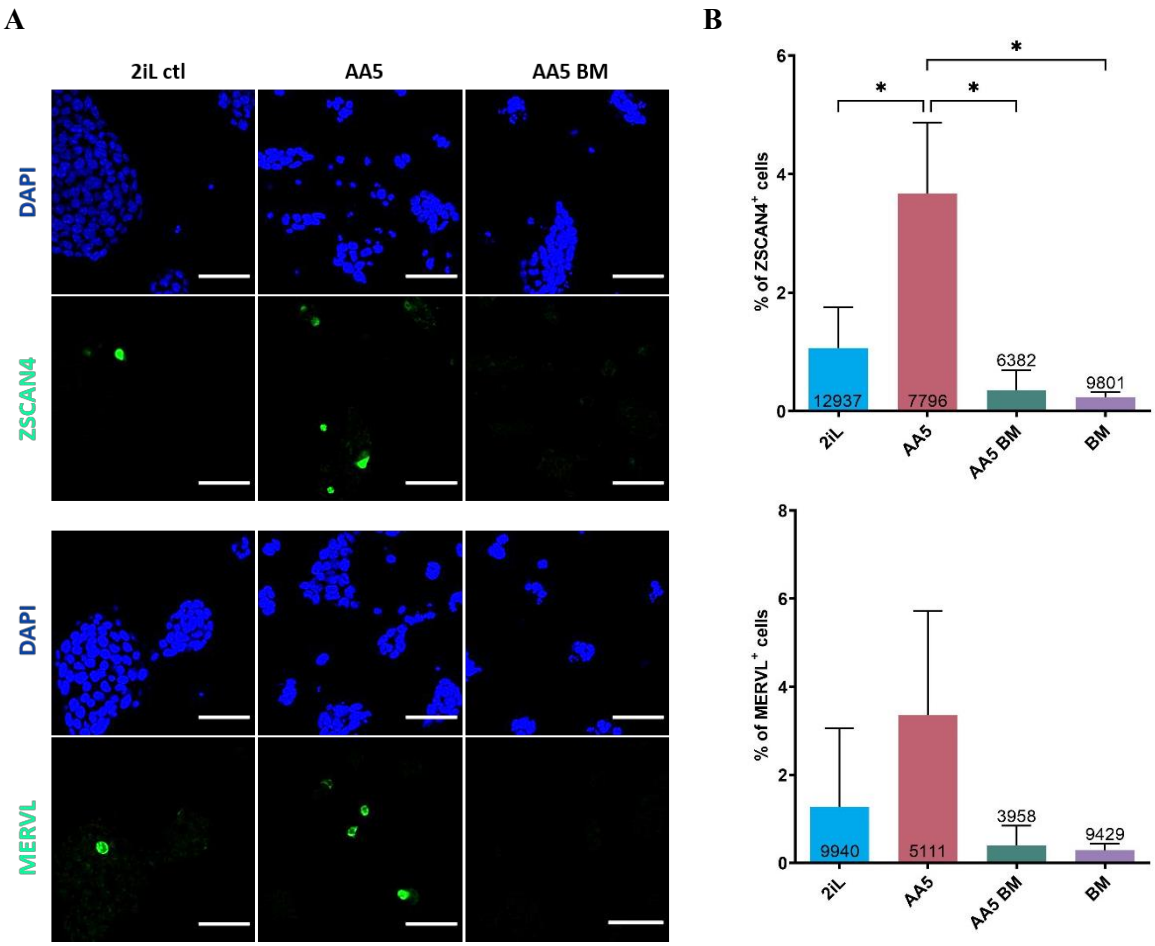

Figure 16. AA5 treatment of naïve mESCs increases the number of ZSCAN4$^+$ and MERVL$^+$ 2CLCs.

(A) Confocal micrographs of naïve (2iL) mESCs treated with 250 nM AA5, with or without 1 µM BM. ZSCAN4 and MERVL-positive cells are immunostained (green), nuclei are counterstained by DAPI. Representative of 4 independent experiments. Scale bar=50 µm.

(B) Quantification of **(A)**, the proportion of ZSCAN4$^+$ and MERVL$^+$ cells in AA5 and BM-treated naïve mESC population. The total number of counted cells is indicated for each condition (ZSCAN4$^+$, n=4; MERVL$^+$, n=3). Results are represented as percentage in mean + S.D. One-way ANOVA and post-hoc Turkey analysis were conducted, * $P < 0.05$.

accumulation (Detraux *et al.*, submitted manuscript) **(Figure 14)**. Similarly, 250 nM AA5-exposed cells exhibit an intensified fluorescence signal across the cell, relatively similar to SA. Although not significant, BM seems to induce a reduction in lysine succinylation **(Figure 14B)**. Altogether these results suggest that AA5 indeed triggers lysine succinylation in the whole cells, generated by a mitochondrial succinate build-up and leakage, that seems to be partially prevented by BM.

3.3. AA5 can induce 2-cell-like features in naïve mESC subpopulations

According to our hypothesis, a build-up of succinate in the mitochondrial matrix leading to its leakage to other cellular compartments would trigger a reprogramming of 2iL mESCs towards a 2C-like state. As a consequence, the expression of specific 2C-like markers upon AA5 exposure was monitored **(Figure 15A)**. The relative expression of 2C-like specific markers studied by RT-qPCR shows an upregulation by 250 nM AA5 (with a 6- to 7-fold overexpression for *Tcstv1*). Interestingly, this increase is inhibited by the addition of 1 µM BM, incriminating the succinate exit out of mitochondria, in accordance with our assumptions.

These results are confirmed by western blot analysis of the protein abundance of ZSCAN4, a well-known marker of 2CLCs. Results coincides with the RT-qPCR observations, exhibiting an upregulation of *Zscan4* at transcript and protein levels. Also, in the presence of BM, ZSCAN4 abundance is maintained at a control level **(Figure 15B)**. All of the results above advocate the effect of AA5 and thus succinate accumulation to upregulate 2-cell-like markers in naïve mESCs.

3.4. AA5 provokes the emergence of ZSCAN4$^+$ and MERVL$^+$ mESC subpopulations

As explained in **Section 1.3.3.**, the 2CLCs are an actual subpopulation of naïve mESCs. We thus aimed to confirm the increase of 2CLC markers observed above at the population level. Thus, in order to explore the emergence of 2CLCs subpopulation among naïve mESCs when in presence of AA5, we assessed the occurrence of ZSCAN4$^+$ and MERVL$^+$ cells by immunostaining **(Figure 16A-B)**. ZSCAN4$^+$ and MERVL$^+$ cells were observed by confocal microscopy and counted. Both 2CLC-specific markers were observable and reached an almost 4-fold increase when cells were treated with AA5. Interestingly, BM alone seems to reduce the 2CLC emergence compared to the control. Although not statistically significant, this supports a role of succinate in endogenous the process of 2CLC emergence.

To confirm the previous observations, the emergence of the MERVL$^+$ subpopulation has been also evaluated by flow cytometry. We took advantage of a previously published cell line (Tbg4)

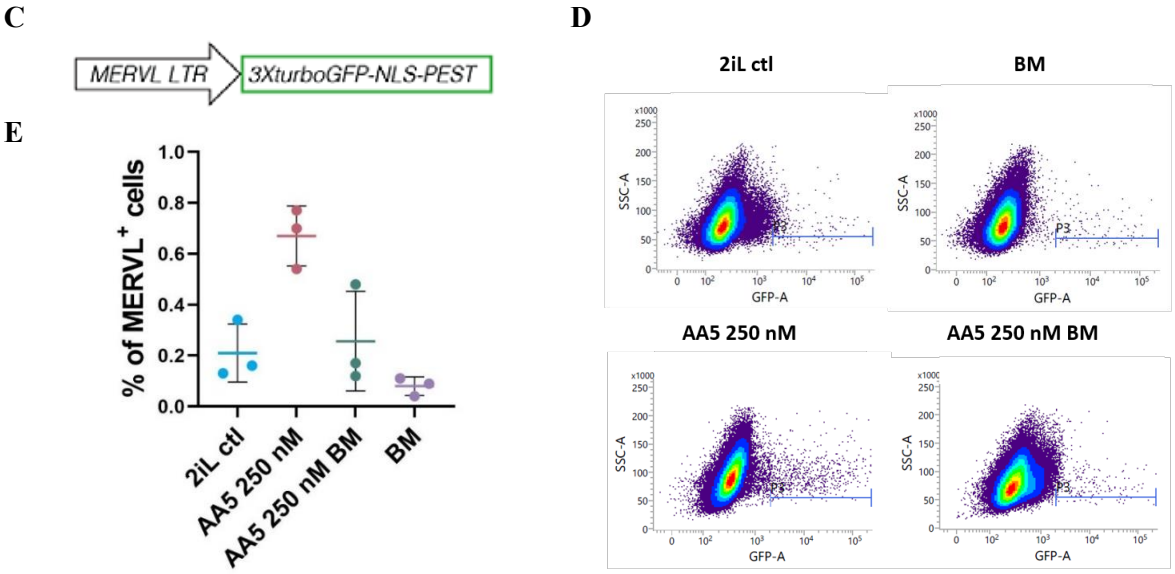

Figure 16. AA5 treatment of naïve mESCs increases the number of ZSCAN4$^+$ and MERVL$^+$ 2CLCs.

(C) Schematic representation of the construct in the mESCs Tbg4 line, displaying a turboGFP under the control of *Mervl* long terminal repeat (LTR) region (Ishiuchi *et al.*, 2015; Rodriguez-Terrones *et al.*, 2020).

(D) Flow cytometry obtained scatter plots. Results are represented as the side scatter in function of GFP signal intensity. One-way ANOVA was conducted for cell count and flow cytometry results, although all results were non-significant.

(E) Flow cytometry results of 2iL mESCs treated with AA5 and/or BM. Results are represented as percentage of MERVL$^+$ cells in the tested population as mean ± S.D. (n=3).

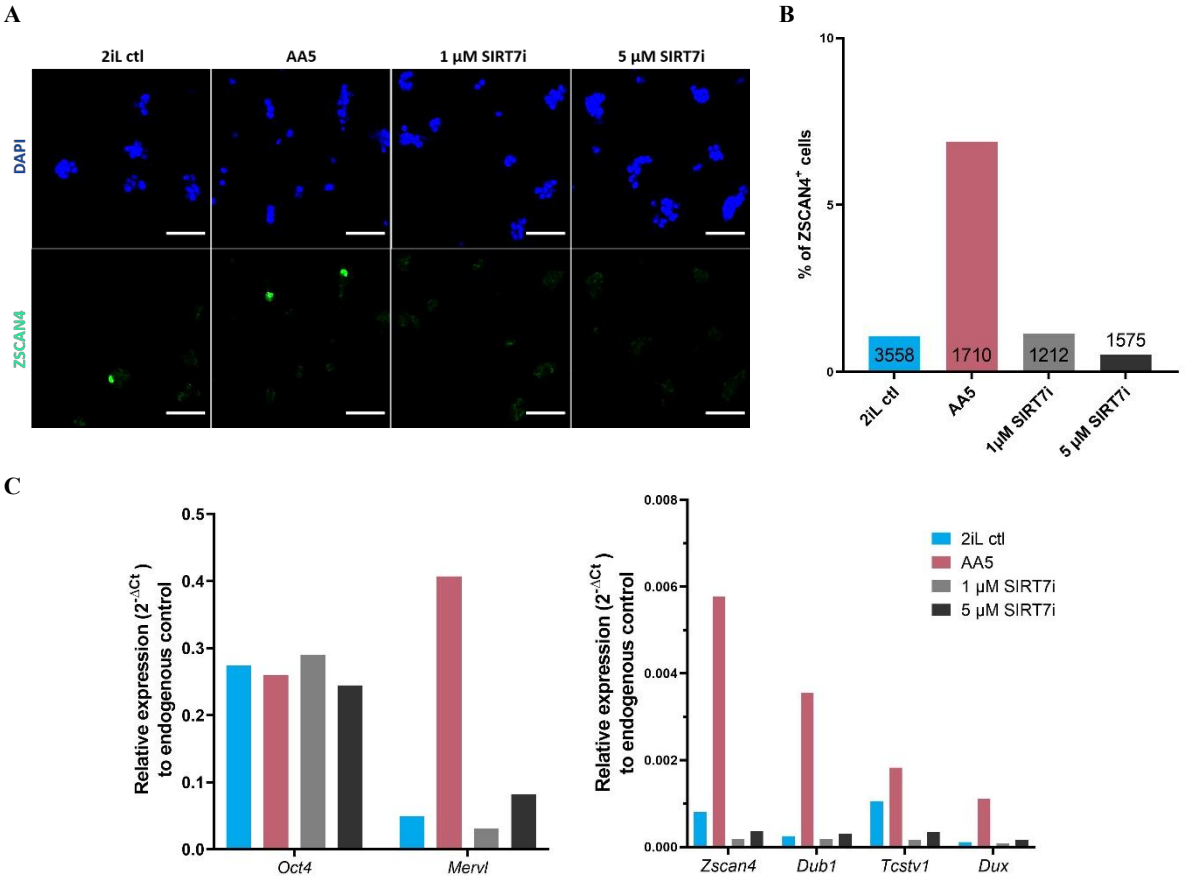

Figure 17. The inhibition of SIRT7-mediated desuccinylation does not favour the 2C-like reprogramming.

(A) Confocal micrographs of naïve (2iL) mESCs treated with 250 nM AA5, 1 µM or 5 µM SIRT7i. ZSCAN4-positive cells are immunostained (green), nuclei are counterstained by DAPI. Representative of 2 independent experiments. Scale bar=50 µm.

(B) Count of ZSCAN4-positive cells in naïve mESCs exposed to 250 nM AA5, 1 µM or 5 µM SIRT7i. The total number of cells counted is indicated for each condition on the histogram. The results are representative of 2 independent replicates.

(C) Relative expression of 2C-like-specific markers determined by RT-qPCR, relative to *Gapdh* as endogenous control of naïve mESCs untreated (2iL ctl), treated with 250 nM AA5, 1 µM and 5 µM SIRT7i (n=2 independent experiments).

expressing a turboGFP construct under the control of *Mervl*'s LTR **(Figure 16C)** (Ishiuchi *et al.*, 2015; Rodriguez-Terrones *et al.*, 2020) enabling the detection of cells expressing the retrotransposon by fluorescence. A higher proportion of $MERVL^+$ cells is expectedly observed upon AA5 treatment, such effect inhibited by BM as shown by the scatterplot shift of population **(Figure 16D-E)**. These results strengthen the assumed AA5 potential to provoke an enhanced reprogramming towards a 2C-like state which is testified by upregulated 2C-specific markers such as *Zscan4* and *Mervl*.

3.5. Protein succinylation is not critical for the 2C-like reprogramming

After the assessment that AA5 is able both to provoke succinate accumulation and to promote 2C-like reprogramming of naïve mESCs, we decided to explore the possible underlying mechanisms. As explained in the introduction **(Section 1.5.3.)**, succinate could mediate the observed induction of 2CLCS either through lysine succinylation of proteins or through the inhibition of 2OGXs. We thus decided to investigate two possibilities in parallel.

On the one hand, a pull-down of succinylated peptides followed by mass spectrometry identification was previously conducted in the laboratory to compare succinylated peptides/proteins between 2iL control and SA-treated mESCs. This analysis confirmed an increase in protein identification after SA treatment. Even more interestingly, the analysis of proteins enriched in SA (FC $\geq$ 1.5) also revealed an important proportion of proteins tagged with nucleus, nucleoplasm or even cytoplasm gene ontology cellular compartment **(Suppl. data 1)**. This suggests that the accumulating mitochondrial succinate is able to leak out of this organelle and that succinate can reach the nucleus and modify lysine residues there. Indeed, we suspect succinate to maybe act in the cytosol but also within the nuclear compartment where it could play an important role in the 2C-like reprogramming since proteins like NCL or TRIM28, already pointed as mediating the mESC-to-2CLC transition (Percharde *et al.*, 2018), were identified among the succinylated proteins.

To investigate if this increase in nuclear protein succinylation is responsible for the increase in 2CLCs, we assumed that a decreased sirtuin desuccinylase activity would augment the amount of lysine succinylation events. Similar to AA5, the proportion in the 2CLC subpopulation would be expected to rise as well as 2C-like features in case of SIRT inhibition. We thus tested the effects of a SIRT7 inhibitor (SIRT7i) (Kim *et al.*, 2019) at two concentrations (1 µM and 5 µM) on naïve mESCs. A 48h-treatment with SIRT7i of mESCs of the Tbg4 cell line was first analysed by immunofluorescence. Interestingly, we observed that in $MERVL^+$ Tbg4 mESCs, the latter exhibited an enhanced level of succinylated lysine residues upon SIRT7i treatment **(Suppl. data 2)**. However, immunofluorescence observations at both concentrations do not exhibit a rise in the 2CLC ($ZSCAN4^+$) population. On the contrary, a decrease is even observed **(Figure 17A-B)**. Similarly, at the RNA level, a downregulation of 2C-like markers is

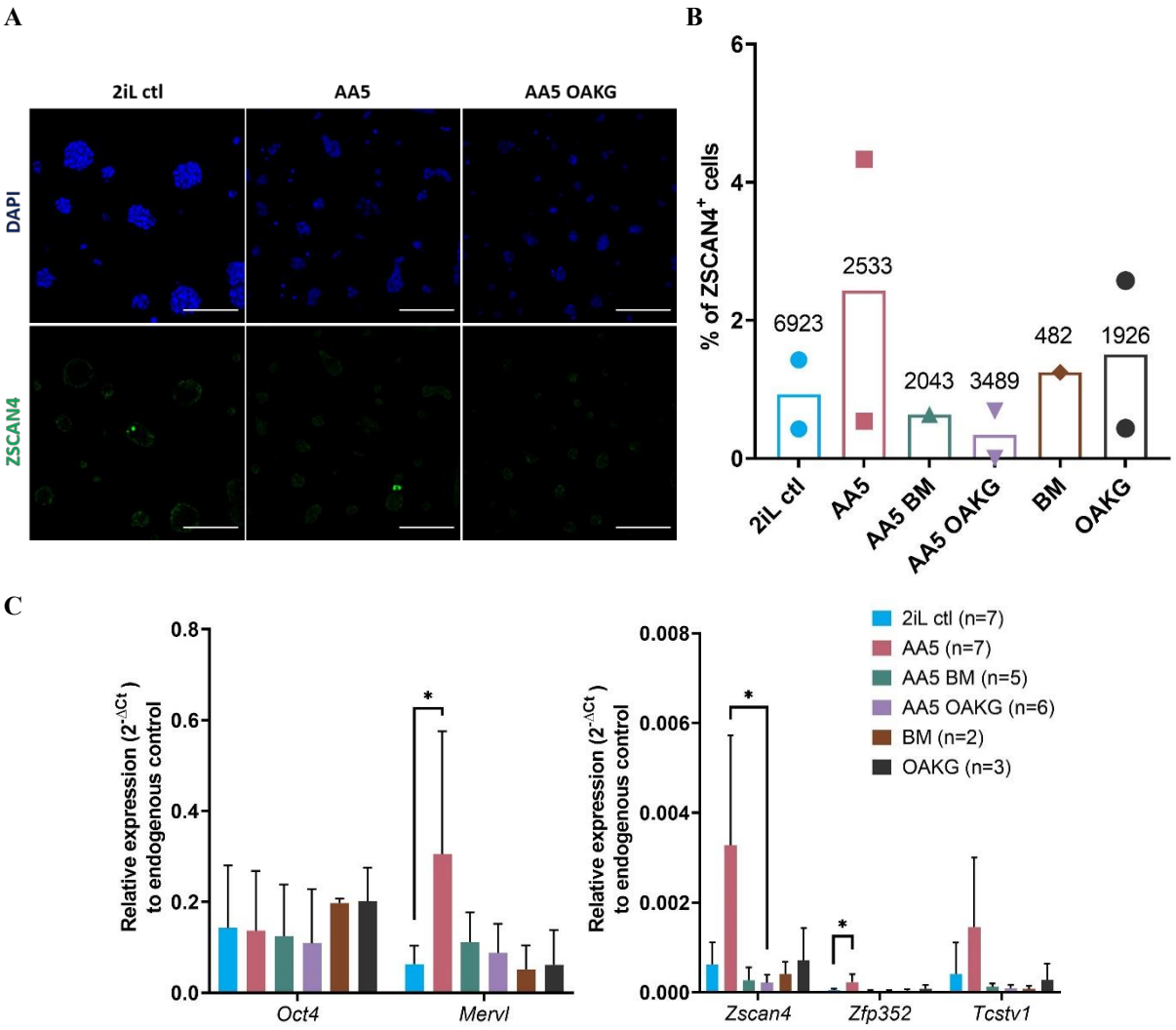

Figure 18. OAKG supplementation of AA5 is preventing the 2C-like reprogramming of naïve mESCs, suggesting a succinate-mediated inhibition of 2OGXs.

(A) Confocal micrographs of naïve (2iL) mESCs treated with 250 nM AA5 and 1 µM OAKG. ZSCAN4-positive cells are immunostained (green), nuclei are counterstained by DAPI. Representative of 2 independent experiments. Scale bar=100 µm.

(B) Quantification of **(A)**, the proportion of ZSCAN4$^+$ cells in 250 nM and corresponding 1µM BM and 1µM OAKG-treated naïve mESC population. The total number of counted cells is indicated for each condition, as well as the number of biological replicates. n=2 biological replicates except for AA5+BM and BM, where n=1.

(C) Relative expression of 2C-like-specific markers determined by RT-qPCR, relative to *Gapdh* as endogenous control of naïve mESCs untreated (2iL ctl), treated with 250 nM AA5, corresponding BM and OAKG conditions, 1 µM BM and 1 µM OAKG (the number of replicates for each condition is indicated on the graph). One-way ANOVA and post-hoc Turkey test were conducted on the results. Non-significant results are not labelled. * $P < 0.05$.

D

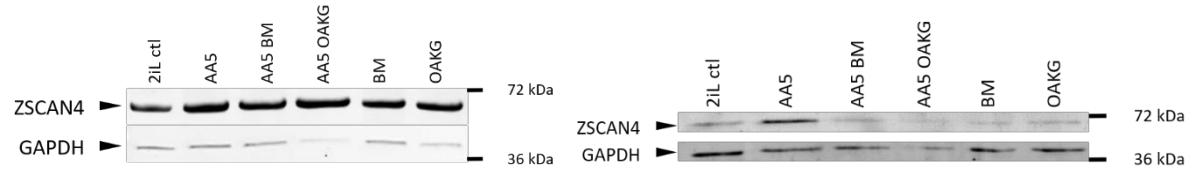

E

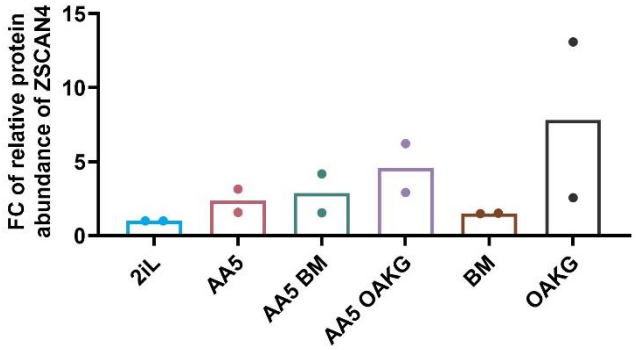

Figure 18. OAKG supplementation of AA5 is preventing the 2C-like reprogramming of naïve mESCs, suggesting a succinate-mediated inhibition of 2OGXs.

(D) Western blot analysis of the abundance of ZSCAN4 of naïve mESCs untreated (2iL ctl), treated with 250 nM AA5, corresponding BM and OAKG conditions, 1 µM BM and 1 µM OAKG 250 nM AA5, corresponding BM and OAKG conditions, 1 µM BM and 1 µM OAKG, relative to GAPDH as loading control. n=2 independent replicates.

(E) Quantification of **(D)**, western blot quantification of the fold change of ZSCAN4 protein abundance relative to GAPDH endogenous loading control. Results are represented as mean of the 2 biological replicates.

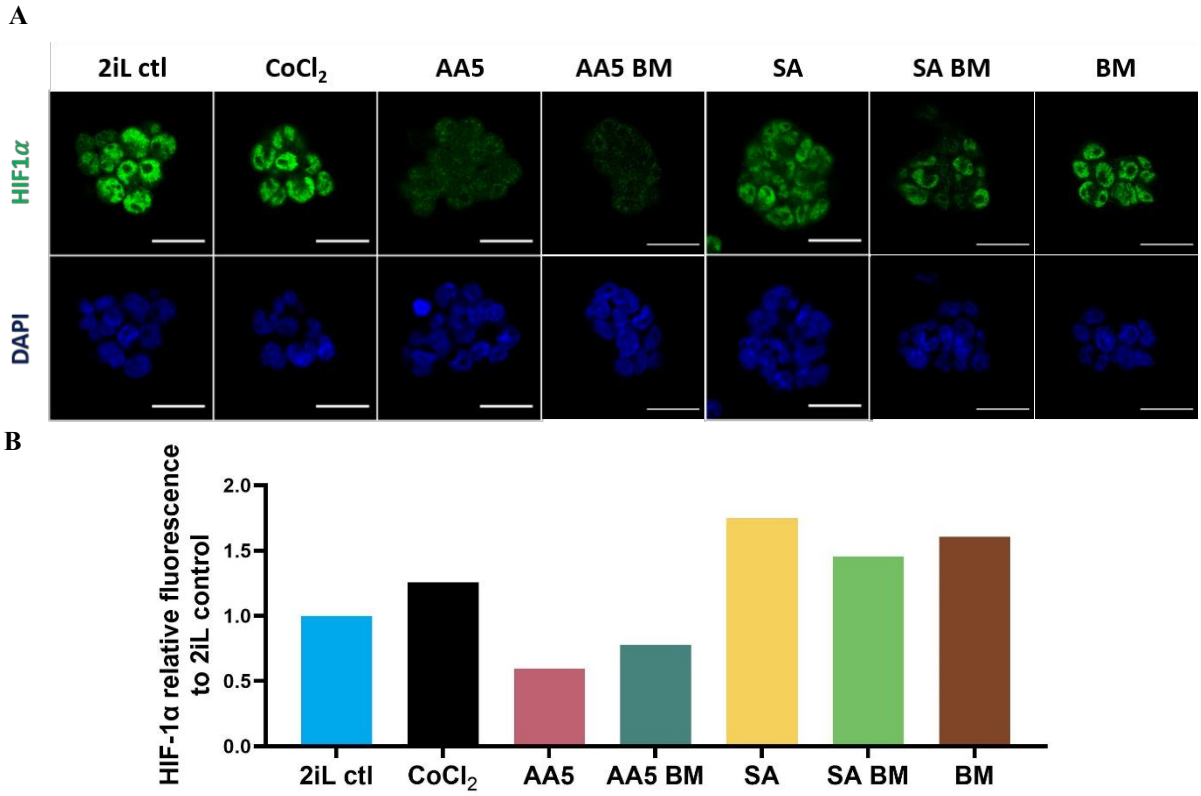

Figure 19. HIF-1α stabilisation is not favouring the 2C-like reprogramming of naïve mESCs.

(A) Representative confocal micrographs of naïve (2iL) mESCs treated with $CoCl_2$, 250 nM AA5, 0.5 mM SA, and corresponding 1 µM BM treatment. ZSCAN4 and MERVL-positive cells are immunostained (green), nuclei are counterstained by DAPI. Representative of 1 independent experiments. Scale bar=20 µm.

(B) Quantification of **(A)**, HIF1A immunofluorescence signal in the nucleus of naïve mESCs treated with $CoCl_2$, 250 nM AA5, 0.5 mM SA, and corresponding 1 µM BM treatment. The results correspond to replicate.

observed **(Figure 17C)**. Altogether these results do not support a role for lysine residues succinylation in the nucleus during the 2C-like reprogramming of naïve mESCs, although we cannot exclude a potential involvement of cytosolic succinylated proteins in the 2CLC reprogramming observed.

3.6. Succinate-enhanced 2C-like reprogramming is due to 2-oxoglutarate dioxygenases product inhibition

On the second hand and simultaneously, we explored the possibility that the effect of succinate accumulation on 2CLC emergence could be due to succinate inhibition of 2OGXs. To counterbalance the inhibitory effect of the accumulated succinate due to AA5 treatment, we opted for a supplementary treatment with octyl-α-ketoglutarate (OAKG), a cell-permeable derivative of 2OG. In the presence of AA5 and OAKG, fewer 2CLCs were counted in the naïve population and 2C-like specific markers were maintained at control-similar levels **(Figure 18A-B)**. In support, the increase of 2C-like-specific markers was prevented upon OAKG supplementation **(Figure 18C)**. Nevertheless, at a protein level, ZSCAN4 relative protein abundance is not coinciding with the observation of the RT-qPCR results. However, we can discuss the quality of two shown western blots on which were assessed the quantifications **(Figure 18E)**, at some point due to the irregular appearance of the GAPDH loading control **(Figure 18D)**. As the relative abundance presents variability between the two replicates, the robustness of the analysis is to be questioned and calls for additional replicates. Anyway, $ZSCAN4^+$ cells count and RT-qPCR results underline an effect of 2OGX activity during the naïve-to-2C-like transition.

Consequently, we started to explore the involvement of the different classes of 2OGX enzymes, starting with the hypoxia-related PHD. From results obtained from an RNA-sequencing experiment comparing naïve mESCs and SA-treated, we compared the expression of some HIF-1α targets and no visible trend is observed between the two conditions **(Suppl. data 3)**. To have a better understanding of whether HIF-1α is stabilised under AA5 or SA treatment, thanks to succinate impeding the action of PHDs, immunofluorescence analysis of HIF-1α was carried out **(Figure 19A-B)**. A basal HIF-1α stabilisation is noticeable in the 2iL control, comparable to the positive control where $CoCl_2$ is used to generate HIF-1α stabilisation. Strikingly, HIF-1α signal illustrates an enhanced stabilisation of HIF-1α upon SA exposure compared to AA5. However, this is in contradiction with the expected succinate-mediated inhibition of PHDs that would end up in improved HIF-1α stabilisation. Additionally to this result, BM does not prevent AA5 effect on HIF-1α stabilisation while its preventive effect has been previously shown with 2CLC count **(Figure 16A-B)**. We concluded that the hypoxia-inducible factor does not have a crucial impact over the transition towards a totipotent-like state of mESCs.

A

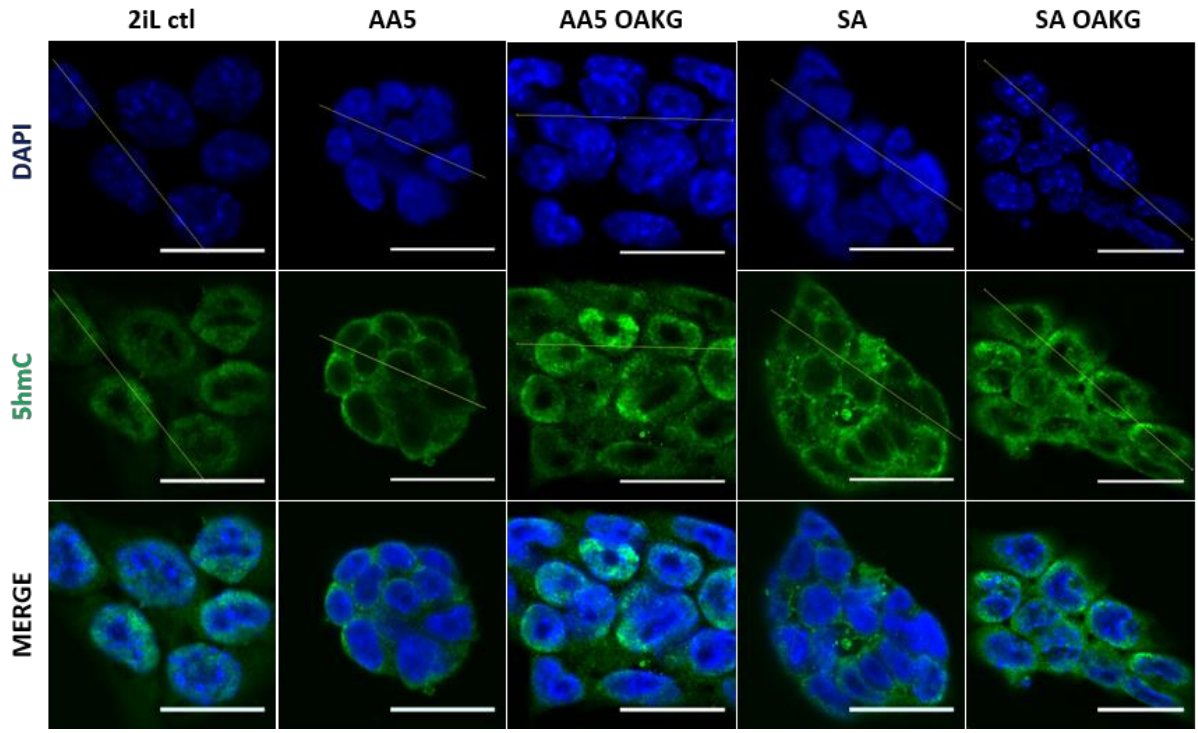

B

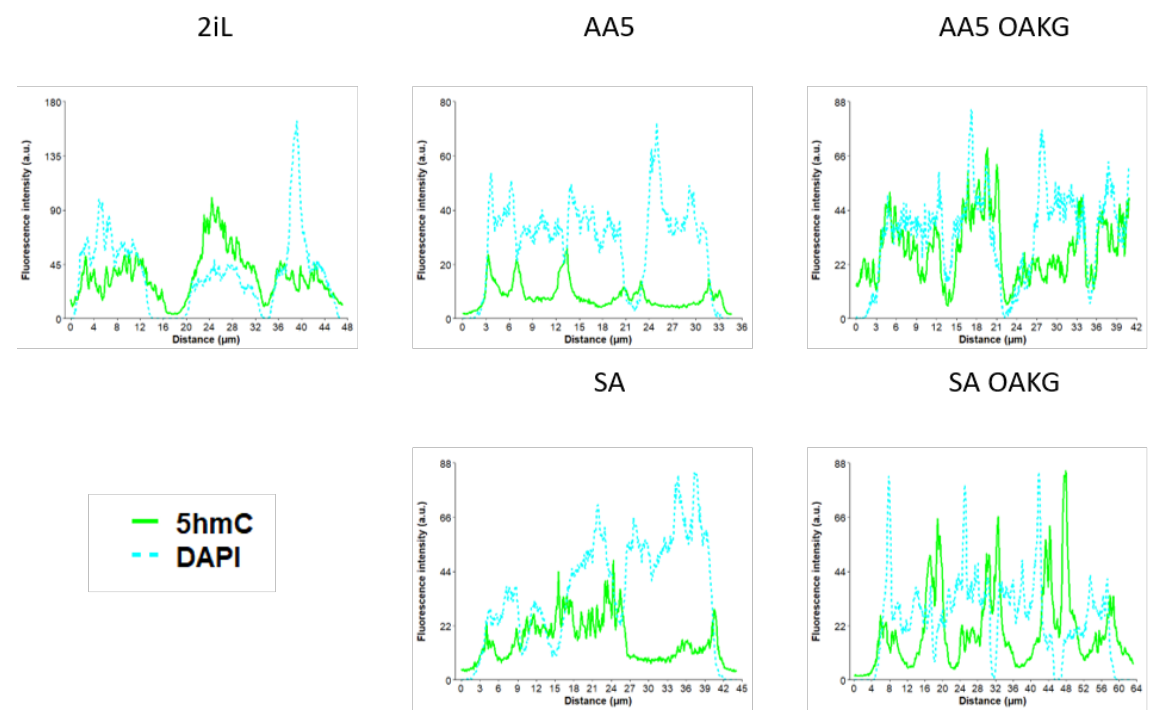

Figure 20. OAKG inhibits the reduction in 5hmC provoked by AA5 and SA treatments.

(A) Representative confocal micrographs of the immunostaining of 5hmC (5-hydroxymethylcytosine; green) of naïve 2iL mESCs treated with 250 nM AA5, 0.5 mM SA, 1 µM BM and 1 µM OAKG. The yellow line is the transect on which quantifications in **(B)** are assessed (n=1 independent experiment). Scale bar=20 µM.

(B) Quantification of **(A)**, of the fluorescence intensity of transect (yellow line) of both the 5hmC immunostaining (green) and DAPI counterstaining for the nuclei (blue). Graphs are represented as the fluorescence intensity (a.u.) in function of the distance (µm) at each point along the transect, the corresponding mESC treatment is indicated above each graph.

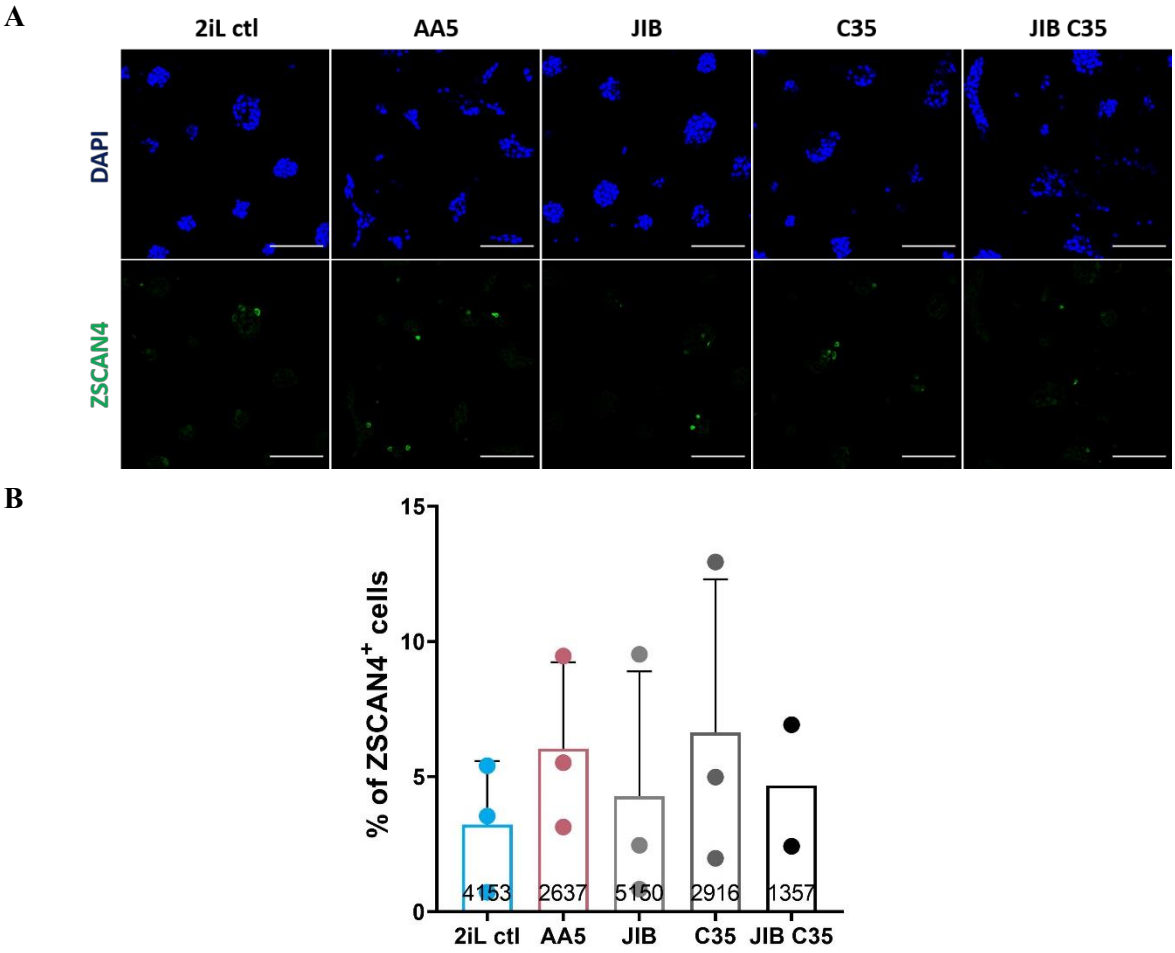

Figure 21. Effect of deficient methylated histones and 5-hydroxymethylcytosine on the proportion of 2CLCs in naïve mESCs.

(A) Representative confocal micrographs of naïve (2iL) mESCs treated with 250 nM AA5, 250 nM JIB, 2.5 µM C35 and JIB+C35. ZSCAN4-positive cells are immunostained (green), nuclei are counterstained by DAPI. Representative of 3 independent experiments. Scale bar=100 µm.

(B) Quantification of **(A)**, the proportion of ZSCAN4^{+} cells in naïve mESC population treated with 250 nM AA5, 250 nM JIB, 2.5 µM C35 and JIB+C35. The total number of counted cells is indicated for each condition. Results are represented as mean + S.D. n=3 biological replicates, except for the JIB+C35 condition (n=2). For n=3 conditions, one-way ANOVA and post-hoc Turkey's test were conducted. No result was significant.

3.7. AA5-enhanced 2C-like reprogramming seems mediated by deficient DNA and histone demethylation

PHDs are not the only target of succinate in the 2OGX enzyme family: the epigenetic modifiers JMJ-domain-containing HDMs and TET 5mC demethylases are also sensitive to this metabolite. This prompted us to test HDM and TET inhibitors: JIB (JIB-04, described as JARID1A, JMJD3 and UTX inhibitor) (Wang *et al.*, 2013) and C35 (TET-C35-INH, shown to inhibit TET1-3) (Singh *et al.*, 2020), in order to inhibit these enzymes directly.

First, their inhibition potential has been assessed. To validate the effect of C35, DNA dot blots followed by 5hmC-immunostaining have been carried out **(Suppl. data 4)**, but unfortunately no clear conclusion could be drawn out of this method. Immunofluorescence analysis of 5hmC was conducted in order to look for variations in global DNA methylation level when mESCs are treated with AA5 **(Figure 20A)**. The fluorescence intensity of both DAPI and 5hmC staining was quantified along a transect line **(Figure 20B)**. This quantification in the AA5 condition sharply shows that the 5hmC is very low within the nuclei (represented by the DAPI counterstain intensity), whereas the signal is a bit higher for the SA treatment. For the conditions with OAKG supplementation, a much more elevated intensity signal is noticeable. Despite the fact that only one replicate has been performed, so it does not allow us to draw any definite conclusions, oneself could consider that AA5 is provoking a decrease in 5hmC that can be explained by the inhibition of the demethylase activity of TETs and that it is prevented with a supplementation with OAKG that counteract this inhibition, which is aligned with our hypothesis. However, as TET-mediated demethylation is sequential **(Figure 7C)**, it rather be more relevant to test for all of the cytosine intermediates (5mC, 5hmC, 5fC and 5caC) of the demethylation process in order to have clear information about the effect of the TET inhibitor. Additionally, the efficiency of C35 to assure TET inhibition should be assessed, before deeper investigations.

Nevertheless, immunofluorescence against trimethylated histones (H3K4me3 and H3K27me3) enabled us to confirm the inhibiting potential of JIB **(Suppl. data 5)**. Accordingly, upon JIB treatment, the signal of the fluorescence of trimethylated H3K4 and H3K27 increases, as observed with AA5 treatment of the cells. This indicates that AA5 by the extent of accumulated succinate can cause histone modifications landscape similar to a deficient demethylation activity on histones. While we cannot yet certify the efficiency of the C35 inhibitor but well the one of the JIB, we tested if the combination of both inhibitors could increase the 2CLC population. Although a high variability between the different replicates prevents from drawing any conclusions, it is interesting to observe that the count of $ZSCAN4^+$ cells in the total naïve population tends to a rise when mESCs are treated with JIB or C35 **(Figure 21)**. However, additional replicates are definitely needed. Altogether, these results suggest a globally methylated epigenetic landscape of naïve mESCs in transition towards a 2C-like state, and these

epigenetic features can be promoted by an accumulation of succinate provoked by AA5-inhibition of SDH.

4. CONCLUSION AND DISCUSSIONS

In this Master's thesis, we hypothesized that an accumulation of succinate in naïve mESCs reprograms them towards a state reminiscing of the 2C-stage embryo, such state being known as the 2C-like state. Based on the following postulates resulting from previous research in the laboratory, it has been demonstrated that an inhibition of the heme biosynthesis pathway is enhancing the 2C-like reprogramming. Moreover, this phenomenon is prevented by BM treatment, which is impeding succinate escape of the mitochondrion (Detraux *et al.*, submitted manuscript). Consequently, we decided to study the outcome of a treatment of naïve mESCs with AA5, an inhibitor of the SDH complex (Miyadera *et al.*, 2003). We demonstrated here that AA5 is able to provoke a rise in succinyllysine levels in the cells and to upregulate 2C-specific markers at transcript and protein levels, also reflected in the 2CLCs ($ZSCAN4^+$ and $MERVL^+$) population increase.

Regarding the multiple possible functions of succinate, we first investigated its role in lysine residues succinylation. To do so, we checked whether blocking the desuccinylase activity of sirtuins, focusing in our case on SIRT7, would intensify Pan-SuccK levels within naïve cells and thus would reinforce the 2C-like reprogramming. The use of SIRT7i allow to conclude more of an opposite effect over 2C-like reprogramming. Indeed, upon SIRT7i treatment, the 2CLC population decreases, ousting post-translational lysine residue succinylations of nuclear proteins as an influent mechanism of the 2C-like reprogramming.

Then, as 2OG is a cosubstrate of the 2OGX reactions and is converted into succinate by these enzymes (Hausinger, 2015), succinate as a consequence can block the enzymatic reaction in the case of its accumulation. This prompted us to use OAKG in order to test whether this supplementary treatment could counterbalance the direction of the reaction in naïve mESCs treated by AA5 and to observe any noticeable effect on the 2CLC subpopulation. Results showed that OAKG can indeed counteract the effects of AA5, reducing 2C-like reprogramming in naïve cells, suggesting an implication of the 2OGXs.

Three relevant 2OGXs were highlighted here: the hypoxia-related PHD, the JMJC-containing domain HDM, and 5mC-demethylase of the TET family. Simultaneously, we aimed to explore the involvement of each of the mentioned OGX. First, we assessed the stabilisation of HIF-1α upon AA5 treatment by immunofluorescence analysis. Confocal micrographs attested no stabilisation of HIF-1α is observed compared to the 2iL control. Supporting these results, RNA-Seq data carried out on untreated and SA-treated naïve mESCs allowed us to conclude that HIF-1α's targets expression is not following any clear trend upon SA treatment. All of this thus implies that PHDs are not involved in the 2CLC reprogramming after AA5 treatment.

Consequently, we continued our study with the putative roles of HDMs and TETs in the process using inhibitors such as JIB, impairing JARID1A, JMJD3 and UTX activity (Wang *et al.*, 2013) and

C35 blocking all 3 TET isoforms (Singh *et al.*, 2020). In short, we claim that a build-up of mitochondrial succinate and its resulting leakage to the rest of the cell is able to inhibit 2OGXs such as the HDMs and the TETs. As a consequence, this would end up in an increase of histone and DNA methylation, respectively, ultimately favouring 2C-like reprogramming of naïve mESCs. Histone methylation levels were thus verified focusing on H3K4me3 and H3K27me3, as they have proven to be relevant according to literature **(Sections 1.7.2. and 1.7.3.)**. Immunofluorescence analyses showed that these two histone modifications were enriched upon AA5 treatment, as well as when cells were treated with a combination of JIB and C35. Although the inhibitory effect of C35 is far from convincing, these results were supported by immunofluorescence, as the percentage of $ZSCAN4^{+}$ cells in the naïve total population increases in AA5, JIB, C35, or JIB-C35-treated cells, even if they were not significant. Unfortunately, even if a trend is observed for a reduced nuclear 5hmC signal in AA5-treated cells, no definite conclusion can be drawn on the levels of methylated DNA. Indeed, the 3 biological replicates were not reached and a deeper study directed towards the other intermediates of the sequential demethylation reaction catalysed by TET 5mC demethylases ought to be addressed.

Together, this suggest that the 2C-like reprogramming of naïve mESCs following succinate accumulation is characterised by a reduced demethylase activity on histones and DNA. This shows a metabolic regulation of the epigenetic landscape of the pluripotent state of mESCs.

Apart from obtaining the three or more replicates for all of the conducted experiments, some aspects of the experiments carried out for this Master's thesis can be discussed. Firstly, the cellular model of mESCs oscillating between the naïve pluripotent and the 2C-like states is not facilitating the study of the 2C-reminiscing state of these cells. Indeed, the well-known heterogeneity of naïve populations can sometimes statistically increase the variability of the final results. In addition of technical variability, this causes large standard deviation, for example, as observed in the RT-qPCR results **(Figure 15A)**. As mentioned in the introduction, 2CLCs reach up to 5% of the total naïve population (Zalzman *et al.*, 2010; Macfarlan *et al.*, 2013), such a relatively small proportion of this subpopulation definitively covers up information as the 2CLCs are 'diluted' in the global population, rendering changes in protein relative abundance, for example, more difficult to observe. It might have as well occurred in the dot blot analysis targeting 5hmC levels in treated mESCs **(Suppl. data 5)**, where no significant modification in the 5hmC signal despite of treating cells with C35, inhibitor of the TETs, at a range of concentrations, even though the 6 replicates. The 'dilution' of information is even more critical as 5mC and 5hmC both reach approximately only 1% of the total amount of cytosines in 2iL mESCs (Burr *et al.*, 2018), rendering any variation at this level harder to observe at the immune-dot blot resolution. This is also noticeable in western blot analyses, where the variation in relative protein

abundance is not really obvious **(Figure 18D)**. To get around this issue, fluorescence activated cell sorting (FACS) could be used in order to sort the cells depending on whether they are 2C-like or not. To do so, the Tbg4 cell line expressing a turboGFP controlled by MERVL's LTR (Ishiuchi *et al.*, 2015; Rodriguez-Terrones *et al.*, 2020) could be used. In addition, other cell lines reported by (Rodriguez-Terrones *et al.*, 2020) could enable such sorting as they allow the sorting of *Zscan4*-expressing and *Mervl*- and *Zscan4*-expressing cells. Following this 2CLC sorting, a lot of experiments can be considered and we will discuss some of them in this discussion.

In this Master's thesis, succinate has been identified to act indirectly on the epigenetic landscape of mESCs. Nonetheless, although immunofluorescence enabled the relative quantification of the succinylated lysine residues, no real quantitative data about the succinate build-up in the cells has been conducted. A colorimetric assay (*e.g.*, Succinate assay kit (Colorimetric), #ab204718, Abcam) could be used to quantify succinate levels, even though one would prefer gas chromatography coupled to mass spectrometry (GC-MS) for more quantitative results, with a possibility of cell sorting of 2CLCs beforehand. Also, we suggest to carry these succinate content measurements with naïve mESCs, 2CLCs and AA5-induced 2CLCs, priorly. Out of these experiments, maybe a correlation between the succinate intracellular concentration and the emergence of 2CLCs will be testified.

The pull-down assay targeting succinylated peptides then identified by mass spectrometry mentioned in the results section was carried out within the global population. We suggest once more that FACS should be done first before such an assay. Single-cell pull-downs are already being used and can still enable further sample processing like microscopic observations (Jain *et al.*, 2011; X. Wang *et al.*, 2018) and maybe mass spectrometry for identification. If through this type of methods, any protein is to be identified as a critical actor in the 2C-like reprogramming, comparing of the phenotype of naïve mESCs and of mESCs expressing this protein in a constitutive succinylated form, thanks to one or several point mutations of the lysine residues into glutamate (Zhang *et al.*, 2011). Such results would force us to re-evaluate the role of protein succinylation in the 2C-like reprogramming.

Oneself could also wonder how cells can survive to SDH inhibition while the complex is part of both the TCA cycle and of the OXPHOS respiratory chain. Actually, naïve ESCs can switch on demand between glycolysis and mitochondrial respiration (Zhou *et al.*, 2012), so it is not really surprising that SDH inhibition to a certain extend do not alter much the phenotype of mESCs. Interestingly, in the mESC CRISPR-Cas9 genome-wide knock out screening mentioned in **Section 1.4.** of the introduction, the A, B and C subunits SDH were identified as critical for the naïve-to-primed transition (Li *et al.*, 2018). Also, the fact that the heme biosynthesis was also shown to prevent the transition (Detraux *et al.*, submitted manuscript), due to a build-up of succinate converges with the importance of SDH subunits. Concomitantly, this is also in line with the accumulation of succinate preventing the differentiation of mESCs and promoting a reprogramming back to an earlier developmental state.

Then, considering succinate as the product of the reactions catalysed by 2OGXs and capable of product inhibition of these enzymes like hypoxia-related PHD, we could go deeper in the study of HIF-1α involvement in the 2C-like reprogramming in order to definitively reject it. The use of $CoCl_2$ enables to stabilise the TF and could allow us to verify for an increase in the 2CLC emergence. In addition, but more technical, thanks to an infection of mESCs by a certain retrovirus, naïve cells can express a stabilised form of HIF-1α (Yan *et al.*, 2007; Mathieu *et al.*, 2014). It would be interesting too to compare the proportion of 2CLCs in such this cell line where HIF-1α is non-degradable. If the TF plays a critical role in the reprogramming, we would expect a rise in the number of 2CLCs compared to the control cell line.

With the aim to investigate the implication of HDMs and TET 5mC demethylases, we opted for the use of two inhibitors, specific to these enzymes but without an entirely great success. First, we can criticize that the efficient concentration has been less carefully defined in our model and rather inspired by literature, and that the inhibitory effect of the JIB has only been partially verified by immunofluorescence. In comparison, C35 concentration has also been selected out of the literature and the inhibitory efficiency has not really been verified. Also, the slight variation observed in trimethylated histone immunofluorescence signal variations may not be much relevant because of the approach that is genome-wide and not restricted to specific genomic regions. Finally, we could not infer anything out of the study of the DNA methylation. Despite the enhanced protocol comprising a DNA denaturation step with HCl, it requires more optimisation in the concentration and incubation time with the acids as several protocols are mentioned in the literature without any consensus [*e.g.*, (Camarena *et al.*, 2017; Zhong *et al.*, 2017)].

Out of this, two conclusions can be underlined. First, a major criticism that could be thrown at this Master's thesis is the extensive use of inhibitors. This implies beforehand preferably rigorous settings of the efficient concentration and also the verification that the molecule is not altering mESCs viability, as we did with AA5. In addition, C35 which has only been reported last year for the first time compared to JIB, is probably less characterized when it comes to possible off-target effects although the whole challenge would be to demonstrate them.

Secondly, immunofluorescence analyses or DNA dot blots are certainly not the best and most contemporary technique for the study of the DNA methylation. As the methylation mainly is lost upon replication step like in the PCR for example, specific methods have been established. One of them is the methylated DNA immunoprecipitation (MeDIP) that allows the production of data about the relative enrichment in methylated cytosine of genomic fragments and that can be followed by next-generation sequencing (MeDIP-Seq) (Zhao *et al.*, 2014). Also, it requires less genomic material compared to other methods of DNA methylation analysis as the bisulfide sequencing (Taiwo *et al.*, 2012; Zhao *et al.*, 2014), which is an advantage accounting the culture characteristics of naïve mESCs that grow in small colonies and that differentiate upon high cell density. Additionally, depending on the antibody selected

for the immunoprecipitation step, the experiment can be adapted according to the demethylation intermediate that is considered, *e.g.*, 5mC, 5hmC (Ficz *et al.*, 2011), 5fC or 5caC (Shen *et al.*, 2013). MeDIP-Seq method would allow us to first, primarily acknowledge the relative DNA methylation differences between naïve mESCs and 2CLCs, and to then identify the differentially methylated genomic regions that followed by bioinformatical analysis might provide insights about critical genes for the 2C-like reprogramming, such as *Dux*, the master regulator gene, as well as inferences about the mechanisms behind this transition. It is to note that as the TET-mediated demethylation of CpG islands is sequential, it might be also of interest to investigate the relative enrichment of at least also 5hmC for better understandings. Furthermore, by taking advantage of TET TKO cell line (Lu *et al.*, 2014), it could be assessed whether AA5 and SA, to test TET involvement, or JIB, for HDMs implication, provoke any effect.

DNA methylation is not the only subject of interest that has not been examined with the most appropriate method, the trimethylation of histones could be better addressed than by immunofluorescence. The immunoprecipitation of trimethylated H3K4 and H3K27 by the mean of chromatin immunoprecipitation followed by next-generation sequencing (ChIP-Seq) is a tempting technique in order to sketch the occupancy of these modified histones on genomic regions genome-wide. Eventually, the comparison between 5mC and other 5-cytosine modifications enrichment along the genome and trimethylated histones occupancy could also highlight some colocalizations of both methylated histones and 5-cytosines. One of the disadvantages of ChIP-Seq is the high quantity of biological material required for the analysis. However, a team has optimized an alternative protocol that they called ultra-low-input micrococcal nuclease-based native ChIP-Seq (ULI-NChIP) that is adapted to small cell subpopulations (Brind'Amour *et al.*, 2015) and that could be transposed to 2CLCs after flow cytometry sorting. The adjective *native* of the ChIP-Seq stands as a substitute to cross-linking using micrococcal nuclease (MNase) digestion, that avoid aspecific signal and improves resolution compared to cross-linking of the histones to the DNA (Alonso, Bernstein and Hasson, 2018).

Another option than the use of inhibitors would be to created KD or KO mutants of the HDMs or TET DNA demethylases, as it has already been done but in different contexts with JMJD3 (Mansour *et al.*, 2012; Ohtani *et al.*, 2013), for KDM5 (JARID1) (Schmitz *et al.*, 2011), and for the three TET enzymes (Dawlaty *et al.*, 2011, 2013, 2014; Lu *et al.*, 2014). Although, the specificity in our case would be to compare the apparition of 2CLCs within the whole population without any treatment at first instance, and to maybe treat the different cell lines with AA5, in order to observe whether or not 2CLCs emerge in different proportions than WT mESCs. To our knowledge, such assays have not been conducted yet.

Whereas the study of the epigenetic landscape of mESCs at a precise timepoint in their oscillation between naïve, 2C-like or even primed state is theoretically assessable with ease, on the contrary, the understanding of the underlying mechanisms provoking the transitions towards one or the other state is

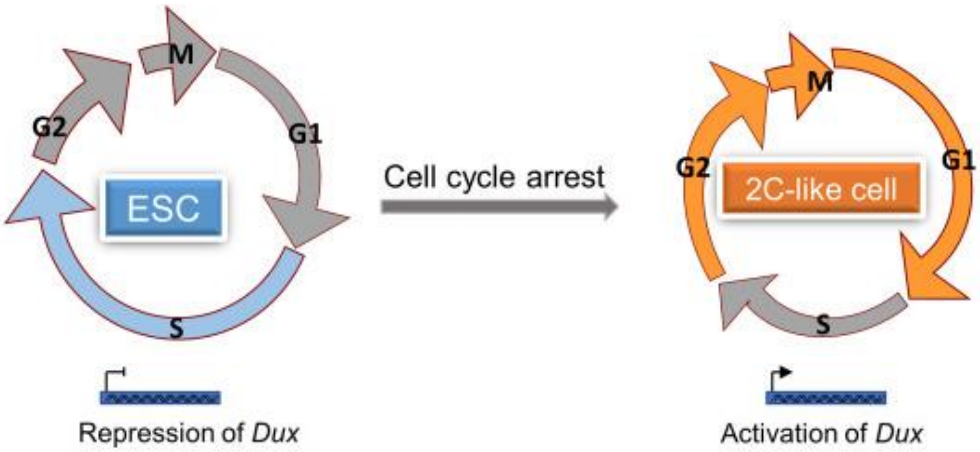

Figure 22. Naïve mESC cell cycle is playing a role in their entry and exit of the 2C-like reprogramming.

By the establishment of transcriptional profiles of 2CLCs by high-throughput methods, a recent report has highlighted a correlation between cell cycle and the naïve-to-2C-like state spontaneous oscillation in mESCs. This study concluded that naïve mESCs were enriched in cells in the S phase of their cell cycle whereas 2CLCs are correlated with the G1 and G2/M phases [modified from (Zhu *et al.*, 2021)].

a challenge, one part due to the multiple layers of epigenetic regulations, *e.g.* DNA methylation, PTMs of histones and chromatin compaction state [reviewed in (Moore, Le and Fan, 2013; Lawrence, Daujat and Schneider, 2016; Quan *et al.*, 2020), respectively], but on the other part because of interactions between these different levels of regulation. As an example, as mentioned previously in the introduction, TETs have also been highlighted at bivalent H3K27me3/H3K4me3 regions of developmental poised genes in mESCs where TET1 interacts with PRC2 for an effective developmental reprogramming (Neri *et al.*, 2013; Shi *et al.*, 2017). Also, a very recent study has reported in mESCs another interplay between histone methylators, being PRC2 and proteins COMPASS family, and DNA methylation for the regulation of developmental genes which expression is dependent on MLL2, a H3K4me2/me3 marks writer (Douillet *et al.*, 2020). Furthermore, H3K4 and H3K27 are not the only histones that alter the epigenetic landscape during the 2C-like reprogramming, other modified histones such as H3K9me3 have also been cited in the literature. Recently, it has been demonstrated that the deposition of H3K9me3 marks could repress MERVL and major satellite repeats due to FOXD3-mediated recruitment of SUV39H1 (a histone methylase), limiting the transition of mESCs towards the 2C-like state. Therefore, the KO of FOXD3 can upregulate MERVL and a subset of other 2C-specific genes (Puri *et al.*, 2021). To conclude, it is needless to mention that these intertwined regulatory mechanisms still need deep investigations for a total understanding of the whole role of epigenetics during the transition from one pluripotent naïve state to a 2C-like state.

One last point that has not been much of an interest in this Master's thesis, is the spontaneous cycling-in and -out of the 2C-like state of naïve mESCs and its dynamical aspects. Thanks to single cell RNA-Seq followed by differentially expressed genes (DEG) and gene set variation analysis (GSVA) analyses to establish the transcriptional profiles of 2CLCs and naïve mESCs at different time points in their 2C-like transition, a team has reported a relationship between the 2C-state and the cell cycle of mESCs. They have concluded that G1 and G2/M phases are correlated to the 2CLCs whereas the S phase characterised by DNA replication is enriched in naïve ESCs **(Figure 22)** (Zhu *et al.*, 2021). This is aligned with previous reports and also with the fast self-renewal exercised by mESCs (Liu *et al.*, 2019). Furthermore, under *Dux* enforced overexpression, a higher proportion of cells were identified as into the G1 and G2/M phases (Zhu *et al.*, 2021). Many other studies have been published about the regulation of the transition and its dynamic (Rodriguez-Terrones *et al.*, 2018; Fu *et al.*, 2020). This is why we suggest to monitor live imaging of Tbg4 naïve mESCs (with additional treatment or not) cycling-in and out- of the 2C-like state.

Finally but not least, a very recent study has underlined the DPPA2 and DPPA4 as essential for 2C-like reprogramming establishment in naïve mESCs (Chen, Xie and Zhang, 2021), supporting a previous report. DPPA2/4 enable the initiation of the 2C-like reprogramming by regulating *Dux* expression (Eckersley-Maslin *et al.*, 2019). However, after *in vivo* experimentations, their conclusions were supporting a rather dispensable implication of DPPA2/4. Due to these diverging results, they have

suggested that 2CLCs might not loyally recapitulate the 2-C stage embryo (Chen, Xie and Zhang, 2021), which is putting into reconsideration the use of this model for the study of totipotent-like state.

To conclude, we have observed a role of a metabolite, succinate, as an actor in the reprogramming of naïve mESCs which consist of a switch towards a totipotent-like state, reminiscent of the 2C-stage embryo. This study has highlighted the impact of the metabolism on the mESCs 2C-like reprogramming as previously suggested by (Rodriguez-Terrones *et al.*, 2020). mESC metabolism has been emphasised to be tightly bound to the epigenetic landscape as the inhibition of histone and DNA demethylating enzymes promotes the 2CLC emergence. Although the omniscient understanding of the mechanism in its globality is still far from being achieved due to the complexity of the process, this matter can be characterised as a scientific hot topic that maybe some advancement in experimentation techniques might solve later on. The very ultimate aim of this research, and possible utopia, would be to manage to stabilise and culture totipotent-like cells enabling multiple and unrestricted differentiation of this type of stem cells for application in regenerative medicine and for the generation of compatible graft supplies for patients. Nevertheless, it is a certainty that such incredible technology ought to be regulated based on ethical debates.

BIBLIOGRAPHY

Abe, K. ichiro *et al.* (2018) 'Minor zygotic gene activation is essential for mouse preimplantation development', *Proceedings of the National Academy of Sciences of the United States of America*, 115(29), pp. E6780–E6788. doi: 10.1073/pnas.1804309115.

Adam Collinson, A. *et al.* (2016) 'Deletion of the Polycomb-Group Protein EZH2 Leads to Compromised Self-Renewal and Differentiation Defects in Human Embryonic Stem Cells Accession Numbers GSE76626', *CellReports*, 17, pp. 2700–2714. doi: 10.1016/j.celrep.2016.11.032.

Alonso, A., Bernstein, E. and Hasson, D. (2018) 'Histone Native Chromatin Immunoprecipitation', in *Methods in Molecular Biology*. Springer Science+Business Media, pp. 77–104. doi: 10.1007/978-1-4939-8663-7_5.

Amano, T. *et al.* (2009) 'Nuclear Transfer Embryonic Stem Cells Provide an In Vitro Culture Model for Parkinson's Disease', *https://home.liebertpub.com/clo*, 11(1), pp. 77–87. doi: 10.1089/CLO.2008.0059.

Amouroux, R. *et al.* (2016) 'De novo DNA methylation drives 5hmC accumulation in mouse zygotes', *Nature Cell Biology 2016 18:2*, 18(2), pp. 225–233. doi: 10.1038/ncb3296.

Andreu-Vieyra, C. V. *et al.* (2010) 'MLL2 is required in oocytes for bulk histone 3 lysine 4 trimethylation and transcriptional silencing', *PLoS Biology*, 8(8), pp. 53–54. doi: 10.1371/journal.pbio.1000453.

Atamna, H. (2004) 'Heme, iron, and the mitochondrial decay of ageing', *Ageing Research Reviews*. Elsevier, pp. 303–318. doi: 10.1016/j.arr.2004.02.002.

Avilion, A. A. *et al.* (2003) 'Multipotent cell lineages in early mouse development depend on SOX2 function', *Genes and Development*, 17(1), pp. 126–140. doi: 10.1101/gad.224503.

Baker, C. L. and Pera, M. F. (2018) 'Capturing Totipotent Stem Cells', *Cell Stem Cell*, 22(1), pp. 25–34. doi: 10.1016/j.stem.2017.12.011.

Bao, S. *et al.* (2009) 'Epigenetic reversion of postimplantation epiblast cells to pluripotent embryonic stem cells', *Nature*, 461(7268), pp. 1292–1295. doi: 10.1038/NATURE08534.

Barski, A. *et al.* (2007) 'High-Resolution Profiling of Histone Methylations in the Human Genome', *Cell*, 129(4), pp. 823–837. doi: 10.1016/J.CELL.2007.05.009.

Batlle-Morera, L., Smith, A. and Nichols, J. (2008) 'Parameters influencing derivation of embryonic stem cells from murine embryos', *genesis*, 46(12), pp. 758–767. doi: 10.1002/dvg.20442.

Bernstein, B. E. *et al.* (2006) 'A Bivalent Chromatin Structure Marks Key Developmental Genes in Embryonic Stem Cells', *Cell*, 125(2), pp. 315–326. doi: 10.1016/j.cell.2006.02.041.

Binó, L. *et al.* (2016) 'The stabilization of hypoxia inducible factor modulates differentiation status and inhibits the proliferation of mouse embryonic stem cells', *Chemico-Biological Interactions*, 244, pp. 204–214. doi: 10.1016/J.CBI.2015.12.007.

Bourque, G. *et al.* (2008) 'Evolution of the mammalian transcription factor binding repertoire via transposable elements', *Genome Research*, 18(11), p. 1752. doi: 10.1101/GR.080663.108.

Brind'Amour, J. *et al.* (2015) 'An ultra-low-input native ChIP-seq protocol for genome-wide profiling of rare cell populations', *Nature Communications*, 6. doi: 10.1038/ncomms7033.

Burchfield, J. S. *et al.* (2015) 'JMJD3 as an epigenetic regulator in development and disease', *The International Journal of Biochemistry & Cell Biology*, 67, pp. 148–157. doi:

10.1016/J.BIOCEL.2015.07.006.

Burgold, T. *et al.* (2012) 'The H3K27 Demethylase JMJD3 Is Required for Maintenance of the Embryonic Respiratory Neuronal Network, Neonatal Breathing, and Survival', *Cell Reports*, 2(5), pp. 1244–1258. doi: 10.1016/J.CELREP.2012.09.013.

Burr, S. *et al.* (2018) 'Oxygen gradients can determine epigenetic asymmetry and cellular differentiation viadifferential regulation of Tet activity in embryonic stem cells', *Nucleic Acids Research*, 46(3). doi: 10.1093/nar/gkx1197.

Burton, A. *et al.* (2020) 'Heterochromatin establishment during early mammalian development is regulated by pericentromeric RNA and characterized by non-repressive H3K9me3', *Nature Cell Biology*, 22(7), pp. 767–778. doi: 10.1038/s41556-020-0536-6.

Camarena, V. *et al.* (2017) 'CAMP signaling regulates DNA hydroxymethylation by augmenting the intracellular labile ferrous iron pool', *eLife*, 6. doi: 10.7554/eLife.29750.

Cao, R. and Zhang, Y. (2004) 'The functions of E(Z)/EZH2-mediated methylation of lysine 27 in histone H3', *Current Opinion in Genetics & Development*, 14(2), pp. 155–164. doi: 10.1016/j.gde.2004.02.001.

Carey, B. W. *et al.* (2015) 'Intracellular α-ketoglutarate maintains the pluripotency of.pdf', *Nature*, 518(7539), pp. 413–416. doi: 10.1038/nature13981.Intracellular.

Cervera, A. M. *et al.* (2009) 'Inhibition of succinate dehydrogenase dysregulates histone modification in mammalian cells', *Molecular Cancer*, 8(1), p. 89. doi: 10.1186/1476-4598-8-89.

Chamberlain, S. J., Yee, D. and Magnuson, T. (2008) 'Polycomb Repressive Complex 2 Is Dispensable for Maintenance of Embryonic Stem Cell Pluripotency', *STEM CELLS*, 26(6), pp. 1496–1505. doi: 10.1634/STEMCELLS.2008-0102.

Chazaud, C. *et al.* (2006) 'Early Lineage Segregation between Epiblast and Primitive Endoderm in Mouse Blastocysts through the Grb2-MAPK Pathway', *Developmental Cell*, 10(5), pp. 615–624. doi: 10.1016/j.devcel.2006.02.020.

Chen, Z., Xie, Z. and Zhang, Y. (2021) 'DPPA2 and DPPA4 are dispensable for mouse zygotic genome activation and preimplantation development', *Development*. doi: 10.1242/dev.200178.

Chinopoulos, C. and Valenti, D. (2021) 'The Mystery of Extramitochondrial Proteins Lysine Succinylation', *International Journal of Molecular Sciences 2021, Vol. 22, Page 6085*, 22(11), p. 6085. doi: 10.3390/IJMS22116085.

Dahl, J. A. *et al.* (2016) 'Broad histone H3K4me3 domains in mouse oocytes modulate maternal-to-zygotic transition', *Nature*, 537(7621), pp. 548–552. doi: 10.1038/nature19360.

Dawlaty, M. M. *et al.* (2011) 'Tet1 is dispensable for maintaining pluripotency and its loss is compatible with embryonic and postnatal development', *Cell Stem Cell*, 9(2), pp. 166–175. doi: 10.1016/j.stem.2011.07.010.

Dawlaty, M. M. *et al.* (2013) 'Combined Deficiency of Tet1 and Tet2 Causes Epigenetic Abnormalities but Is Compatible with Postnatal Development', *Developmental Cell*, 24(3), pp. 310–323. doi: 10.1016/j.devcel.2012.12.015.

Dawlaty, M. M. *et al.* (2014) 'Loss of tet enzymes compromises proper differentiation of embryonic stem cells', *Developmental Cell*, 29(1), pp. 102–111. doi: 10.1016/j.devcel.2014.03.003.

Douillet, D. *et al.* (2020) 'Uncoupling histone H3K4 trimethylation from developmental gene expression via an equilibrium of COMPASS, Polycomb and DNA methylation', *Nature Genetics*, 52(6),

pp. 615–625. doi: 10.1038/s41588-020-0618-1.

Du, J. *et al.* (2011) 'Sirt5 is a NAD-dependent protein lysine demalonylase and desuccinylase', *Science*, 334(6057), pp. 806–809. doi: 10.1126/science.1207861.

Dunn, K. W., Kamocka, M. M. and McDonald, J. H. (2011) 'A practical guide to evaluating colocalization in biological microscopy', *AJP: Cell Physiology*, 300(4), pp. C723–C742. doi: 10.1152/ajpcell.00462.2010.

Eckersley-Maslin, M. *et al.* (2019) 'Dppa2 and Dppa4 directly regulate the Dux-driven zygotic transcriptional program', *Genes and Development*, 33(3–4), pp. 194–208. doi: 10.1101/gad.321174.118.

Eckersley-Maslin, M. A., Alda-Catalinas, C. and Reik, W. (2018) *Dynamics of the epigenetic landscape during the maternal-to-zygotic transition*, *Nature Reviews Molecular Cell Biology*. Nature Publishing Group. doi: 10.1038/s41580-018-0008-z.

Evans, M. J. and Kaufman, M. H. (1981) 'Establishment in culture of pluripotential cells from mouse embryos', *Nature*, 292(5819), pp. 154–156. doi: 10.1038/292154a0.

Fatehullah, A., Tan, S. H. and Barker, N. (2016) 'Organoids as an in vitro model of human development and disease', *Nature Cell Biology*. Nature Publishing Group, pp. 246–254. doi: 10.1038/ncb3312.

Ficz, G. *et al.* (2011) 'Dynamic regulation of 5-hydroxymethylcytosine in mouse ES cells and during differentiation', *Nature*, 473(7347), pp. 398–404. doi: 10.1038/nature10008.

Fu, X. *et al.* (2020) 'A transcriptional roadmap for 2C-like-to-pluripotent state transition', *Science Advances*, 6(22), pp. 5181–5210. doi: 10.1126/SCIADV.AAY5181/SUPPL_FILE/AAY5181_TABLE_S6.XLSX.

Genet, M. and Torres-Padilla, M. E. (2020) 'The molecular and cellular features of 2-cell-like cells: a reference guide', *Development (Cambridge, England)*, 147(16). doi: 10.1242/dev.189688.

Ginno, P. A. *et al.* (2020) 'A genome-scale map of DNA methylation turnover identifies site-specific dependencies of DNMT and TET activity', *Nature Communications*, 11(1), pp. 1–16. doi: 10.1038/s41467-020-16354-x.

Grow, E. J. *et al.* (2015) 'Intrinsic retroviral reactivation in human preimplantation embryos and pluripotent cells', *Nature*, 522(7555), pp. 221–246. doi: 10.1038/nature14308.

Grzenda, A. *et al.* (2009) 'Sin3: Master scaffold and transcriptional corepressor', *Biochimica et Biophysica Acta - Gene Regulatory Mechanisms*. Biochim Biophys Acta, pp. 443–450. doi: 10.1016/j.bbagrm.2009.05.007.

Guallar, D. *et al.* (2018) 'stem cells', *Nature Genetics*. doi: 10.1038/s41588-018-0060-9.

Gui, L. *et al.* (2016) 'Implantable tissue-engineered blood vessels from human induced pluripotent stem cells', *Biomaterials*, 102, pp. 120–129. doi: 10.1016/j.biomaterials.2016.06.010.

Gurusamy, N. *et al.* (2018) *Adult Stem Cells for Regenerative Therapy*. 1st edn, *Progress in Molecular Biology and Translational Science*. 1st edn. Elsevier Inc. doi: 10.1016/bs.pmbts.2018.07.009.

Hackett, J. A. and Azim Surani, M. (2014) 'Regulatory principles of pluripotency: From the ground state up', *Cell Stem Cell*. Cell Press, pp. 416–430. doi: 10.1016/j.stem.2014.09.015.

Hadlaczky, G., Went, M. and Ringertz, N. R. (1986) 'Direct evidence for the non-random localization of mammalian chromosomes in the interphase nucleus', *Experimental Cell Research*, 167(1), pp. 1–15. doi: 10.1016/0014-4827(86)90199-0.

Hägerhäll, C. (1997) 'Succinate: Quinone oxidoreductases. Variations on a conserved theme', *Biochimica et Biophysica Acta - Bioenergetics*. Elsevier, pp. 107–141. doi: 10.1016/S0005-2728(97)00019-4.

Hammoud, S. S. *et al.* (2014) 'Chromatin and Transcription Transitions of Mammalian Adult Germline Stem Cells and Spermatogenesis', *Cell Stem Cell*, 15(2), pp. 239–253. doi: 10.1016/J.STEM.2014.04.006.

Hausinger, R. P. (2015) 'CHAPTER 1. Biochemical Diversity of 2-Oxoglutarate-Dependent Oxygenases', in *RSC Metallobiology*. Royal Society of Chemistry, pp. 1–58. doi: 10.1039/9781782621959-00001.

He, Y. F. *et al.* (2011) 'Tet-mediated formation of 5-carboxylcytosine and its excision by TDG in mammalian DNA', *Science*, 333(6047), pp. 1303–1307. doi: 10.1126/science.1210944.

Hermann, A., Goyal, R. and Jeltsch, A. (2004) 'The Dnmt1 DNA-(cytosine-C5)-methyltransferase methylates DNA processively with high preference for hemimethylated target sites', *Journal of Biological Chemistry*, 279(46), pp. 48350–48359. doi: 10.1074/jbc.M403427200.

Hopkinson, R. J. *et al.* (2010) 'Monitoring the activity of 2-oxoglutarate dependent histone demethylases by NMR spectroscopy: Direct observation of formaldehyde', *ChemBioChem*, 11(4), pp. 506–510. doi: 10.1002/CBIC.200900713.

Huang, D. W., Sherman, B. T. and Lempicki, R. A. (2009a) 'Bioinformatics enrichment tools: Paths toward the comprehensive functional analysis of large gene lists', *Nucleic Acids Research*, 37(1), pp. 1–13. doi: 10.1093/nar/gkn923.

Huang, D. W., Sherman, B. T. and Lempicki, R. A. (2009b) 'Systematic and integrative analysis of large gene lists using DAVID bioinformatics resources', *Nature Protocols*, 4(1), pp. 44–57. doi: 10.1038/nprot.2008.211.

Huang, Y. *et al.* (2014) 'Distinct roles of the methylcytosine oxidases Tet1 and Tet2 in mouse embryonic stem cells', *Proceedings of the National Academy of Sciences of the United States of America*, 111(4), pp. 1361–1366. doi: 10.1073/pnas.1322921111.

Huang, Z. *et al.* (2021) 'The chromosomal protein SMCHD1 regulates DNA methylation and the 2c-like state of embryonic stem cells by antagonizing TET proteins', *Science Advances*, 7(4), pp. 1–16. doi: 10.1126/sciadv.abb9149.

De Iaco, A. *et al.* (2017) 'DUX-family transcription factors regulate zygotic genome activation in placental mammals', *Nature Genetics*, 49(6), pp. 941–945. doi: 10.1038/ng.3858.

Ishiuchi, T. *et al.* (2015) 'Early embryonic-like cells are induced by downregulating replication-dependent chromatin assembly', *Nature Structural and Molecular Biology*, 22(9), pp. 662–671. doi: 10.1038/nsmb.3066.

Islam, M. S. *et al.* (2018) '2-Oxoglutarate-Dependent Oxygenases', *Annual Review of Biochemistry*. Annual Reviews, pp. 585–620. doi: 10.1146/annurev-biochem-061516-044724.

Ito, S. *et al.* (2010) 'Role of tet proteins in 5mC to 5hmC conversion, ES-cell self-renewal and inner cell mass specification', *Nature*, 466(7310), pp. 1129–1133. doi: 10.1038/nature09303.

Ito, S. *et al.* (2011) 'Tet proteins can convert 5-methylcytosine to 5-formylcytosine and 5-carboxylcytosine', *Science*, 333(6047), pp. 1300–1303. doi: 10.1126/science.1210597.

Itoh, F., Watabe, T. and Miyazono, K. (2014) 'Roles of TGF-β family signals in the fate determination of pluripotent stem cells', *Seminars in Cell and Developmental Biology*. Elsevier Ltd, pp. 98–106. doi: 10.1016/j.semcdb.2014.05.017.

Ivan, M. *et al.* (2001) 'HIFα targeted for VHL-mediated destruction by proline hydroxylation: Implications for O2 sensing', *Science*, 292(5516), pp. 464–468. doi: 10.1126/science.1059817.

Jachowicz, J. W. *et al.* (2017) 'LINE-1 activation after fertilization regulates global chromatin accessibility in the early mouse embryo', *Nature Genetics*, 49(10), pp. 1502–1510. doi: 10.1038/ng.3945.

Jain, A. *et al.* (2011) 'Probing cellular protein complexes using single-molecule pull-down', *Nature*, 473(7348), pp. 484–488. doi: 10.1038/nature10016.

Johnson, J. D. *et al.* (1998) 'Genetic evidence for the expression of ATP- and GTP-specific succinyl- CoA synthetases in multicellular eucaryotes', *Journal of Biological Chemistry*, 273(42), pp. 27580–27586. doi: 10.1074/jbc.273.42.27580.

Jones, R. S. and Gelbart, W. M. (1993) 'The Drosophila Polycomb-group gene Enhancer of zeste contains a region with sequence similarity to trithorax', *Molecular and Cellular Biology*, 13(10), pp. 6357–6366. doi: 10.1128/mcb.13.10.6357-6366.1993.

Jukam, D., Shariati, S. A. M. and Skotheim, J. M. (2017) 'Zygotic Genome Activation in Vertebrates', *Developmental Cell*. Cell Press, pp. 316–332. doi: 10.1016/j.devcel.2017.07.026.

Kagiwada, S. *et al.* (2013) 'Replication-coupled passive DNA demethylation for the erasure of genome imprints in mice', *EMBO Journal*, 32(3), pp. 340–353. doi: 10.1038/emboj.2012.331.

Kebede, A. F., Schneider, R. and Daujat, S. (2015) 'Novel types and sites of histone modifications emerge as players in the transcriptional regulation contest', *FEBS Journal*, 282(9), pp. 1658–1674. doi: 10.1111/febs.13047.

Kenneth, N. S. and Rocha, S. (2008) 'Regulation of gene expression by hypoxia', *Biochemical Journal*, 414(1), pp. 19–29. doi: 10.1042/BJ20081055.

Kim, Ji Hye *et al.* (2019) 'Identification of a novel SIRT7 inhibitor as anticancer drug candidate', *Biochemical and Biophysical Research Communications*, 508(2), pp. 451–457. doi: 10.1016/j.bbrc.2018.11.120.

Kinoshita, M. and Smith, A. (2018) 'Pluripotency Deconstructed', *Development Growth and Differentiation*. Blackwell Publishing, pp. 44–52. doi: 10.1111/dgd.12419.

Klose, R. J., Kallin, E. M. and Zhang, Y. (2006) 'JmjC-domain-containing proteins and histone demethylation', *Nature Reviews Genetics*, 7(9), pp. 715–727. doi: 10.1038/nrg1945.

Kluckova, K. and Tennant, D. A. (2018) 'Metabolic implications of hypoxia and pseudohypoxia in pheochromocytoma and paraganglioma', *Cell and Tissue Research*. Springer Verlag, pp. 367–378. doi: 10.1007/s00441-018-2801-6.

Ko, M. S. H. (2016) 'Zygotic Genome Activation Revisited: Looking Through the Expression and Function of Zscan4', *Current Topics in Developmental Biology*, 120, pp. 103–124. doi: 10.1016/bs.ctdb.2016.04.004.

Koivunen, P. *et al.* (2007) 'Inhibition of hypoxia-inducible factor (HIF) hydroxylases by citric acid cycle intermediates: Possible links between cell metabolism and stabilization of HIF', *Journal of Biological Chemistry*, 282(7), pp. 4524–4532. doi: 10.1074/JBC.M610415200.

Kolios, G. and Moodley, Y. (2012) 'Introduction to stem cells and regenerative medicine', *Respiration*. Karger Publishers, pp. 3–10. doi: 10.1159/000345615.

Kornberg, R. D. (1974) 'Chromatin Structure: A Repeating Unit of Histones and DNA', *Science*, 184(4139), pp. 868–871. doi: 10.1126/science.184.4139.868.

Kouzarides, T. (2007) 'Chromatin Modifications and Their Function', *Cell*. Cell, pp. 693–705. doi: 10.1016/j.cell.2007.02.005.

Kumar, P., Nagarajan, A. and Uchil, P. D. (2018) 'Analysis of Cell Viability by the MTT Assay', pp. 469–472. doi: 10.1101/pdb.prot095505.

de la Rica, L. *et al.* (2016) 'TET-dependent regulation of retrotransposable elements in mouse embryonic stem cells.', *Genome Biology*, 17(1), p. 234. doi: 10.1186/s13059-016-1096-8.

Lancaster, M. A. and Huch, M. (2019) 'Disease modelling in human organoids', *DMM Disease Models and Mechanisms*, 12(7). doi: 10.1242/dmm.039347.

Laugesen, A., Højfeldt, J. W. and Helin, K. (2019) 'Molecular Mechanisms Directing PRC2 Recruitment and H3K27 Methylation', *Molecular Cell*, 74(1), pp. 8–18. doi: 10.1016/J.MOLCEL.2019.03.011.

Laukka, T. *et al.* (2016) 'Fumarate and succinate regulate expression of hypoxia-inducible genes via TET enzymes', *Journal of Biological Chemistry*, 291(8), pp. 4256–4265. doi: 10.1074/jbc.M115.688762.

Lawrence, M., Daujat, S. and Schneider, R. (2016) 'Lateral Thinking: How Histone Modifications Regulate Gene Expression', *Trends in Genetics*, 32(1), pp. 42–56. doi: 10.1016/J.TIG.2015.10.007.

Le, R. *et al.* (2021) 'Dcaf11 activates Zscan4-mediated alternative telomere lengthening in early embryos and embryonic stem cells', *Cell Stem Cell*, 28(4), pp. 732-747.e9. doi: 10.1016/j.stem.2020.11.018.

Lee, S.-W. W. *et al.* (2012) 'Hypoxic priming of mESCs accelerates vascular-lineage differentiation through HIF1-mediated inverse regulation of Oct4 and VEGF', *EMBO Molecular Medicine*, 4(9). doi: 10.1002/EMMM.201101107.

Lee, Y. M. *et al.* (2001) 'Determination of hypoxic region by hypoxia marker in developing mouse embryos in vivo: A possible signal for vessel development', *Developmental Dynamics*, 220(2), pp. 175–186. doi: 10.1002/1097-0177(20010201)220:2<175::AID-DVDY1101>3.0.CO;2-F.

Lemarie, A. and Grimm, S. (2009) 'Mutations in the heme b-binding residue of SDHC inhibit assembly of respiratory chain complex II in mammalian cells', *Mitochondrion*, 9(4), pp. 254–260. doi: 10.1016/j.mito.2009.03.004.

Li, E. and Zhang, Y. (2014) 'DNA methylation in mammals', *Cold Spring Harbor Perspectives in Biology*, 6(5). doi: 10.1101/cshperspect.a019133.

Li, L. *et al.* (2016) 'SIRT7 is a histone desuccinylase that functionally links to chromatin compaction and genome stability', *Nature Communications*, 7. doi: 10.1038/ncomms12235.

Li, M. *et al.* (2018) 'Genome-wide CRISPR-KO Screen Uncovers mTORC1-Mediated Gsk3 Regulation in Naive Pluripotency Maintenance and Dissolution', *Cell Reports*, 24(2), pp. 489–502. doi: 10.1016/j.celrep.2018.06.027.

Lister, R. *et al.* (2009) 'Human DNA methylomes at base resolution show widespread epigenomic differences', *Nature*, 462(7271), pp. 315–322. doi: 10.1038/nature08514.

Liu, L. *et al.* (2019) 'The cell cycle in stem cell proliferation, pluripotency and differentiation', *Nature Cell Biology*. Nature Publishing Group, pp. 1060–1067. doi: 10.1038/s41556-019-0384-4.

Lu, C. C., Brennan, J. and Robertson, E. J. (2001) 'From fertilization to gastrulation: Axis formation in the mouse embryo', *Current Opinion in Genetics and Development*, pp. 384–392. doi: 10.1016/S0959-437X(00)00208-2.

Lu, F. *et al.* (2014) 'Role of Tet proteins in enhancer activity and telomere elongation', *Genes & Development*, 28(19), pp. 2103–2119. doi: 10.1101/gad.248005.114.

Luger, K. *et al.* (1997) 'Crystal structure of the nucleosome core particle at 2.8 Å resolution', *Nature*, 389(6648), pp. 251–260. doi: 10.1038/38444.

Macfarlan, T. S. *et al.* (2011) 'Endogenous retroviruses and neighboring genes are coordinately repressed by LSD1/KDM1A', *Genes & Development*, 25(6), pp. 594–607. doi: 10.1101/GAD.2008511.

Macfarlan, T. S. *et al.* (2013) 'HHS Public Access', 487(7405), pp. 57–63. doi: 10.1038/nature11244.ES.

Mahon, P. C., Hirota, K. and Semenza, G. L. (2001) 'FIH-1: A novel protein that interacts with HIF-1α and VHL to mediate repression of HIF-1 transcriptional activity', *Genes and Development*, 15(20), pp. 2675–2686. doi: 10.1101/GAD.924501.

Maiti, A. and Drohat, A. C. (2011) 'Thymine DNA glycosylase can rapidly excise 5-formylcytosine and 5-carboxylcytosine: Potential implications for active demethylation of CpG sites', *Journal of Biological Chemistry*, 286(41), pp. 35334–35338. doi: 10.1074/jbc.C111.284620.

Mandai, M. *et al.* (2017) 'Autologous Induced Stem-Cell–Derived Retinal Cells for Macular Degeneration', *http://dx.doi.org/10.1056/NEJMoa1608368*, 376(11), pp. 1038–1046. doi: 10.1056/NEJMOA1608368.

Mansour, A. A. *et al.* (2012) 'The H3K27 demethylase Utx regulates somatic and germ cell epigenetic reprogramming', *Nature*. Nature Publishing Group, pp. 409–413. doi: 10.1038/nature11272.

Martin, G. R. (1981) 'Isolation of a pluripotent cell line from early mouse embryos cultured in medium conditioned by teratocarcinoma stem cells', *Proceedings of the National Academy of Sciences of the United States of America*, 78(12 II), pp. 7634–7638. doi: 10.1073/pnas.78.12.7634.

Massagué, J., Seoane, J. and Wotton, D. (2005) 'Smad transcription factors', *Genes and Development*. Cold Spring Harbor Laboratory Press, pp. 2783–2810. doi: 10.1101/gad.1350705.

Mathieu, J. *et al.* (2014) 'Hypoxia-inducible factors have distinct and stage-specific roles during reprogramming of human cells to pluripotency', *Cell Stem Cell*, 14(5), pp. 592–605. doi: 10.1016/j.stem.2014.02.012.

Mathieu, J. *et al.* (2019) 'Folliculin regulates mTORC1/2 and WNT pathways in early human pluripotency', *Nature Communications*, 10(1). doi: 10.1038/s41467-018-08020-0.

Matsushita, N. *et al.* (2011) 'Distinct regulation of mitochondrial localization and stability of two human Sirt5 isoforms', *Genes to Cells*, 16(2), pp. 190–202. doi: 10.1111/j.1365-2443.2010.01475.x.

Maxwell, P. H., Pugh, C. W. and Ratcliffe, P. J. (2001) 'The pVHL-HIF-1 system: A key mediator of oxygen homeostasis', in *Advances in Experimental Medicine and Biology*. Kluwer Academic/Plenum Publishers, pp. 365–376. doi: 10.1007/978-1-4757-3401-0_24.

McDonough, M. A. *et al.* (2010) 'Structural studies on human 2-oxoglutarate dependent oxygenases', *Current Opinion in Structural Biology*, 20(6), pp. 659–672. doi: 10.1016/j.sbi.2010.08.006.

Melchiorri, A. J. *et al.* (2016) '3D-Printed Biodegradable Polymeric Vascular Grafts', *Advanced Healthcare Materials*, 5(3), pp. 319–325. doi: 10.1002/ADHM.201500725.

Meng, H. *et al.* (2015) 'DNA methylation, its mediators and genome integrity', *International Journal of Biological Sciences*, 11(5), pp. 604–617. doi: 10.7150/ijbs.11218.

Mihajlović, A. I. and Bruce, A. W. (2017) 'The first cell-fate decision of mouse preimplantation embryo development: Integrating cell position and polarity', *Open Biology*. Royal Society Publishing. doi: 10.1098/rsob.170210.

Mikkelsen, T. S. *et al.* (2007) 'Genome-wide maps of chromatin state in pluripotent and lineage-committed cells', *Nature*, 448(7153), pp. 553–560. doi: 10.1038/nature06008.

Miyadera, H. *et al.* (2003) 'Atpenins, potent and specific inhibitors of mitochondrial complex II (succinate-ubiquinone oxidoreductase)', *Proceedings of the National Academy of Sciences of the United States of America*, 100(2), pp. 473–477. doi: 10.1073/pnas.0237315100.

Moore, L. D., Le, T. and Fan, G. (2013) 'DNA methylation and its basic function', *Neuropsychopharmacology*. Neuropsychopharmacology, pp. 23–38. doi: 10.1038/npp.2012.112.

Morey, L. and Helin, K. (2010) 'Polycomb group protein-mediated repression of transcription', *Trends in Biochemical Sciences*, 35(6), pp. 323–332. doi: 10.1016/J.TIBS.2010.02.009.

Mosmann, T. (1983) 'Rapid colorimetric assay for cellular growth and survival: Application to proliferation and cytotoxicity assays', *Journal of Immunological Methods*, 65(1–2), pp. 55–63. doi: 10.1016/0022-1759(83)90303-4.

Müller, J. *et al.* (2002) 'Histone Methyltransferase Activity of a Drosophila Polycomb Group Repressor Complex', *Cell*, 111(2), pp. 197–208. doi: 10.1016/S0092-8674(02)00976-5.

Myllyharju, J. and Kivirikko, K. I. (2004) 'Collagens, modifying enzymes and their mutations in humans, flies and worms', *Trends in Genetics*, 20(1), pp. 33–43. doi: 10.1016/J.TIG.2003.11.004.

Nagarajan, P. *et al.* (2013) 'Histone Acetyl Transferase 1 Is Essential for Mammalian Development, Genome Stability, and the Processing of Newly Synthesized Histones H3 and H4', *PLoS Genetics*, 9(6), p. 1003518. doi: 10.1371/journal.pgen.1003518.

Neri, F. *et al.* (2013) 'Genome-wide analysis identifies a functional association of Tet1 and Polycomb repressive complex 2 in mouse embryonic stem cells', *Genome Biology*, 14(8), p. R91. doi: 10.1186/gb-2013-14-8-r91.

Nestor, C. E. *et al.* (2012) 'Tissue type is a major modifier of the 5-hydroxymethylcytosine content of human genes', *Genome Research*, 22(3), pp. 467–477. doi: 10.1101/gr.126417.111.

Ng, S. S. *et al.* (2007) 'Crystal structures of histone demethylase JMJD2A reveal basis for substrate specificity', *Nature*, 448(7149), pp. 87–91. doi: 10.1038/nature05971.

Nichols, J. *et al.* (2009) 'Validated germline-competent embryonic stem cell lines from nonobese diabetic mice', *Nature Medicine 2009 15:7*, 15(7), pp. 814–818. doi: 10.1038/nm.1996.

Nichols, J. and Smith, A. (2009) 'Naive and Primed Pluripotent States', *Cell Stem Cell*, 4(6), pp. 487–492. doi: 10.1016/j.stem.2009.05.015.

Nishimura, B. J. S. (1986) 'Succinyl-coa synthetase structure-function relationships and other considerations', 58.

Niwa, H. *et al.* (1998) 'Self-renewal of pluripotent embryonic stem cells is mediated via activation of STAT3', *Genes and Development*, 12(13), pp. 2048–2060. doi: 10.1101/gad.12.13.2048.

Ohtani, K. *et al.* (2013) 'Jmjd3 controls mesodermal and cardiovascular differentiation of embryonic stem cells', *Circulation Research*, 113(7), pp. 856–862. doi: 10.1161/CIRCRESAHA.113.302035.

Okano, M. *et al.* (1999) 'DNA methyltransferases Dnmt3a and Dnmt3b are essential for de novo

methylation and mammalian development', *Cell*, 99(3), pp. 247–257. doi: 10.1016/S0092-8674(00)81656-6.

Oudet, P., Gross-Bellard, M. and Chambon, P. (1975) 'Electron microscopic and biochemical evidence that chromatin structure is a repeating unit', *Cell*, 4(4), pp. 281–300. doi: 10.1016/0092-8674(75)90149-X.

Palmieri, F. *et al.* (1971) 'Kinetic Study of the Dicarboxylate Carrier in Rat Liver Mitochondria', *European Journal of Biochemistry*, 22(1), pp. 66–74. doi: 10.1111/j.1432-1033.1971.tb01515.x.

Park, J.-M. and Kang, T.-H. (2015) 'DNA Slot Blot Repair Assay', *BIO-PROTOCOL*, 5(8). doi: 10.21769/bioprotoc.1453.

Park, J. *et al.* (2013) 'SIRT5-Mediated Lysine Desuccinylation Impacts Diverse Metabolic Pathways', *Molecular Cell*, 50(6), pp. 919–930. doi: 10.1016/j.molcel.2013.06.001.

Pasini, D. *et al.* (2010) 'JARID2 regulates binding of the Polycomb repressive complex 2 to target genes in ES cells', *Nature 2010 464:7286*, 464(7286), pp. 306–310. doi: 10.1038/nature08788.

Peaston, A. E. *et al.* (2004) 'Retrotransposons regulate host genes in mouse oocytes and preimplantation embryos', *Developmental Cell*, 7(4), pp. 597–606. doi: 10.1016/j.devcel.2004.09.004.

Pei, J. and Grishin, N. V. (2013) 'A new family of predicted krüppel-like factor genes and pseudogenes in placental mammals', *PLoS ONE*, 8(11), p. 81109. doi: 10.1371/journal.pone.0081109.

Percharde, M. *et al.* (2018) 'A LINE1-Nucleolin Partnership Regulates Early Development and ESC Identity.', *Cell*, 174(2), pp. 391-405.e19. doi: 10.1016/j.cell.2018.05.043.

Puri, D. *et al.* (2021) 'Foxd3 controls heterochromatin-mediated repression of repeat elements and 2-cell state transcription', *EMBO reports*, 22(12). doi: 10.15252/embr.202153180.

Quan, H. *et al.* (2020) 'Chromatin structure changes during various processes from a DNA sequence view', *Current Opinion in Structural Biology*. Elsevier Current Trends, pp. 1–8. doi: 10.1016/j.sbi.2019.10.010.

Ramsahoye, B. H. *et al.* (2000) 'Non-CpG methylation is prevalent in embryonic stem cells and may be mediated by DNA methyltransferase 3a', *Proceedings of the National Academy of Sciences of the United States of America*, 97(10), pp. 5237–5242. doi: 10.1073/pnas.97.10.5237.

Robinson, B. H. and Williams, G. R. (1970) 'The sensitivity of dicarboxylate anion exchange reactions to transport inhibitors in rat-liver mitochondria', *BBA - Bioenergetics*, 216(1), pp. 63–70. doi: 10.1016/0005-2728(70)90159-3.

Rodriguez-Terrones, D. *et al.* (2018) 'A molecular roadmap for the emergence of early-embryonic-like cells in culture', *Nature Genetics*, 50(1), pp. 106–119. doi: 10.1038/s41588-017-0016-5.

Rodriguez-Terrones, D. *et al.* (2020) 'A distinct metabolic state arises during the emergence of 2-cell-like cells', *EMBO reports*, 21(1), pp. 1–14. doi: 10.15252/embr.201948354.

Romero-Lanman, E. E. *et al.* (2012) 'Id1 Maintains Embryonic Stem Cell Self-Renewal by Up-Regulation of Nanog and Repression of Brachyury Expression', *Stem Cells and Development*, 21(3), pp. 384–393. doi: 10.1089/scd.2011.0428.

Romito, A. and Cobellis, G. (2016) 'Pluripotent stem cells: Current understanding and future directions', *Stem Cells International*. Hindawi Publishing Corporation. doi: 10.1155/2016/9451492.

Santos-Rosa, H. *et al.* (2002) 'Active genes are tri-methylated at K4 of histone H3', *Nature 2002*

419:6905, 419(6905), pp. 407–411. doi: 10.1038/nature01080.

Sassa, S. and Kappas, A. (1983) 'Hereditary tyrosinemia and the heme biosynthetic pathway. Profound inhibition of δ-aminolevulinic acid dehydratase activity by succinylacetone', *Journal of Clinical Investigation*, 71(3), pp. 625–634. doi: 10.1172/JCI110809.

Schardin, M. *et al.* (1985) 'Specific staining of human chromosomes in Chinese hamster x man hybrid cell lines demonstrates interphase chromosome territories', *Human Genetics*, 71(4), pp. 281–287. doi: 10.1007/BF00388452.

Schindelin, J. *et al.* (2012) 'Fiji: An open-source platform for biological-image analysis', *Nature Methods*. Nature Publishing Group, pp. 676–682. doi: 10.1038/nmeth.2019.

Schmitz, S. U. *et al.* (2011) 'Jarid1b targets genes regulating development and is involved in neural differentiation', *EMBO Journal*, 30(22), pp. 4586–4600. doi: 10.1038/emboj.2011.383.

Selak, M. A. *et al.* (2005) 'Succinate links TCA cycle dysfunction to oncogenesis by inhibiting HIF-α prolyl hydroxylase', *Cancer Cell*, 7(1), pp. 77–85. doi: 10.1016/j.ccr.2004.11.022.

Sendžikaitė, G. and Kelsey, G. (2019) 'The role and mechanisms of DNA methylation in the oocyte', *Essays in Biochemistry*. Portland Press, pp. 691–705. doi: 10.1042/EBC20190043.

Shafi, R. *et al.* (2000) 'The O-GlcNAc transferase gene resides on the X chromosome and is essential for embryonic stem cell viability and mouse ontogeny', *Proceedings of the National Academy of Sciences of the United States of America*, 97(11), pp. 5735–5739. doi: 10.1073/pnas.100471497.

Shen, L. *et al.* (2013) 'Genome-wide analysis reveals TET- and TDG-dependent 5-methylcytosine oxidation dynamics', *Cell*, 153(3), pp. 692–706. doi: 10.1016/j.cell.2013.04.002.

Shi, D. Q. *et al.* (2017) 'New insights into 5hmC DNA modification: Generation, distribution and function', *Frontiers in Genetics*. Frontiers Media S.A., p. 100. doi: 10.3389/fgene.2017.00100.

Shpargel, K. B. *et al.* (2012) 'UTX and UTY Demonstrate Histone Demethylase-Independent Function in Mouse Embryonic Development', *PLOS Genetics*, 8(9), p. e1002964. doi: 10.1371/JOURNAL.PGEN.1002964.

Shpargel, K. B. *et al.* (2014) 'KDM6 Demethylase Independent Loss of Histone H3 Lysine 27 Trimethylation during Early Embryonic Development', *PLoS Genetics*. Edited by J. T. Lee, 10(8), p. e1004507. doi: 10.1371/journal.pgen.1004507.

Singh, A. K. *et al.* (2020) 'Selective targeting of TET catalytic domain promotes somatic cell reprogramming', *Proceedings of the National Academy of Sciences of the United States of America*, 117(7), pp. 3621–3626. doi: 10.1073/pnas.1910702117.

Smestad, J. *et al.* (2018) 'Chromatin Succinylation Correlates with Active Gene Expression and Is Perturbed by Defective TCA Cycle Metabolism', *iScience*, 2, pp. 63–75. doi: 10.1016/j.isci.2018.03.012.

Smith, A. G. (2001) 'E MBRYO -D ERIVED S TEM C ELLS : Of Mice and Men', *Cell*, Annu. Rev.

Smith, Z. D. and Meissner, A. (2013) 'DNA methylation: roles in mammalian development', *Nature Reviews Genetics 2013 14:3*, 14(3), pp. 204–220. doi: 10.1038/nrg3354.

Sobhani, A. *et al.* (2017) 'Multipotent stem cell and current application', *Acta Medica Iranica*, 55(1), pp. 6–23. Available at: https://acta.tums.ac.ir/index.php/acta/article/view/4962/4885 (Accessed: 15 April 2021).

Sperber, H. *et al.* (2015) 'The metabolome regulates the epigenetic landscape during naive-to-primed human embryonic stem cell transition', *Nature Cell Biology*, 17(12), pp. 1523–1535. doi: 10.1038/ncb3264.

Sreedhar, A., Wiese, E. K. and Hitosugi, T. (2020) 'Enzymatic and metabolic regulation of lysine succinylation', *Genes & Diseases*, 7(2), pp. 166–171. doi: 10.1016/j.gendis.2019.09.011.

Sugie, K. *et al.* (2020) 'Expression of Dux family genes in early preimplantation embryos', *Scientific Reports*, 10(1). doi: 10.1038/s41598-020-76538-9.

Sun, F. *et al.* (2005) 'Crystal structure of mitochondrial respiratory membrane protein Complex II', *Cell*, 121(7), pp. 1043–1057. doi: 10.1016/j.cell.2005.05.025.

Sun, L. *et al.* (2021) 'Chromatin and Epigenetic Rearrangements in Embryonic Stem Cell Fate Transitions', *Frontiers in Cell and Developmental Biology*. Frontiers Media S.A. doi: 10.3389/fcell.2021.637309.

Šustáčková, G. *et al.* (2012) 'Differentiation-independent fluctuation of pluripotency-related transcription factors and other epigenetic markers in embryonic stem cell colonies', *Stem Cells and Development*, 21(5), pp. 710–720. doi: 10.1089/scd.2011.0085.

Tahiliani, M. *et al.* (2009) 'Conversion of 5-methylcytosine to 5-hydroxymethylcytosine in mammalian DNA by MLL partner TET1', *Science*, 324(5929), pp. 930–935. doi: 10.1126/science.1170116.

Taiwo, O. *et al.* (2012) 'Methylome analysis using MeDIP-seq with low DNA concentrations', *Nature Protocols*, 7(4), pp. 617–636. doi: 10.1038/nprot.2012.012.

Takahashi, K. and Yamanaka, S. (2006) 'Induction of Pluripotent Stem Cells from Mouse Embryonic and Adult Fibroblast Cultures by Defined Factors', *Cell*, 126(4), pp. 663–676. doi: 10.1016/j.cell.2006.07.024.

TeSlaa, T. *et al.* (2016) 'α-Ketoglutarate Accelerates the Initial Differentiation of Primed Human Pluripotent Stem Cells', *Cell Metabolism*, 24(3), pp. 485–493. doi: 10.1016/j.cmet.2016.07.002.

Thomson, J. A. *et al.* (1998) 'Embryonic Stem Cell Lines Derived from Human Blastocysts', *Science*, 282(5391), pp. 1145–1147. doi: 10.1126/science.282.5391.1145.

Tretter, L., Patocs, A. and Chinopoulos, C. (2016) 'Succinate, an intermediate in metabolism, signal transduction, ROS, hypoxia, and tumorigenesis', *Biochimica et Biophysica Acta - Bioenergetics*, 1857(8), pp. 1086–1101. doi: 10.1016/j.bbabio.2016.03.012.

Tschiersch, B. *et al.* (1994) 'The protein encoded by the Drosophila position-effect variegation suppressor gene Su(var)3-9 combines domains of antagonistic regulators of homeotic gene complexes', *EMBO Journal*, 13(16), pp. 3822–3831. doi: 10.1002/j.1460-2075.1994.tb06693.x.

Vella, P. *et al.* (2013) 'Tet Proteins Connect the O-Linked N-acetylglucosamine Transferase Ogt to Chromatin in Embryonic Stem Cells', *Molecular Cell*, 49(4), pp. 645–656. doi: 10.1016/j.molcel.2012.12.019.

Wang, C. *et al.* (2018) 'Reprogramming of H3K9me3-dependent heterochromatin during mammalian embryo development', *Nature Cell Biology 2018 20:5*, 20(5), pp. 620–631. doi: 10.1038/s41556-018-0093-4.

Wang, G. L. and Semenza, G. L. (1995) 'Purification and characterization of hypoxia-inducible factor', *Journal of Biological Chemistry*, 270(3), pp. 1230–1237. doi: 10.1074/jbc.270.3.1230.

Wang, L. *et al.* (2013) 'A small molecule modulates Jumonji histone demethylase activity and

selectively inhibits cancer growth', *Nature Communications*, 4. doi: 10.1038/ncomms3035.

Wang, X. *et al.* (2018) 'Toward Single-Cell Single-Molecule Pull-Down', *Biophysical Journal*, 115(2), pp. 283–288. doi: 10.1016/j.bpj.2018.05.013.

Weinert, B. T. *et al.* (2013) 'Lysine succinylation is a frequently occurring modification in prokaryotes and eukaryotes and extensively overlaps with acetylation', *Cell Reports*, 4(4), pp. 842–851. doi: 10.1016/j.celrep.2013.07.024.

Welford, R. W. D. *et al.* (2005) 'Incorporation of oxygen into the succinate co-product of iron(II) and 2-oxoglutarate dependent oxygenases from bacteria, plants and humans', *FEBS Letters*, 579(23), pp. 5170–5174. doi: 10.1016/j.febslet.2005.08.033.

Williams, K. *et al.* (2011) 'TET1 and hydroxymethylcytosine in transcription and DNA methylation fidelity', *Nature*, 473(7347), pp. 343–348. doi: 10.1038/nature10066.

Wobus, A. M. and Boheler, K. R. (2005) 'Embryonic stem cells: Prospects for developmental biology and cell therapy', *Physiological Reviews*. American Physiological Society, pp. 635–678. doi: 10.1152/physrev.00054.2003.

Wolf, S. F. *et al.* (1984) 'Complete concordance between glucose-6-phosphate dehydrogenase activity and hypomethylation of 3′ CpG clusters: Implications for X chromosome dosage compensation', *Nucleic Acids Research*, 12(24), pp. 9333–9348. doi: 10.1093/nar/12.24.9333.

Wray, J., Kalkan, T. and Smith, A. G. (2010) 'The ground state of pluripotency', *Biochemical Society Transactions*, pp. 1027–1032. doi: 10.1042/BST0381027.

Wu, H. *et al.* (2011) 'Genome-wide analysis of 5-hydroxymethylcytosine distribution reveals its dual function in transcriptional regulation in mouse embryonic stem cells', *Genes and Development*, 25(7), pp. 679–684. doi: 10.1101/gad.2036011.

Wu, H. *et al.* (2013) 'Structure of the Catalytic Domain of EZH2 Reveals Conformational Plasticity in Cofactor and Substrate Binding Sites and Explains Oncogenic Mutations', *PLoS ONE*. Edited by S. Rocha, 8(12), p. e83737. doi: 10.1371/journal.pone.0083737.

Xia, W. *et al.* (2019) 'Resetting histone modifications during human parental-to-zygotic transition', *Science*, 365(6451), pp. 353–360. doi: 10.1126/SCIENCE.AAW5118.

Xia, W. and Xie, W. (2020) 'Rebooting the Epigenomes during Mammalian Early Embryogenesis', *Stem Cell Reports*, 15(6), pp. 1158–1175. doi: 10.1016/j.stemcr.2020.09.005.

Xiang, Y. *et al.* (2019) 'Epigenomic analysis of gastrulation identifies a unique chromatin state for primed pluripotency', *Nature Genetics 2019 52:1*, 52(1), pp. 95–105. doi: 10.1038/s41588-019-0545-1.

Xiao, M. *et al.* (2012) 'Inhibition of α-KG-dependent histone and DNA demethylases by fumarate and succinate that are accumulated in mutations of FH and SDH tumor suppressors', *Genes and Development*, 26(12), pp. 1326–1338. doi: 10.1101/gad.191056.112.

Xu, Y. *et al.* (2012) 'Tet3 CXXC domain and dioxygenase activity cooperatively regulate key genes for xenopus eye and neural development', *Cell*, 151(6), pp. 1200–1213. doi: 10.1016/j.cell.2012.11.014.

Yamanaka, S. (2020) 'Pluripotent Stem Cell-Based Cell Therapy—Promise and Challenges', *Cell Stem Cell*. Cell Press, pp. 523–531. doi: 10.1016/j.stem.2020.09.014.

Yan, Q. *et al.* (2007) 'The Hypoxia-Inducible Factor 2α N-Terminal and C-Terminal Transactivation Domains Cooperate To Promote Renal Tumorigenesis In Vivo', *Molecular and Cellular*

Biology, 27(6), pp. 2092–2102. doi: 10.1128/mcb.01514-06.

Yang, G. *et al.* (2021) 'Histone acetyltransferase 1 is a succinyltransferase for histones and non-histones and promotes tumorigenesis', *EMBO reports*, 22(2), p. e50967. doi: 10.15252/embr.202050967.

Ye, S. *et al.* (2013) 'Embryonic stem cell self-renewal pathways converge on the transcription factor Tfcp2l1', *The EMBO Journal*, 32, pp. 2548–2560. doi: 10.1038/emboj.2013.175.

Ying, Q.-L. *et al.* (2008) 'The ground state of embryonic stem cell self-renewal', 453. doi: 10.1038/nature06968.

Ying, Q. L. *et al.* (2003) 'BMP induction of Id proteins suppresses differentiation and sustains embryonic stem cell self-renewal in collaboration with STAT3', *Cell*, 115(3), pp. 281–292. doi: 10.1016/S0092-8674(03)00847-X.

Zakariyah, A. *et al.* (2019) 'Combinatorial Utilization of Murine Embryonic Stem Cells and In Vivo Models to Study Human Congenital Heart Disease', *Current Protocols in Stem Cell Biology*, 48(1). doi: 10.1002/cpsc.75.

Zalzman, M. *et al.* (2010) 'Zscan4 regulates telomere elongation and genomic stability in ES cells', *Nature*, 464(7290), pp. 858–863. doi: 10.1038/nature08882.

Zhang, B. *et al.* (2016) 'Allelic reprogramming of the histone modification H3K4me3 in early mammalian development', *Nature*, 537(7621), pp. 553–557. doi: 10.1038/nature19361.

Zhang, T. *et al.* (2020) 'Histone H3K27 acetylation is dispensable for enhancer activity in mouse embryonic stem cells', *Genome Biology*, 21(1). doi: 10.1186/s13059-020-01957-w.

Zhang, Z. *et al.* (2011) 'Identification of lysine succinylation as a new post-translational modification', *Nature Chemical Biology*, 7(1), pp. 58–63. doi: 10.1038/nchembio.495.

Zhao, M. T. *et al.* (2014) 'Methylated DNA immunoprecipitation and high-throughput sequencing (MeDIP-seq) using low amounts of genomic DNA', *Cellular Reprogramming*, 16(3), pp. 175–184. doi: 10.1089/cell.2014.0002.

Zheng, H. *et al.* (2016) 'Resetting Epigenetic Memory by Reprogramming of Histone Modifications in Mammals', *Molecular Cell*, 63(6), pp. 1066–1079. doi: 10.1016/J.MOLCEL.2016.08.032.

Zhong, S. *et al.* (2017) 'Immunofluorescence Imaging Strategy for Evaluation of the Accessibility of DNA 5-Hydroxymethylcytosine in Chromatins', *Analytical Chemistry*, 89(11), pp. 5702–5706. doi: 10.1021/acs.analchem.7b01428.

Zhou, W. *et al.* (2012) 'HIF1α induced switch from bivalent to exclusively glycolytic metabolism during ESC-to-EpiSC/hESC transition', *The EMBO Journal*, 31(9), pp. 2103–2116. doi: 10.1038/emboj.2012.71.

Zhu, Y. *et al.* (2021) 'Cell cycle heterogeneity directs spontaneous 2C state entry and exit in mouse embryonic stem cells', *Stem Cell Reports*, 16(11), pp. 2659–2673. doi: 10.1016/J.STEMCR.2021.09.003.

SUPPLEMENTARY DATA

Sublist	Category	Term	RT	Genes	Count	%	P-Value	Fold Enrichment	Benjamini
☐	GOTERM_CC_DIRECT	extracellular exosome	RT		94	58,8	1,3E-40	4,3	3,3E-38
☐	GOTERM_CC_DIRECT	intracellular ribonucleoprotein complex	RT		36	22,5	9,2E-30	13,9	1,2E-27
☐	GOTERM_CC_DIRECT	cytoplasm	RT		114	71,2	1,9E-22	2,1	1,7E-20
☐	GOTERM_CC_DIRECT	focal adhesion	RT		31	19,4	4,9E-21	9,8	3,2E-19
☐	GOTERM_CC_DIRECT	ribosome	RT		24	15,0	7,5E-21	15,8	3,9E-19
☐	GOTERM_CC_DIRECT	nucleus	RT		96	60,0	1,4E-14	2,0	6,1E-13
☐	GOTERM_CC_DIRECT	cytosolic large ribosomal subunit	RT		14	8,8	3,9E-13	19,0	1,5E-11
☐	GOTERM_CC_DIRECT	cytosol	RT		44	27,5	3,0E-11	3,0	9,7E-10
☐	GOTERM_CC_DIRECT	myelin sheath	RT		16	10,0	4,4E-11	10,3	1,3E-9
☐	GOTERM_CC_DIRECT	nucleoplasm	RT		44	27,5	4,0E-10	2,8	1,0E-8

Supplementary data 1. Protein succinylation also occurs outside the mitochondria upon SA treatment of mESCs.
Gene ontology (GO) analysis of proteins identified as over-succinylated in SA-treated mESCs after pull-down of succinylated peptides and mass spectrometry analysis. Only proteins with a FC ≥ 1.5 compared to the untreated control group (278 proteins out of 829) were selected for the analysis. The results represent the ten first 'cellular-component' (CC) GO terms classified by *P*-value and obtained with DAVID Annotation Tool.

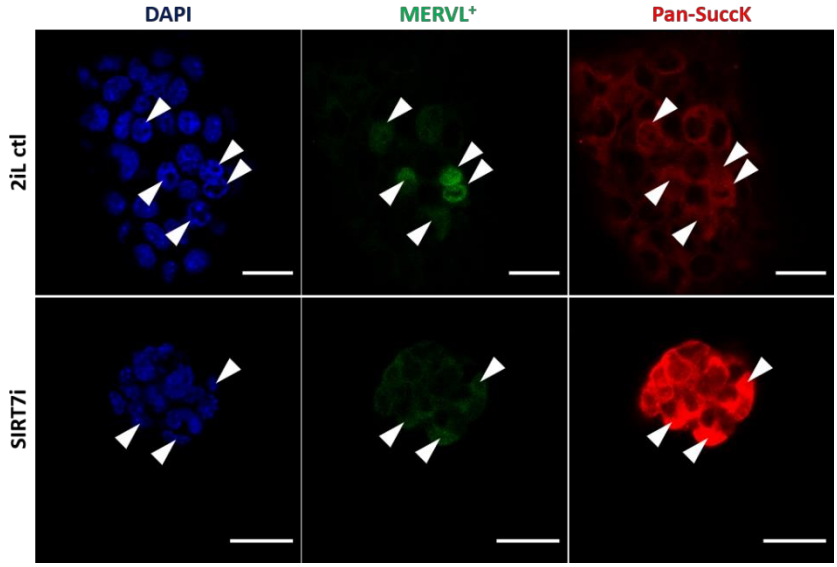

Supplementary data 2. SIRT7i, a sirtuin 7 inhibitor, engenders slight increase in nuclear succinylation.
Confocal micrographs untreated (2iL ctl) or treated with 5 µM SIRT7i of naïve mESCs of the TBG4 cell line that expresses a turboGFP under the control of MERVL's LTR (Ishiuchi *et al.*, 2015; Rodriguez-Terrones *et al.*, 2020). Pan-succinyllysine residues (Pan-SuccK) are immunostained (red) and nuclei are counterstained by DAPI. White triangles point MERVL-expressing cells with exhibit enhanced pan-succinyllysine immunofluorescence signal. Representative of 1 independent experiment. Scale bar=20 µm.

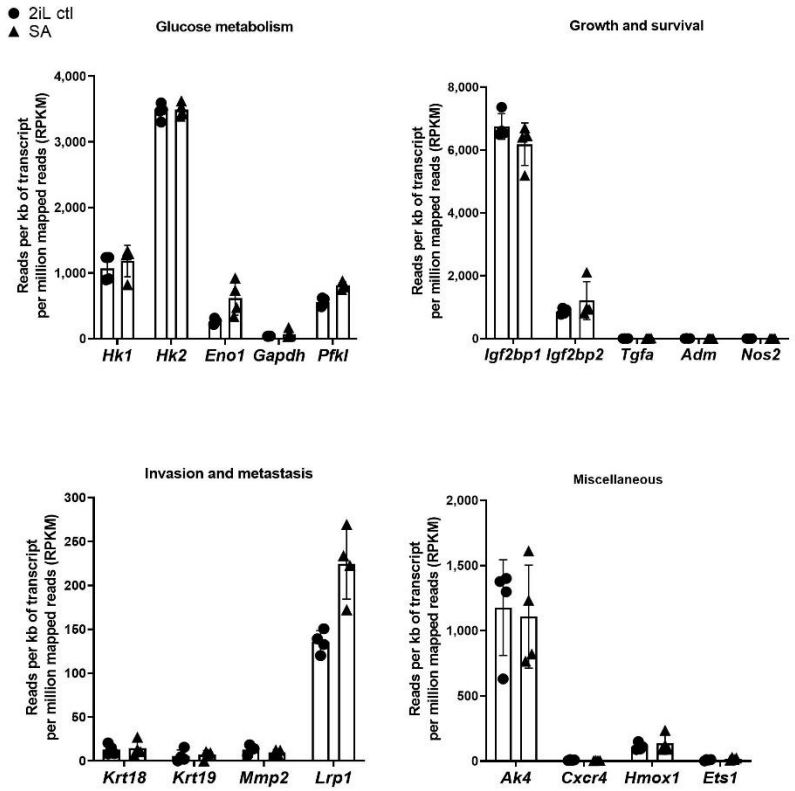

Supplementary data 3. HIF-1α targets expression is impacted by SA treatment although no fashion is noticeable.
This bar plot represents the reads per kilobase (kb) of transcript per million mapped reads (RPKM) of an exhaustive list of HIF-1α targets classified according to their biological context (glucose metabolism, growth and survival, invasion and metastasis, and miscellaneous) of untreated and SA-treated naïve mESCs of four independent replicates. *Ak4*, *Ndgr1*(Hu *et al.*, 2006) *Cxcr4, Hmox1* (Pawlus *et al.*, 2012), *Hk1*, *Hk2*, *Eno1*, *Gapdh*, *Pfkl*, *Igf2bp1*, *Igf2bp2*, *Tgfa*, *Adm*, *Nos2*, *Krt18*, *Krt19*, *Mmp2*, *Lrp1*, *Ets1* (Hong, Lee and Kim, 2004).

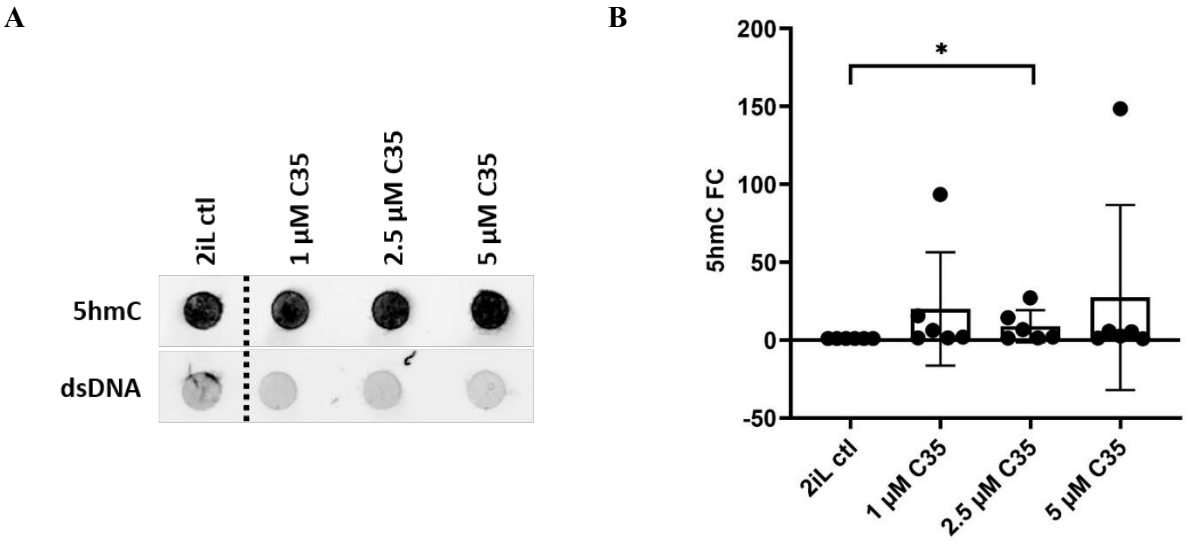

Supplementary data 4. TET inhibitors do not seem to increase the global 5hmC level in treated naïve mESCs.

(A) Dot blot analysis of the 5hmC global level in naïve mESCs treated with the C35 TET inhibitor, at 1, 2.5 and 5 µM. These results represent only one replicate with the separated 5hmC and dsDNA (double-strand DNA) immunostainings, the latter serving as loading control.

(B) Quantification of **(A)**, the 5hmC (5-hydroxymethlcytosine) immunostaining of mESCs DNA treated with TET inhibitors, C35 (1, 2.5 and 5 µM) established by dot blot analysis. Results are representative of 6 independent experiments. Results are shown as mean ± S.D. and each independent value are represented by dots. Dunnett's mixed-effect statistical analysis has been conducted with the Geisser-Greenhouse correction. * $P < 0.05$, non-significant results are not labelled.

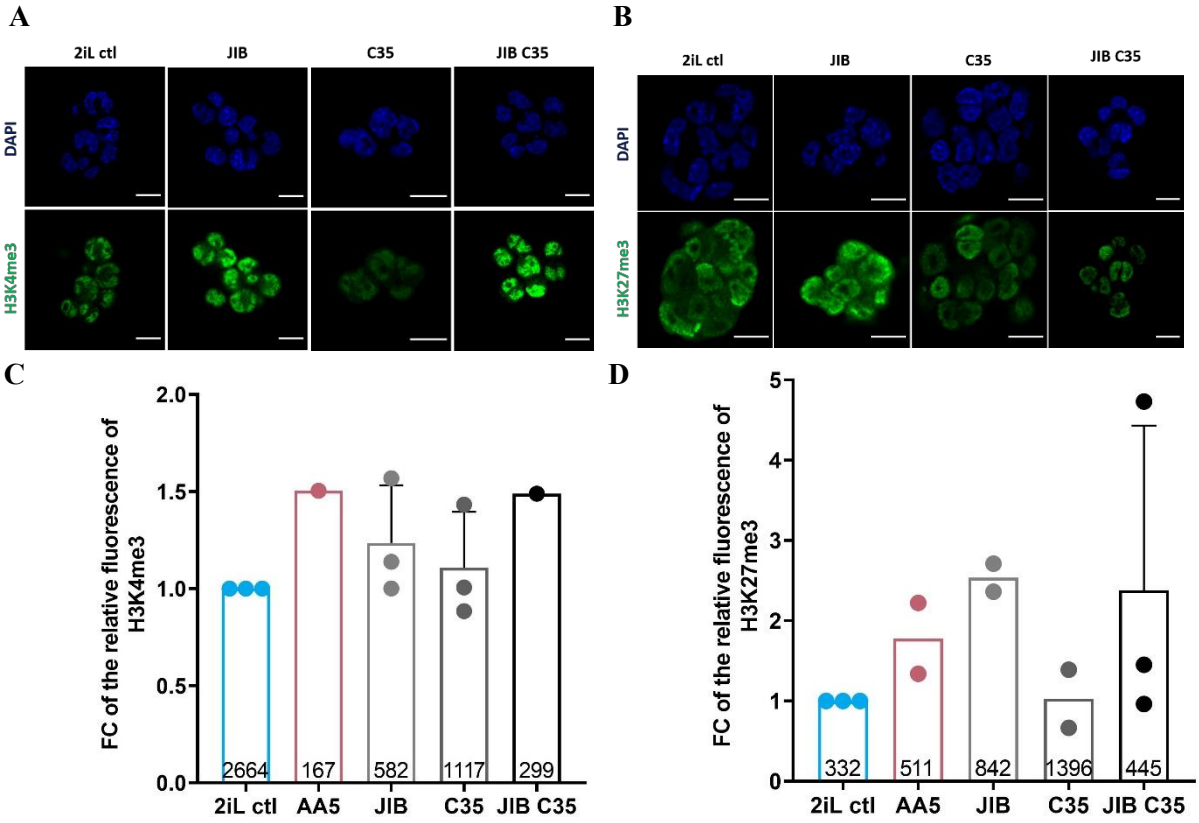

Supplementary data 5. Assessment of the inhibitory effect of the JIB HDM inhibitor and C35 TET inhibitor.

(A) and (B) Representative confocal micrographs of naïve (2iL) mESCs treated with 250 nM AA5, 250 nM JIB (HDM inhibitor), 2.5 µM C35 (TET inhibitor) or with both JIB and C35. H3K4me3 in **(A)** and H3K27me3 in **(B)** are immunostained (green), nuclei are counterstained by DAPI. Scale bar=10 µm.

(C) and (D) Relative fluorescence of H3K4me3 **(C)** and H3K27me3 **(D)** immunofluorescence signal to 2iL control in nuclei of naïve mESCs exposed to 250 nM AA5, 250 nM JIB (HDM inhibitor), 2.5 µM C35 (TET inhibitor) or to both JIB and C35. The number of biological replicates is **(C)** n=3, 1, 3, 3 and 1, **(D)** n=3, 2, 2, 2, and 3, respectively for 2iL, 250 nM AA5, 250 nM JIB, 2.5 µM C35 and JIB+C35.